The NaStA project aims to support and improve the operational environment of the SMEs by increasing knowledge on natural stones used in historical constructions, their origin and possible substitutes in restoration works. The main objective is to promote the uniqueness of rapakivi granites used in buildings, constructions and the architectural monuments. The European Union has partly been funded the project by the ENI CBC Programme 2014–2020 between South-eastern Finland and Russia.

NaStA

History and future of natural stones in architecture – bridge between South East Finland and Russia (ENI CBC)

Altering visual appearance on surface of rapakivi granite

LUT Team: Maaret Paakkunainen, Satu-Pia Reinikainen, Tuomas Sihvonen, Elisa Raiskio, Zina-Sabrina Duma

GTK Team: Paavo Härmä, Nike Luodes, Heidi Laxström

28.11.2022

The project is funded by European Union.

Contents

1. Introduction

Restoration of old stone buildings often requires new stones to be added to the building, but the difference in appearance between the old and new building stone due to the years of weathering causes an aesthetical problem. This study is a part of NaStA (History and future of natural stones in architecture – bridge between South East Finland and Russia) ENI CBC project (activity 3). One aim of the NaStA project is to identify potential means to artificially change the appearance of rapakivi granite used as building stones and to study how the old appearance can be achieved. This research focused to the two most common Finnish rapakivi varieties applied in Russian historical buildings, wiborgite and pyterlite, (Panova, Vlasov & Luodes 2014), and two commercially interesting rapakivi varieties: dark rapakivi granite and dark green wiborgite.

1.1 Methods

This study aims to alter the chemical composition of rapakivi granite surface by different means of treatments. The main procedures were thermal treatment by exposing the surface of rapakivi granite to high temperatures such as 400°C and 600 °C, and chemical treatment by exposing the surface to acids and metal salts solutions. A combination of these treatments was also applied. The changes were observed visually, and various analytical measurements were carried out to see the changes in the chemical structure of the stone surface (for example XRF, FTIR and SEM/EDS) (Figure 1).

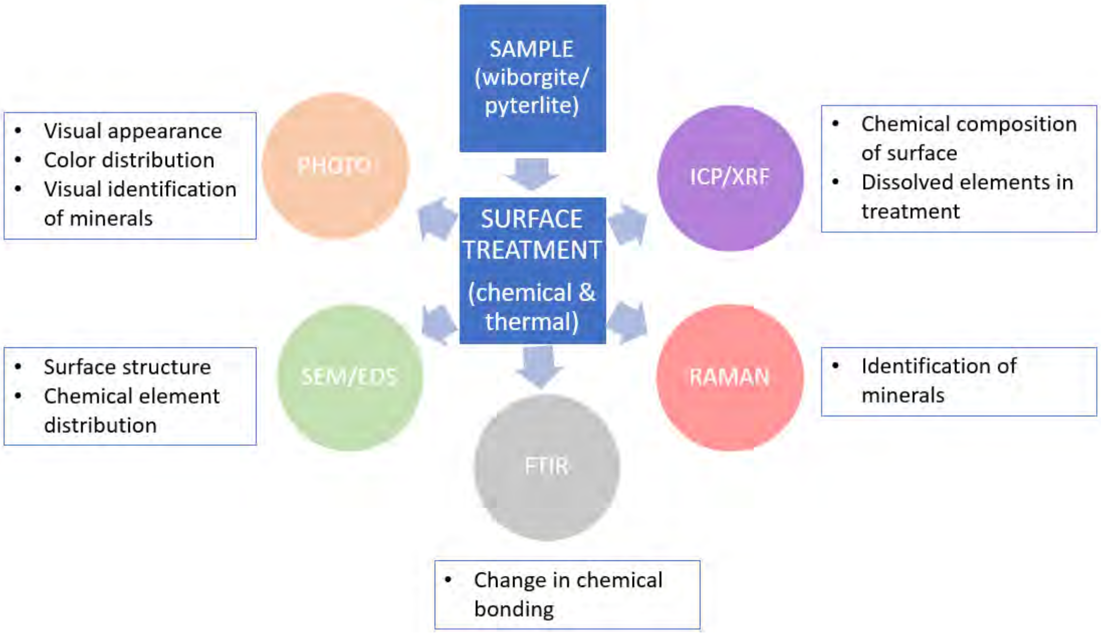

Figure 1: Analytical methods and devices used and their purposes in studying the changes in the stone sample surfaces.

Visual appearance is particularly important when substitution of stones in old buildings is required. Photogrammetry and colorimetric methods were applied in defining visual changes in texture, pattern, and colours. Scanning electron microscope (SEM) and energy dispersive X-ray spectroscopy (EDS) provided information about the changes in surface structure and elemental distribution on microscopic scale. Spectroscopic methods, such as Raman and FT-IR, were applied in mineral identification or mineral mixture monitoring. XRF (X-ray fluorescence) was applied as a non-destructive analytical technique to determine the elemental composition of the surfaces. The chemical solutions applied in treatments were analysed for leached or adsorbed chemicals with Inductively Coupled Plasma Mass Spectrometry (ICP-MS).

1.2 Rapakivi granite samples

Stone samples were delivered by GTK to LUT. In course of the project several granite varieties were studied. The main stone types utilized in this research were:

1) wiborgite rapakivi granite (called here W or A1)
2) pyterlite rapakivi granite (called here P of C1)
3) dark rapakivi granite (called D or B)
4) dark green wiborgite (called DG or BG).

In Chapter 3 these four rapakivi granite varieties are presented with photos.

1) Wiborgite (marked W or A1)

Wiborgite rapakivi granite has a typical texture of rapakivi granites with large megacrysts (ovoids) 1–4 cm in diameter in medium-grained matrix. The K-feldspar ovoids are surrounded by a rim of plagioclase, which are set in a medium-grained matrix of main minerals, quartz, feldspars, biotite and hornblende. The chemical formulas for these minerals are SiO_2, $KAlSi_3O_8$,$K(Mg,Fe)_3AlSi_3O_{10}(OH,F)_2$ and $(Ca,Na)_{2–3}(Mg,Fe,Al)_5(Al,Si)_8O_{22}(OH,F)_2$, respectively. The size of the K-feldspar ovoids can range from 1-10 cm in diameter and the size of the plagioclase rim is often between 1-5 mm. Wiborgite is typically brown coloured, but green and red wiborgites can also be found. An example of chemical composition of wiborgite found from literature is presented in Table 1 together with measurements achieved with XRF analysis from samples used in these experiments. (Härmä 2020, Simonen 1987).

Compared to the literature, the iron and kalium concentration of wiiborgite seems a bit higher than expected. The surfaces have been cleaned, but one reason might be contamination from sample extraction. The results are computed from 99 XRF measurements, and with expanded uncertainty (95 %), the result would be for iron 7.7 % +/- 1.1 %, and for kalium 10.8 % +/- 0.8 %. Table 10 shows elemental concentration from the XRF measurements with expanded 95 % confidence values for all 4 granite varieties in this study.

Table 1. Chemical composition of wiborgite rapakivi granite: the literature (Simonen, 1987), and experimentally determined in the present study. n.a. = not analyzed.

	SiO_2	TiO_2	Al_2O_3	Fe_2O_3	FeO	MnO	MgO	CaO	Na_2O	K_2O	P_2O_5	F
m-% literature	69.45	0.47	13.78	1.02	3.27	0.05	0.43	2.00	3.03	5.66	0.11	0.20
m-% XRF measurement	66.30	0.66	25.53	7.73*		0.05	0.26	1.53	n.a.	10.80	n.a.	n.a.

*Distribution of Fe between Fe_2O_3 and FeO is unknown.

2) Pyterlite (marked P or C1)

Pyterlite is a porphyritic rapakivi granite variety with rounded, densely dispersed K-feldspar megacrysts 1–4 cm in diameter in medium-grained matrix (Fig. 1). In this rapakivi type, megacrysts lack the rim of plagioclase. The colour of pyterlite is typically pale red, brown or green. The main mineral composition of pyterlite rapakivi granite is K-feldspar, quartz, plagioclase and biotite that is very similar to wiborgite rapakivi granite, but usually lacking hornblende. Chemically pyterlite contains more quartz, K-feldspar and silicic acids than wiborgite, but it contains less plagioclase, iron, magnesium and calcium when compared to wiborgite. An example of chemical composition of pyterlite found from literature Table 2￼

together with measurements achieved with XRF analysis from samples used in these experiments. (Härmä 2020, Simonen 1987).

Table 2. Chemical composition of pyterlite rapakivi granite: the literature (Simonen, 1987), and experimentally determined in the present study.

	SiO_2	TiO_2	Al_2O_3	Fe_2O_3	FeO	MnO	MgO	CaO	Na_2O	K_2O	P_2O_5	F
m-% literature	76.02	0.23	11.12	0.92	1.70	0.02	0.16	0.92	2.32	5.51	0.40	0.33
m-% XRF measurement	74.17	0.24	21.74	2.56*		0.02	0.20	0.59	n.a.	11.26	0.07	n.a.

3) Dark rapakivi granite (marked D or B)

Dark rapakivi granites comprise a lithological group that consists of rock types with varying texture, but which are similar in mineralogical composition. They can be dark green, dark greenish brown or black. The dark rapakivi granites contain quartz, plagioclase and K-feldspar in varying proportions as main minerals. Hornblende, olivine, biotite and clinopyroxene are the mafic minerals, which together amount to up to 20 vol%. In all of the dark rapakivi granites, fayalitic olivine is present with hornblende and magnetite. (Härmä 2020, Simonen 1987).

Dark and dark green rapakivi studied seem to have lower silica concentration, and higher iron, aluminium and calcium concentrations than wiborgite and pyterlite in general. Table 3 shows chemical composition of the dark rapakivi granite and the dark green wiborgite of samples.

Table 3 Chemical composition of pyterlite rapakivi granite: Dark rapakivi granite and Dark green wiborgite samples studied.

	SiO_2	TiO_2	Al_2O_3	Fe_2O_3	FeO	MnO	MgO	CaO	Na_2O	K_2O	P_2O_5	F
m-% Dark rapakivi	65.83	1.01	25.73	9.81		0.07	0.50	2.26	n.a.	9.51	0.31	n.a.
m-% Dark Green	61.55	0.68	26.51	8.62		0.06	3.00	2.02	n.a.	10.50	0.42	n.a.

4) Dark green wiborgite (marked DG or BG)

Dark wiborgite is a variety of wiborgite carrying K-feldspar megacrysts (ovoids), occasionally mantled with plagioclase, as well as angular plagioclase crysts of andesine composition (1–5 cm in diameter) in a dark-coloured matrix (Figure 19). The main colours of the rock are dark brown and black, with occasional shades of dark greenish brown. The main minerals are K-feldspar, quartz, plagioclase and hornblende. In addition, fayalitic olivine, magnetite and biotite are found as accessory minerals. (Härmä 2020, Simonen 1987).

2. METHOLOGY AND METHODS

The study started with a campaign aiming to define the most potential chemicals and treatment methods. In this report the results gathering the main finding and the results from the final experiment are presented. The effects of thermal, chemical and the combination of chemical and thermal treatments to granite surface were studied.

All the stone samples were photographed before and after every treatment for comparison of visual appearance. First chemical treatments were done to the samples. After the chemical treatments, the analyses of the sample surface were made to determine the changes that chemical treatment caused. The results of the treatments were analysed with SEM/EDS, ICP-MS, XRF, FTIR and RAMAN. Then the samples continued to thermal treatment to determine the effect of the combination of chemical and thermal treatment to the sample surface. Some samples were only treated with thermal treatment. Then the samples were analysed again to determine the changes the treatment caused.

2.1 CHEMICAL TREATMENT

One of the goals of this research was to study, how chemical treatment affects the granite surface. The effect of chemicals was studied with several different acid and metal solutions. The stone samples were treated with solutions of sulfuric acid, H_3PO_4, $CaCl_2$, $FeCl_2$ and $NaSO_4$, all in the strength of 2 M. For $FeCl_2$ and $NaSO_4$ solution some sulfuric acid was added to enhance the solubility of the metal salts. Chemical treatments were also conducted with a combination of acid and metal solutions. The stone samples were treated with a combination of 2 M sulfuric acid and 2 M $NaSO_4$ and a combination of 2 M sulfuric acid and 2 M $FeCl_2$.

Table 4. Stone samples labels and the treatments applied to them.

Treatment		Sample name			
1st	2nd	A1 or W	C1 or P	B or D	BG or DG
SA (=H_2SO_4)	Thermal^2	6	6, 8	1	1
SA+$FeCl_2$	Thermal^2	7	7, 15	2	2
SA+Na_2SO_4	Thermal^2	9	9	4	4
Na_2SO_4	Thermal^2	12	12	7	7
$FeCl_2$	Thermal^2	11	11	6	6
$CaCl_2$	Thermal^2	10	10	5	5
H_3PO_4	Thermal^2	13	13	8	8
Thermal^1	-	14	14	9	9
Thermal^2	-	8	16	3	-

Thermal^1: 600 °C for 45 minutes
Thermal^2: 400 °C for 30 minutes

The summary of the treated stone samples and the treatments applied is presented in Table 4. For example Dark green wiborgite sample DG-1 was first chemically treated with 2 M sulfuric acid for 72 h and analyzed. The treatment continued with thermal treatment at 400 °C for 30 minutes.

EXPERIMENTAL PROCEDURES

The chemical treatment solutions were prepared by calculating the needed amount of concentrated substance or solid powder needed to make 2 M solutions. For the metal salts $FeCl_2$ and Na_2SO_4, some concentrated sulfuric acid was added to the 2 M solutions to ease their solubility.

To conduct the chemical treatment experiments, approximately 50 % of the stone sample area was submerged in the acid, metal, and combination solutions for 72 hours, similarly as in Figure 2. Some glass cullet was placed on the bottom of the decanter glass used for treatment to ensure that the solution reacted with most of the bottom surface of the sample too. Samples of acid acting as solvent substance were taken after leaching and were brought to ICP-MS analysis.

Figure 2. Sample W-6 and approximately 50 % of its area submerged in 2 M sulfuric acid.

After the treatment, the rock samples were washed in de-ionized water, gently tapped with paper towel, and left to dry in room temperature in a fume hood overnight, for about 16 hours. The dry-stone samples were photographed for visual analysis and analyzed with XRF and SEM/EDS. After analysis, the samples were treated further with thermal treatments, as described in chapter 2.2.

2.2 PHYSICAL TREATMENT

Physical treatment methods applied were thermal and UV treatment. In pretests effect of UV treatment on visual appearance was minor and it was excluded from latter experiments. APPENDIX UV treatment shows analytical results and instrumentation in UV treatment. Results from UV experiments are discussed in B. Sc. Thesis of Juhani Ilonen (Ilonen, 2020).

Thermal treatments for the stone samples were done in two different ways: Thermal^1 and Thermal^2. In the Thermal^1 treatment the stone samples were placed in a 600 °C oven for 45 minutes. After 45 minutes the stone sample was taken out of the oven and left to cool in room temperature in a fume hood for 1-2 hours. In the Thermal^2 treatment the stone samples were placed in a 400°C oven for 30 minutes. After 30 minutes the stone sample was taken out of the oven and left to cool in room temperature in a fume hood for 1-2 hours.

The oven used for the thermal treatments was Naber Industrieofenbau 2804, as seen in Figure 3. After the thermal treatments, the samples were photographed for visual analysis and analyzed with XRF and SEM/EDS.

Figure 3. *Oven used for thermal treatment.*

2.3 METHOLOGY IN VISUAL ANALYSIS

Photos were taken of all samples before treatments, after treatment 1 and after treatment 2. The setup of photo studio is described in Figure 4. Visual analysis was applied to the samples using colour information obtained from the surfaces using Image Processing Toolbox provided within MATLAB.

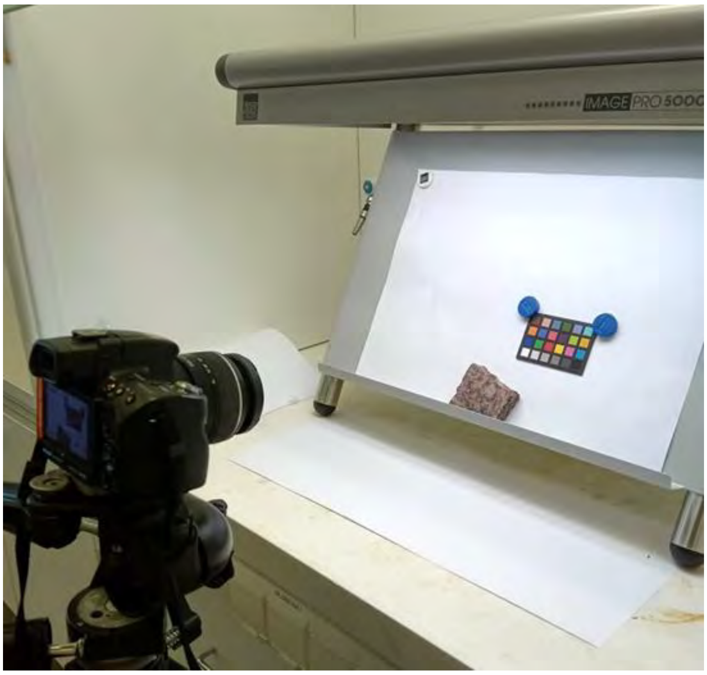

Figure 4. Setup of camera, photo studio and colour palette.

COLOUR CORRECTION

The images, taken with single-lens reflex camera, needed to be colour-corrected before processing, because of the different RGB values being captured by cameras of the same objects from one image to another. By applying colour calibration, the colours are transformed in such a way that the difference in colour between images is minimized, converting it into a standard space (*Akkaynak et al.,* 2014). The pictures were taken next to the plate consisting of target colour patches that includes an almost complete majority of the reflectance spectrum that occurs naturally.

Before the colour thresholding could be applied to the images, the camera-taken images needed to be linearized from the RGB space. This was done in order to avoid any gamma correction that is applied by the camera.

The colour correction first began by taking location of the colour plate’s corners, which were fixed in each of the images, and the difference in colour is measured between the plate colour and the standard, manufacturer-given values, *colourChekcer()* function resulting in ΔE values for each colour and *measureColour*() resulting in the correction matrix to be applied to the images. Then, each colour is adjusted based on the correction matrix generated. MATLAB's *imapplymatrix()* that linearly combines colour channels is used for combining the colour correction matrix to the image. The colour corrected image that results is then converted back to the RGB space for further processing, using the *lin2rgb()* function.

IMAGE SEGEMENTING IN COLOUR CHANNELS

Before applying any colour segmentation, the background from the image needed to be removed. A very simple solution was to draw an circle on the image using *drawcircle*, getting the pixel coordinates of the circular sample and getting a mask of the circle. Everything outside of the circular mask could then be cropped and the rest of the background could be turned to black colour.

Now that the object of interest only remained in the image the colours could be divided into separate masks. This was achieved by using MATLAB's Colour Thresholder tool and dividing samples colour information in YCbCr colour space into three different regions representing each of the three different tones of colour: red, dark, and light. With the created colour masks each of the images could now be divided into three separate binary pictures using the colour thresholds provided by the masks. By combining these masks information such as the area covered by the binary picture and overlaps between the different binary pictures could be captured. The area which is not covered by the masks is referred to as *other*. Each of the different colour mask coverages are calculated with:

$$\mathrm{A}_{mask\%} = \frac{nnz(A_{mask})}{nnz(A_{tot})} * 100 \tag{1}$$

where *nnz()* refers to number of nonzero elements in the mask, A_{mask} is the colour mask and A_{tot} is the mask that covers the entire object.

Each of the different sample groups had their own colour masks created. Difference between the colour areas could now be calculated by subtracting the colour area after the treatments from the original colour coverage.

2.4 DETERMINATION OF CHEMICAL CONCENTRATIONS

During the chemical treatment, the samples were treated in different solvents. Before and after the treatment, liquid samples were taken from the solvent, filtrated, diluted, and analyzed with Agilent 7900 ICP-MS (Figure 5). With ICP-MS the metal concentrations of the solutions were measured. included elements studied were from included rare earth elements (REE's) standard, multi element standard Multi26 and standard PA Tuning 1. Metals analyzed were: Ag, Al, As, Au, Ba, Be, Bi, Ca, Cd, Ce, Co, Cr, Cu, Dy, Er, Eu, Fe, Hg, Ho, In, K, La, Li, Lu, Mg, Mn, Mo, Na, Nd, Ni, P, Pb, Pr, Sb, Sc, Se, Sm, Sn, Sr, Tb, Te, Th, Tl, Tm U, V, Zn, Y and Yb. For most of the metals the concentrations were below the detection limits. The result which were in the analytical working range are discussed in this report.

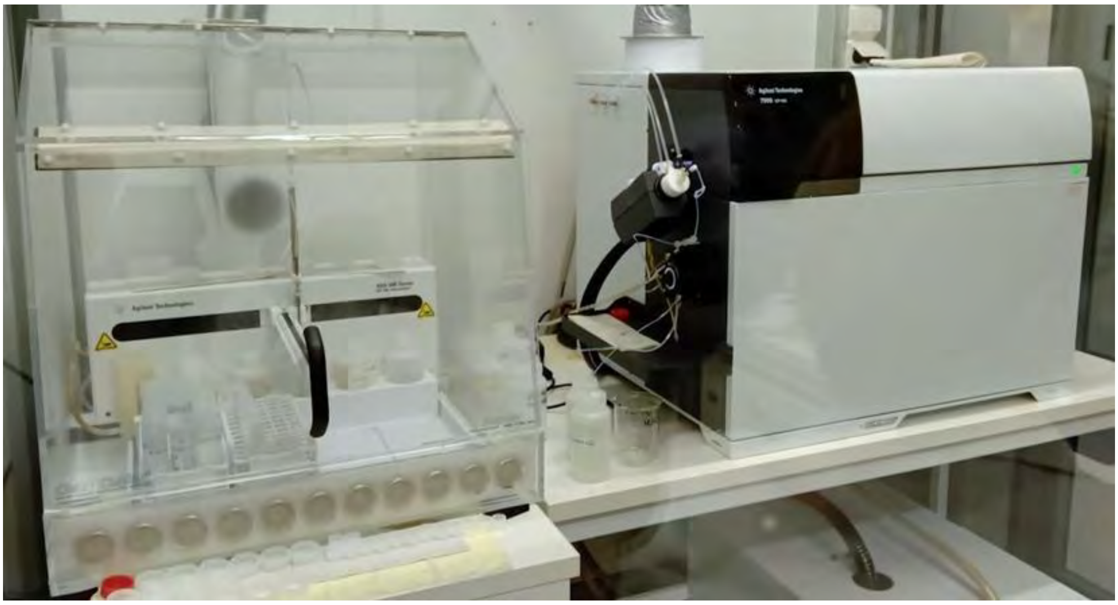

Figure 5. Agilent Technologies 7900 ICP-MS used in examining the elements in solvents.

The XRF measurements were acquired using the hand device shown in Figure 6. Hand-held device used for XRF measurements All XRF measurements were acquired from samples before and after the chemical and thermal treatments. Elements analyzed with the XRF were: Mg, Al, Si, P, S, K, Ca, Ti, V, Cr, Mn, Fe, Co, Ni, Cu, Zn, As, Se, Rb, Sr, Y, Zr, Nb, Mo, Ag, Cd, Sn, Sb, W, Au, Hg, Pb, Bi, Th, U. Methods applied were GeoChem REE and GeoChem.

Figure 6. Hand-held device used for XRF measurements.

Scanning electron microscope -energy dispersive X-ray spectrometer (SEM-EDS) provide SEM images on surface and elemental distribution connected to it. The SEM/EDS pictures were acquired using the Scanning Electron Microscope SU3500 and Thermo Scientific UltraDry SDD EDS, dual detector. The device is shown in Figure 7. SEM-EDS used to analyse the surface structure and element distribution on the sample surface.

Figure 7. SEM-EDS used to analyse the surface structure and element distribution on the sample surface.

2.5 SPECTRAL MEASUREMENTS

Raman spectroscopy, and Fourier transform infrared (FTIR) techniques found many applications in the field of geology, archaeology and cultural heritage analysis due to its non-invasiveness. In these spectroscopic methods, samples are exposed to IR radiation and a fraction of the IR radiation is absorbed at wavelengths that are specific to the molecular excitation states of covalently bonded atoms. Each molecule has its own specific absorption spectrum, and the IR spectra are represented as a plot of transmittance across the IR band.

Spectral instruments for qualification the individual components of rock samples applied were 1) laboratory implemented attenuated total reflectance – Fourier transform infrared spectral device (ATR-FTIR), 2) handheld FT-IR with Diffuse Reflectance probe, and 3) Raman spectrometer.

Majority of the FT-IR measurements were acquired using the handheld device, Agilent 4300, in Figure 8. The sample interface used for FT-IR was Diffuse Reflectance probe due to the samples low light reflectance. The Perkin Elmer 2000 FT-IR with microscope were applied in quarry rock surface imaging and in gaining reference spectra.

Mineral identification was performed with Raman imaging microscope (Thermo Scientific, DXR3xi with OMNICxi software, Figure 9) for selected wiborgite and pyterlite samples.

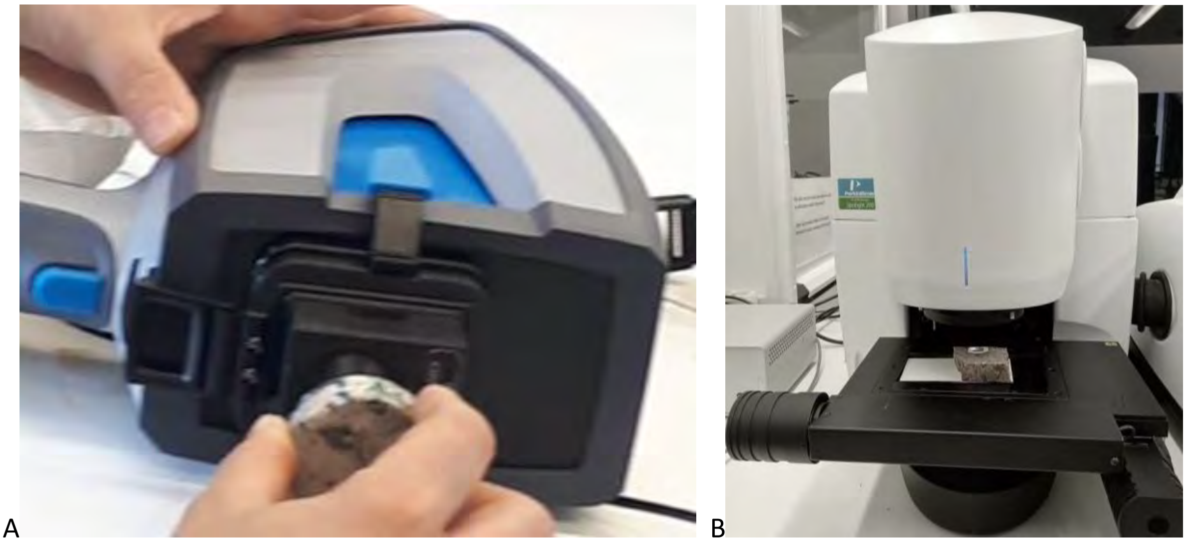

Figure 8. A) Agilent 4300 Handheld FTIR spectrometer applied in most FTIR measurements. B) FT-IR spectrometer Perkin-Elmer 2000 equipped with a germanium on a KBr beam splitter and liquid nitrogen cooled MCT detector. The spectrometer was attached to a microscope with a camera and a stage that is moveable in x, y and z directions enabling measuring rock surfaces.

Figure 9 Mineral identification was performed with Raman imaging microscope (Thermo Scientific, DXR3xi with OMNICxi software).

3. CHANGE IN VISUAL APPEARANCE

During chemical concentrations and visual appearance analysis, the aim was to visually examine the change of sample surface mineral and chemical composition. This was done visually by comparing the change of colour distributions on the surface before and during the treatments done to the samples,

Visual changes in surface are visualized in colour corrected figures. Main procedure contains 2 steps and figures contain photo of 1) original surface, 2) chemically treated surface, and 3) thermally treated surface. From the photos the change in colours, areas covered with them, and tones are described mathematically to support human vision.

The colour tones were divided into 4 classes: 1) light, 2) dark, 3) reddish/brownish, and 4) other. Table 5 illustrates the colour distribution in original samples before treatment. Wiborgite and pyterlite samples are dominated with dark and brownish or reddish patterns. Pyterlite seems to have more heterogeneity in the pattern since even 9 % surface is clustered outside of the main colour classes. Surfaces of dark rapakivi granite and dark green wiborgite have black/dark minerals dominating. However, dark green wiborgite has also high coverage of light colours (34 %). *Figure* 10 - *Figure* 20 show the original and treated surfaces.

Feldspars belong most likely to the Brown-Red class, but in general in this 4 colours classification method the colour cannot be applied as identifier of minerals. Dark and Light regions contain several minerals, and for example thin quartz layers on top of others might lead to confusion in classification.

Table 5 Colour distribution on surfaces of granite variates: mean value (%) and expanded uncertainty of the mean based on the 9 samples (N = 9).

		Brown/Red	**Dark**	**Light**	**Other**
Wiborgite	Mean, %	**31.3**	**45.5**	18.7	4.5
	+/- U(95)	3.9	2.0	2.7	0.6
Pyterlite	Mean, %	**43.8**	**39.3**	7.5	9.3
	+/- U(95)	5.7	4.8	1.1	0.6
Dark Rapakivi Granite	Mean, %	3.9	**91.1**	4.9	0.0
	+/- U(95)	1.7	2.2	1.2	0.0
Dark Green wiborgite	Mean, %	2.2	**60.7**	**34.2**	2.9
	+/- U(95)	0.6	2.2	1.5	0.6

Table 6 - Table 9 show changes in color colors after treatment steps. It was a clear conclusion that portion of the dark colored minerals decreased in thermal and acidic treatments. At the same time portion of reddish-brownish surface are increased together with visually light regions. However, effect of acidic treatment seemed mainly effect on dark/light region rate. Dark regions were covered with

light or opaque layers. The effect of chloride and sulphate compounds on the granite varieties vary. More detailed discussion can be found from table captions.

Table 6 Change in colour percentage ((after treatment) – (before treatment)) at sample surface. ***Thermal treatment in 400ºC or 600ºC*** *increased the reddish surface area and decreased dark areas. In visual observation, it was found that dark minerals were often covered with a light (plagioclase) layer. In colourimetric analysis it was classified partially as reddish, light, or other, however. Visual observation of samples before and after treatment are in the latter chapters.*

Sample ID	Brown-Red Area Change	Dark Area Change	Light Area Change	Other Area Change	Brightness Change
	[%]	[%]	[%]	[%]	
W_08 Thermal, 400	19.3	-6.4	-7.9	-2.0	145
P_16 Thermal, 400	6.0	-13.3	1.7	5.6	139
D_03 Thermal, 400	36.2	-11.2	-1.7	0.2	28
W_14 Thermal, 600	11.3	-12.1	-6.3	5.2	151
P_14 Thermal, 600	18.5	-25.2	3.3	3.4	162
D_09 Thermal, 600	8.0	-36.3	7.0	20.8	56
DG_09 Thermal, 600	31.9	-35.5	24.4	5.3	102

Table 7 Change in colour percentage ((after treatment) – (original untreated surface)) at sample surface. ***Step 1 Acidic (with H2SO4 or H3PO4) treatment was followed by a thermal step in 400ºC***. *Step 1 decreased the dark colour and increased light areas. This phenomenon continued in the thermal treatment (2nd step), but in addition a clear increase in reddish area was detected in colourimetric analysis. the Visual observation of samples before and after treatment are in the latter chapters.*

Sample ID	Brown-Red Area Change	Dark Area Change	Light Area Change	Other Area Change	Brightness Change
	[%]	[%]	[%]	[%]	
Step 1 with sulphuric acid - original					
W_06 SA (H_2SO_4)	10.0	-3.4	-2.9	-2.5	132
P_08 SA (H_2SO_4)	4.7	-9.2	3.4	1.2	143
D_01 SA (H_2SO_4)	-1.6	-12.2	14.1	0.0	44
DG_01 SA (H_2SO_4)	-1.1	-23.2	25.0	-1.6	6
Step 2 in 400ºC - original					
W_06 SA (H_2SO_4)	31.6	-13.3	-7.8	-5.3	141
P_08 SA (H_2SO_4)	17.5	-32.5	10.9	4.1	139
D_01 SA (H_2SO_4)	5.7	-44.8	44.6	0.1	80
DG_01 SA (H_2SO_4)	1.8	-36.4	36.9	-0.4	6
Step 1 with phosphoric acid - original					
W_13 H_3PO_4	6.0	-4.2	-0.3	-1.3	137
P_13 H_3PO_4	6.7	-12.9	3.3	2.8	158
D_08 H_3PO_4	-5.9	-7.9	9.1	0.0	44
DG_08 H_3PO_4	-3.1	-19.9	24.1	-3.6	6
Step 2 in 400ºC - original					
W_13 H_3PO_4	25.8	-13.3	-10.6	-1.8	136
P_13 H_3PO_4	14.0	-23.7	1.7	8.0	139
D_08 H_3PO_4	16.0	-24.3	22.5	0.2	49
DG_08 H_3PO_4	4.5	-29.3	26.0	2.9	6

Table 8 Change in colour percentage at sample surface ((after treatment, %) – (original untreated surface, %)). ***Step 1 chemical treatment was followed by thermal step in 400ºC****. Iron and calcium chlorides increased the reddish area of Wiborgite and Pyterlite. Thermal treatment increased the phenomenon: reddish colour area increased, and dark areas decreased. Iron treatment of Dark rapakivi granite and Dark Green wiborgite increased the light minerals and decreased dark regions. Sulphuric Acid (SA) did not show clear benefits when combined to iron chloride. Calcium chloride had only minor effects. Thermal treatment had very clear effect on appearances of all samples. Visualization is in the latter chapters.*

Sample ID	**Red Area Change**	**Dark Area Change**	**Light Area Change**	**Other Area Change**	**Brightness Change**
Step 1 chemical treatment - original					
W_10 $CaCl_2$	5.8	-1.0	-0.3	-1.4	6
W_11 $FeCl_2$	18.6	-3.7	-10.7	-2.5	6
W_07 SA+$FeCl_2$	7.0	-4.8	-3.8	0.5	143
P_10 $CaCl_2$	**3.8**	**-2.6**	**0.4**	**-1.6**	**151**
P_11 $FeCl_2$	**9.7**	**-13.0**	**1.1**	**2.3**	**34**
P_15 SA+$FeCl_2$	**7.7**	**-14.5**	**2.2**	**4.5**	**142**
D_05 $CaCl_2$	-1.7	1.4	-1.6	0.0	12
D_06 $FeCl_2$	4.2	-12.0	12.8	0.0	45
D_02 SA+$FeCl_2$	-1.0	-26.9	28.6	0.0	44
DG_05 $CaCl_2$	**-1.1**	**1.2**	**-0.8**	**-0.3**	**12**
DG_06 $FeCl_2$	**-2.1**	**-23.6**	**27.1**	**-3.2**	**6**
DG_02 SA+$FeCl_2$	**-0.7**	**-24.5**	**25.8**	**-1.1**	**6**
Step 2 in 400ºC - original					
W_10 $CaCl_2$	12.9	-9.9	0.4	-0.7	99
W_11 $FeCl_2$	38.7	-14.5	-18.6	-4.5	6
W_07 SA+$FeCl_2$	35.0	-12.3	-15.0	-4.6	133
P_10 $CaCl_2$	**5.0**	**-8.9**	**1.3**	**2.6**	**132**
P_11 $FeCl_2$	**31.1**	**-40.7**	**-4.9**	**14.4**	**147**
P_15 SA+$FeCl_2$	**30.7**	**-37.8**	**-4.7**	**11.7**	**138**
D_05 $CaCl_2$	23.3	1.4	-2.9	0.0	30
D_06 $FeCl_2$	61.5	-38.6	-4.9	0.2	62
D_02 SA+$FeCl_2$	52.2	-38.4	11.0	0.1	70
DG_05 $CaCl_2$	**20.3**	**-15.7**	**-0.8**	**8.7**	**6**
DG_06 $FeCl_2$	**82.2**	**-48.3**	**20.0**	**-0.3**	**114**
DG_02 SA+$FeCl_2$	**65.7**	**-50.1**	**33.9**	**5.3**	**6**

Table 9 Change in colour percentage at sample surface ((after treatment, %) – (original untreated surface, %)). ***Step 1 chemical treatment was followed by thermal step in 400ºC****. Sodium sulphate had less effect on colour distribution than Sulphuric Acid (SA, Table 7). When SA was combined into Sodium Sulphate solution, it slightly increased the phenomena. In Wiborgite and Pyrite samples the sulphates increased reddish colours and decreased dark regions. For dark rapakivi granite varieties the changes are in appearance of dark (-) and light (+) regions mainly. Thermal treatment had again very clear effect on appearances of all samples repeated in all experiments. Visualization is in the latter chapters.*

Sample ID	**Red Area Change**	**Dark Area Change**	**Light Area Change**	**Other Area Change**	**Brightness Change**
Step 1 chemical treatment					
W_12 Na_2SO_4	3.3	-1.7	-1.7	-0.2	136
W_09 SA+Na_2SO_4	6.3	-2.6	-2.0	-1.5	6
P_12 Na_2SO_4	**9.4**	**-11.3**	**2.8**	**-1.0**	**159**
P_09 SA+Na_2SO_4	**11.7**	**-9.8**	**-1.0**	**-0.9**	**147**
D_07 Na_2SO_4	0.9	-12.3	12.8	0.0	44
D_04 SA+Na_2SO_4	-1.4	-13.2	14.4	0.0	44
DG_07 Na_2SO_4	**-2.7**	**-18.4**	**21.1**	**-2.4**	**6**
DG_04 SA+Na_2SO_4	**-2.0**	**-24.7**	**29.1**	**-3.8**	**6**
Step 2 in 400ºC					
W_12 Na_2SO_4	18.6	-8.1	-8.9	-2.5	142
W_09 SA+Na_2SO_4	18.9	-12.5	-4.5	-0.9	144
P_12 Na_2SO_4	**14.2**	**,-24.97**	**6.3**	**4.5**	**133**
P_09 SA+Na_2SO_4	**14.5**	**-19.2**	**-1.6**	**6.3**	**139**
D_07 Na_2SO_4	12.7	-23.8	13.7	1.0	45
D_04 SA+Na_2SO_4	7.2	-28.7	23.8	0.8	54
DG_07 Na_2SO_4	**1.9**	**-30.6**	**30.5**	**-0.2**	**6**
DG_04 SA+Na_2SO_4	**4.6**	**-40.0**	**39.0**	**0.9**	**113**

3.1 Visual changes in wiborgite

Figure 10 illustrates changes in wiborgite samples after treatment with sulphuric acid, phosphoric acid and calcium chloride. After chemical treatment step, the samples were heated to 400 ºC, to complete procedure.

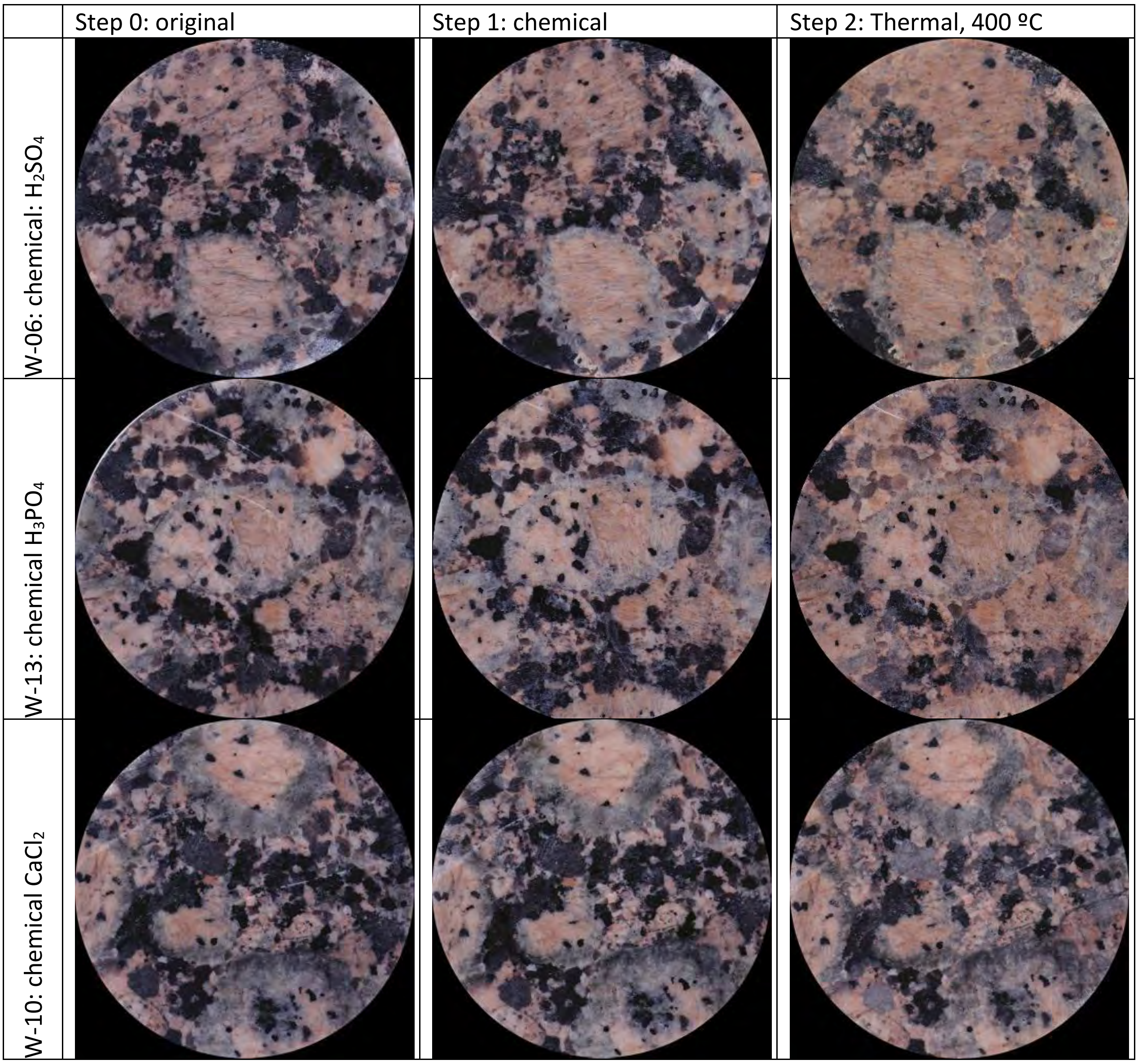

Figure 10 Wiborgite sample surfaces; 1): original surface 2) after 1st treatment with sulphuric acid (H_2SO_4), phosphoric acid (H_3PO_4) or calcium chloride ($CaCl_2$), and 3) after 2nd treatment step in 400ºC (30 min thermal treatment). Visual changes are a few, mainly felsic minerals (light coloured minerals) have been faded. In thermal treatment the feldspar tone has slightly changed and dark minerals have been partially covered with silica compound layers.

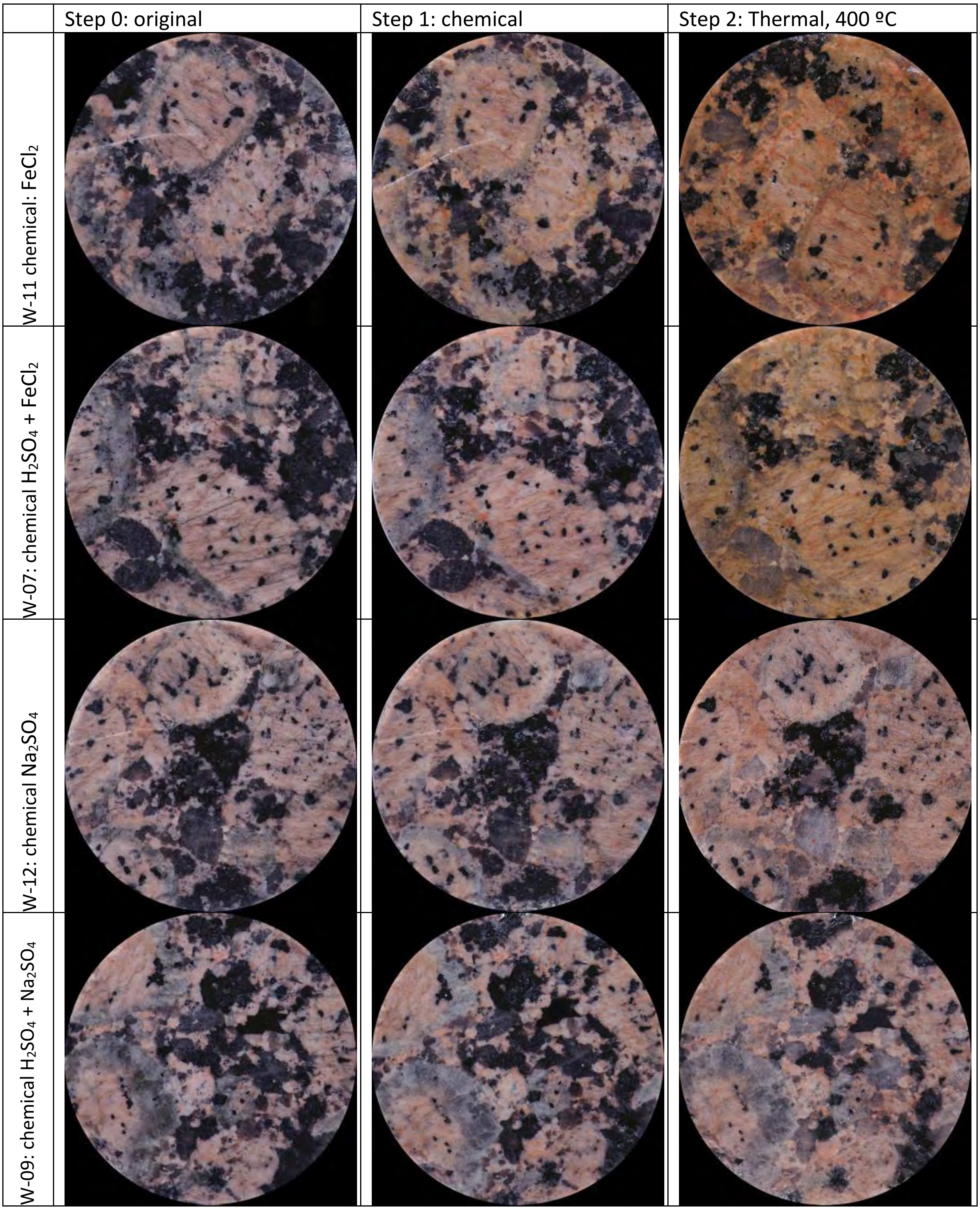

Figure 11 Wiborgite sample surfaces; 1): original surface 2) after 1st treatment with chemicals ($FeCl_2$, and Na_2AO_4), and 3) after 2nd treatment step in 400ºC (30 min thermal treatment) There are quite a few visual changes, mainly the felsic minerals (light minerals) are coloured by $FeCl_2$ in the chemical treatment. Light opaque layers have appeared on top of dark minerals and iron compounds have coloured the surfaces.

	Step 0: original	Step 2: Thermal
W-08: 400 ºC, 30 min	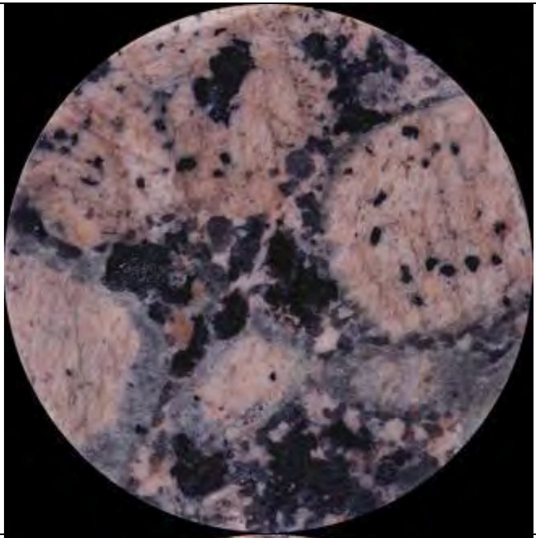	
W-14: 600ºC, 45 min	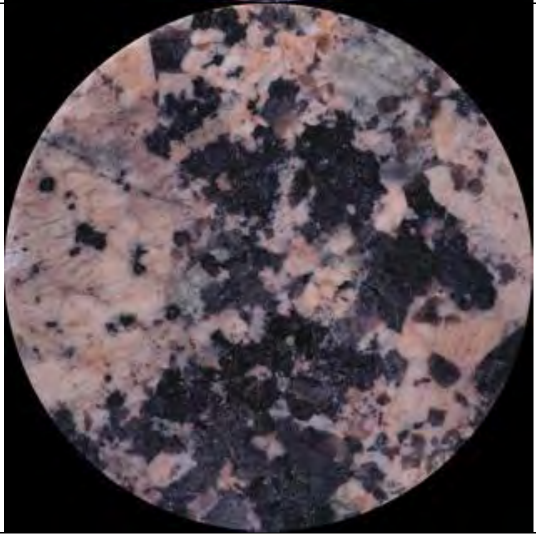	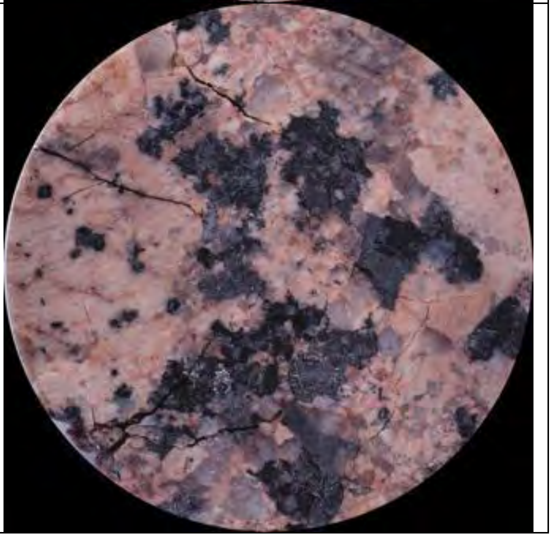

Figure 12 Wiborgite sample surfaces; 1): original surface 2) and after thermal treatment step in 400ºC or 600ºC. Thermal expansion has caused mechanical weathering as the microcracks have opened.

3.2 Visual changes in pyterlite

	Step 0: original	Step 1: chemical	Step 2: Thermal, 400 ºC
P-08: chemical: H_2SO_4		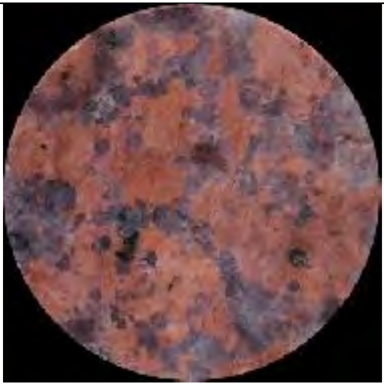	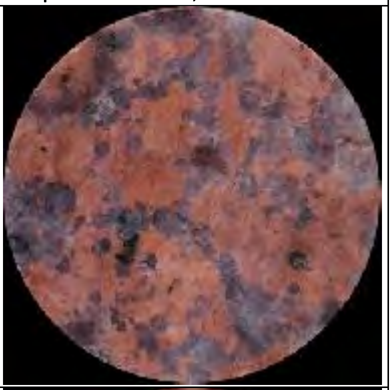
P-13: chemical H_3PO_4	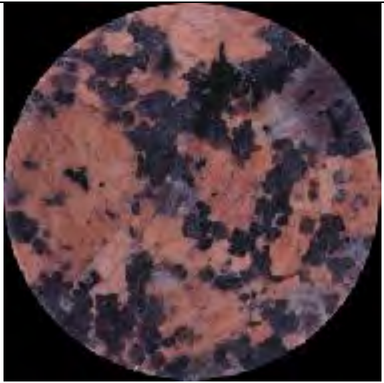		
P-10: chemical $CaCl_2$	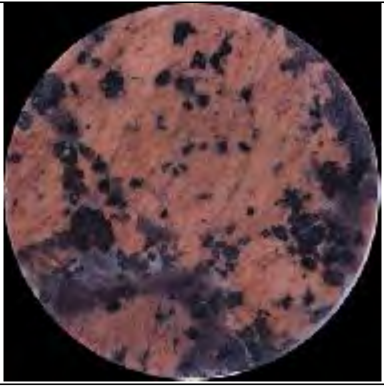	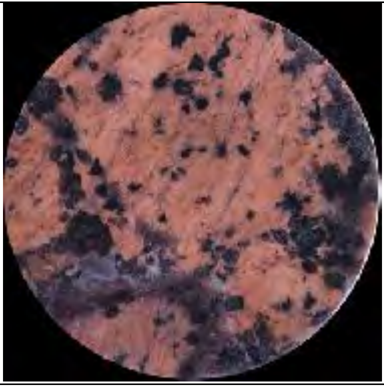	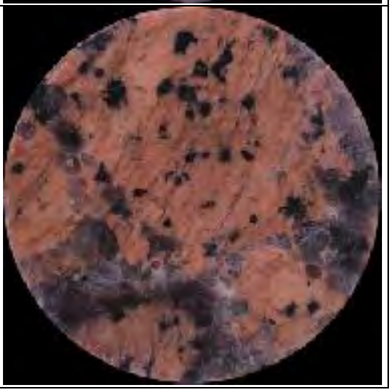

Figure 13 Pyterlite sample surfaces; 1): original surface 2) after 1st treatment with sulphuric acid (H_2SO_4), phosphoric acid (H_3PO_4) or calcium chloride ($CaCl_2$), and 3) after 2nd treatment step in 400ºC (30 min thermal treatment). The treatments have only caused slightly fading of the stone surface in the first two tests. Light opaque layers have appeared on top of dark regions.

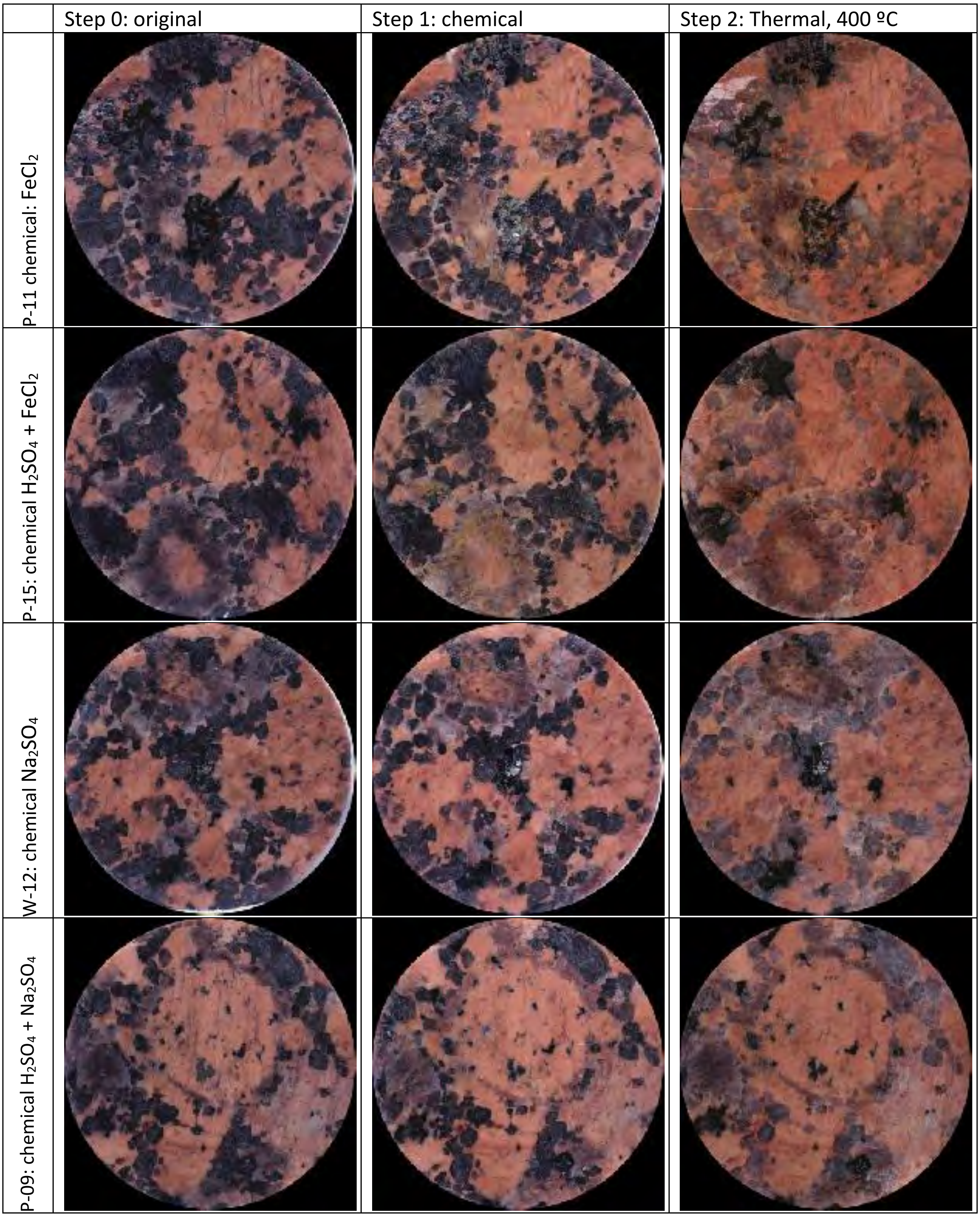

Figure 14 Pyterlite sample surfaces; 1): original surface 2) after 1st treatment with chemicals ($FeCl_2$, and Na_2SO_4), and 3) after 2nd treatment step in 400ºC (30 min thermal treatment). The felsic minerals (light minerals) are coloured by FeCl2 in the first two tests. Light opaque layers have appeared on top of dark regions.

	Step 0: original	Step 2: Thermal, 400 ºC
P-16: 400 ºC, 30 min	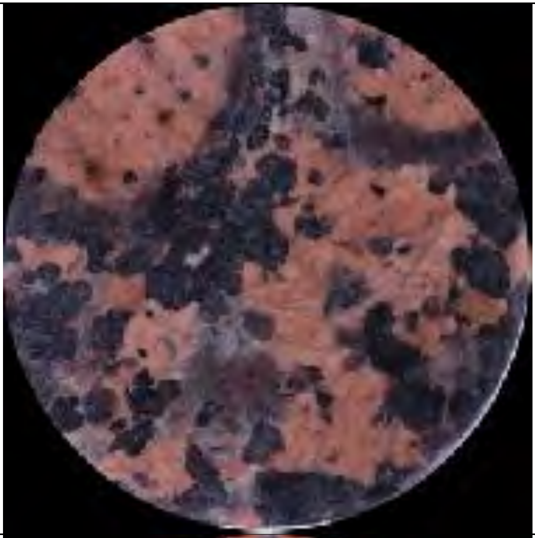	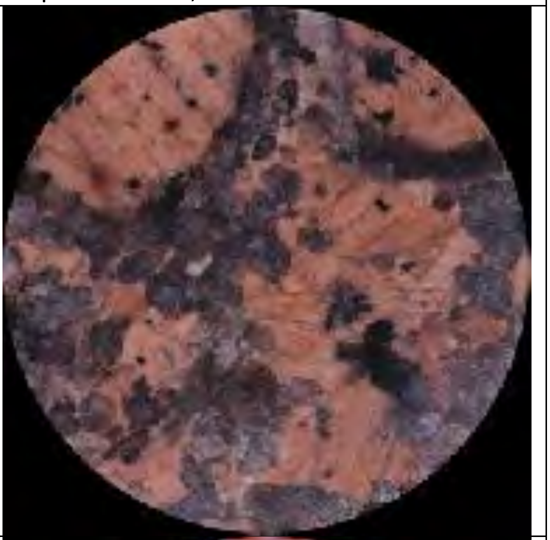
P-14: 600ºC, 45 min	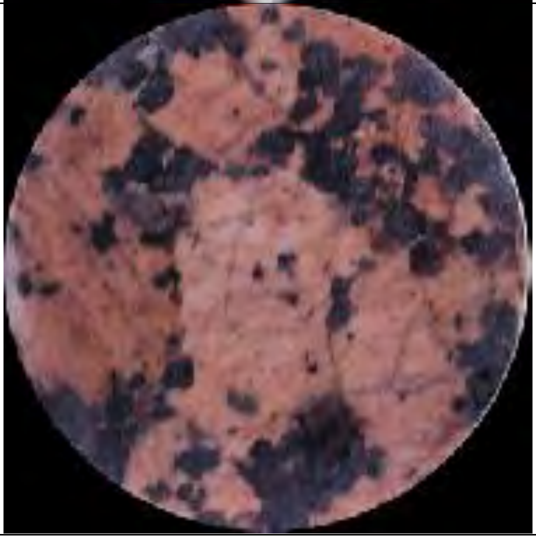	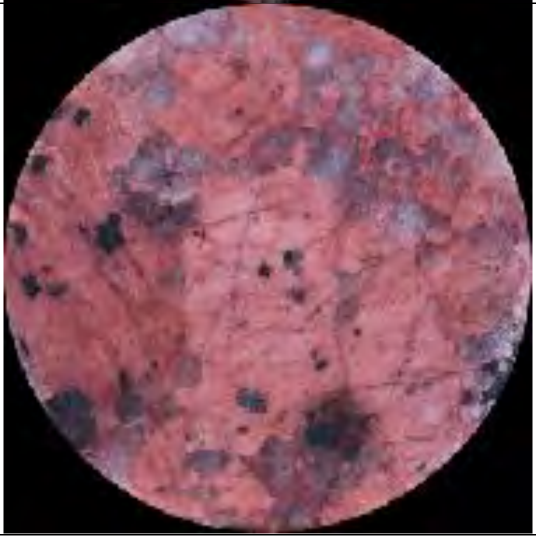

Figure 15 Pyterlite sample surfaces; 1): original surface 2) and after thermal treatment step in 400ºC or 600ºC. A clear change in pyterlite at 600ºC reflects an accelerated weathering of stone and this might demonstrate how pyterlite will weather in natural conditions.

3.3 Visual changes in dark rapakivi

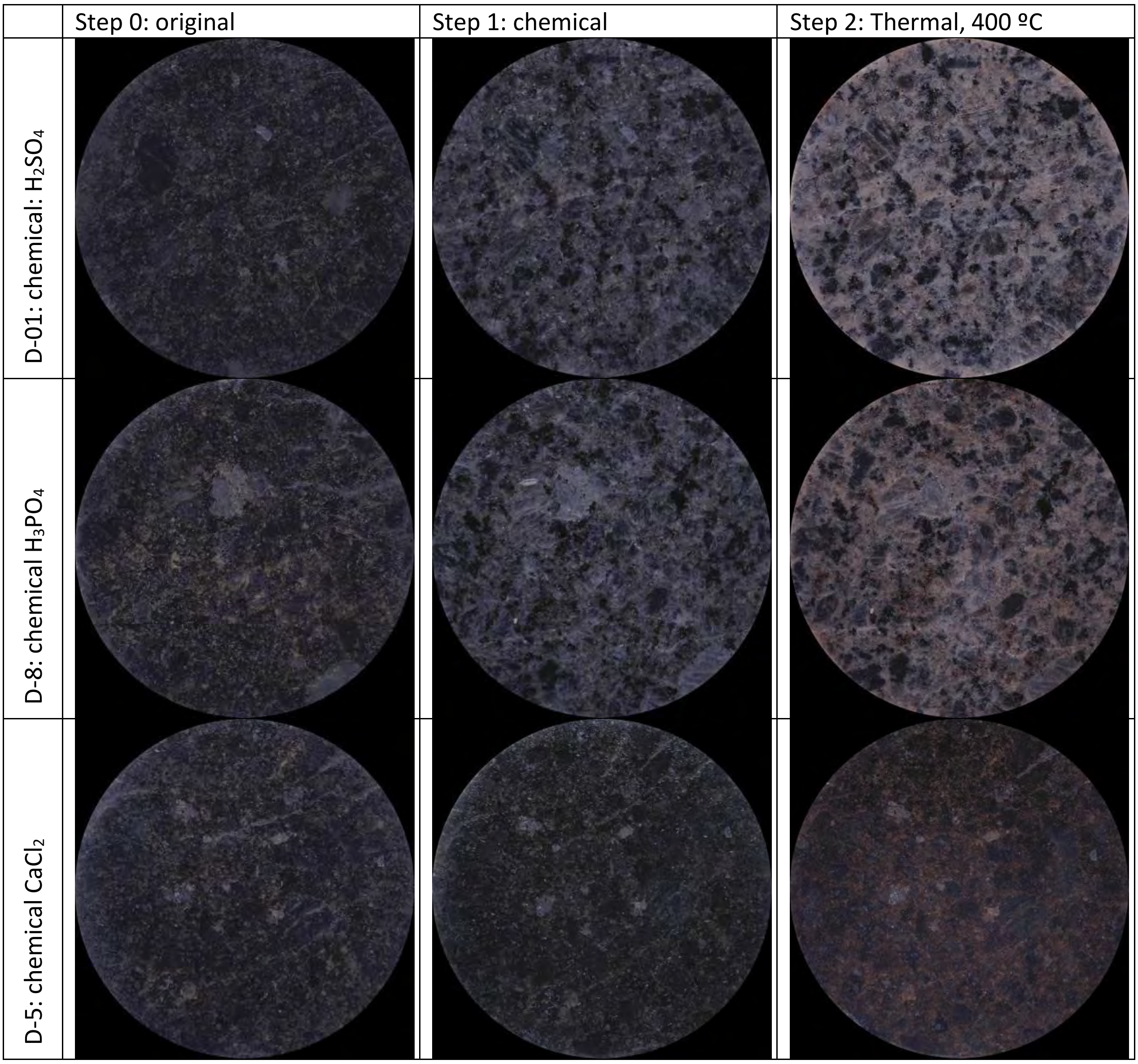

Figure 16 Dark rapakivi granite sample surfaces; 1): original surface 2) after 1st treatment with sulphuric acid (H_2SO_4), phosphoric acid (H_3PO_4) or calcium chloride ($CaCl_2$), and 3) after 2nd treatment step in 400ºC (30 min thermal treatment). The treatments have disclosed mafic (dark coloured) and felsic (light coloured) minerals on the stone surface in the first two tests.

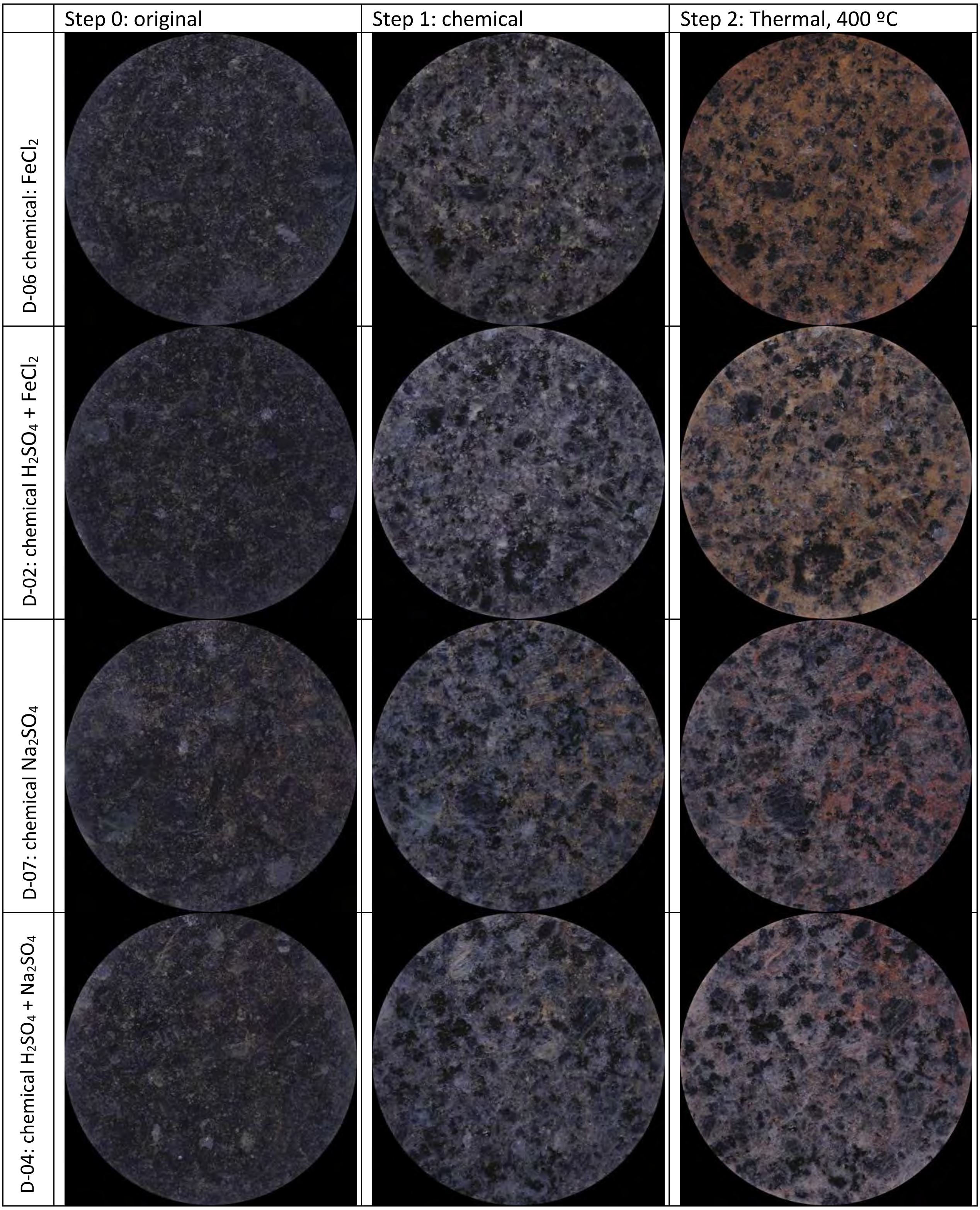

Figure 17 Dark rapakivi granite sample surfaces; 1): original surface 2) after 1st treatment with chemicals ($FeCl_2$, and Na_2AO_4), and 3) after 2nd treatment step in 400ºC (30 min thermal treatment. ***The treatments have disclosed mafic (dark coloured) and felsic (light coloured) minerals on the stone surface and felsic minerals are coloured by FeCl2 in the first two tests.***

	Step 0: original	Step 2: Thermal, 400 ºC
D-03: 400 ºC, 30 min	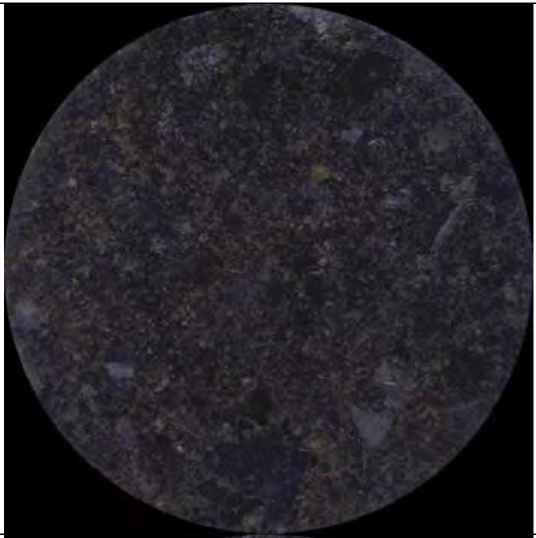	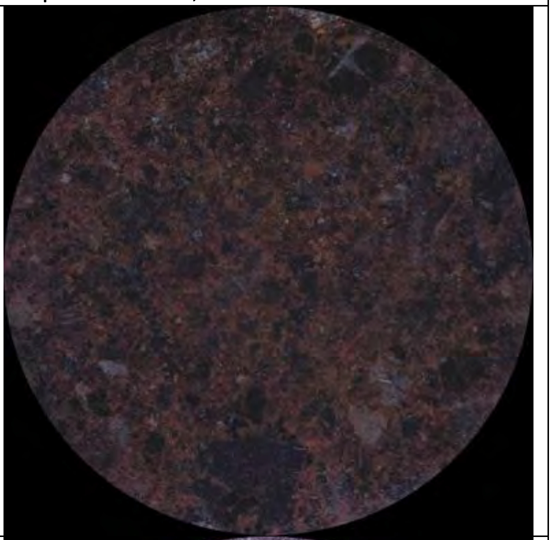
D09: 600ºC, 45 min	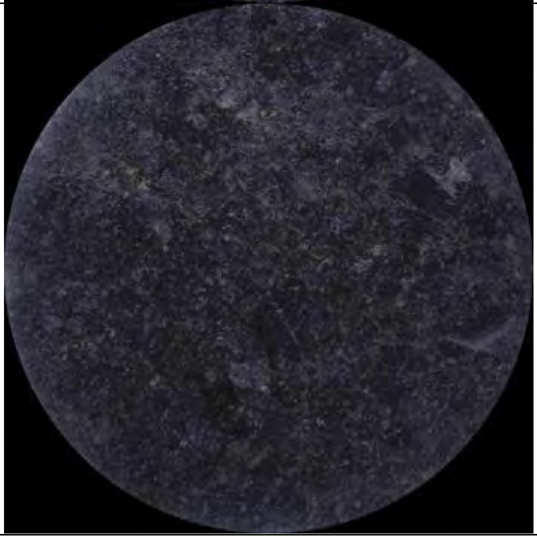	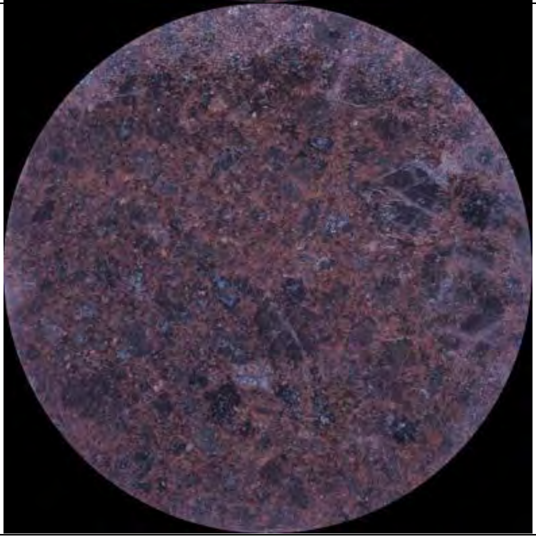

Figure 18 Dark rapakivi granite sample surfaces; 1): original surface 2) and after thermal treatment step in 400ºC or 600ºC. Changes at 600ºC demonstrate the features on surface of stone that might be seen in the surface on naturally weathered dark rapakivi granite.

3.4 Visual changes in dark green wiborgite

	Step 0: original	Step 1: chemical	Step 2: Thermal, 400 ºC
DG-01: chemical: H_2SO_4		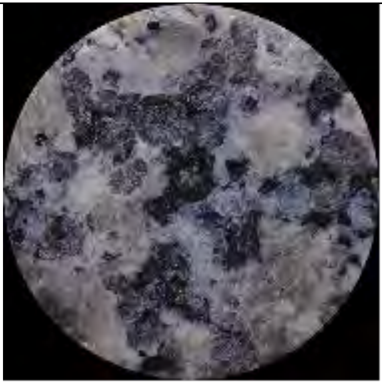	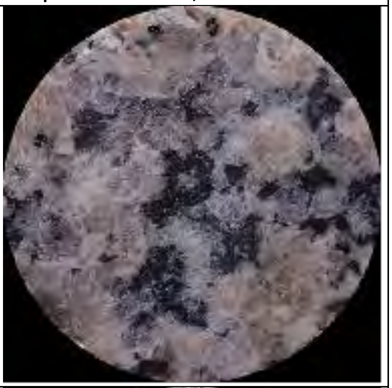
DG-08: chemical H_3PO_4	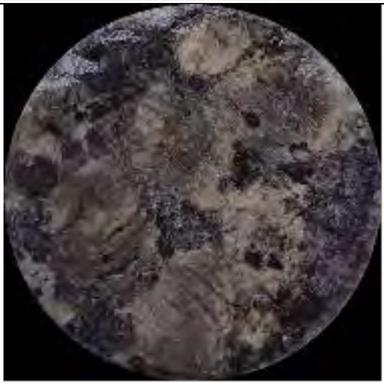	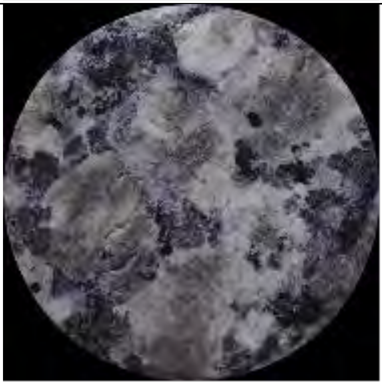	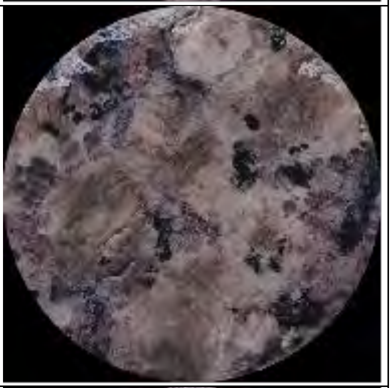
DG-05: chemical $CaCl_2$			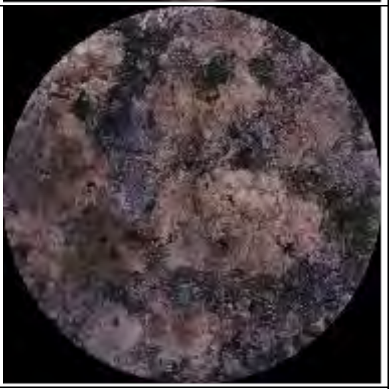
DG-09: thermal 600ºC	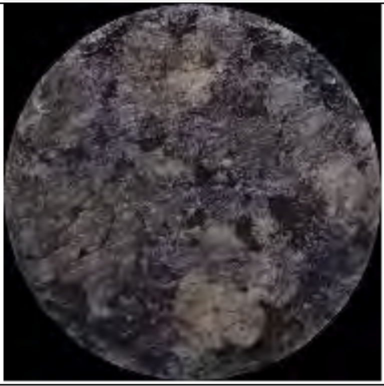		

Figure 19 Dark green wiborgite sample surfaces; 1): original surface 2) after 1st treatment with sulphuric acid (H_2SO_4), phosphoric acid (H_3PO_4) or calcium chloride ($CaCl_2$), and 3) after 2nd treatment step in 600ºC (30 min thermal treatment). The treatments have disclosed mafic (dark coloured) and felsic (light coloured) minerals on the stone surface. Changes at 600ºC demonstrate the features on surface of stone that might be seen in the surface on naturally weathered dark green wiborgite.

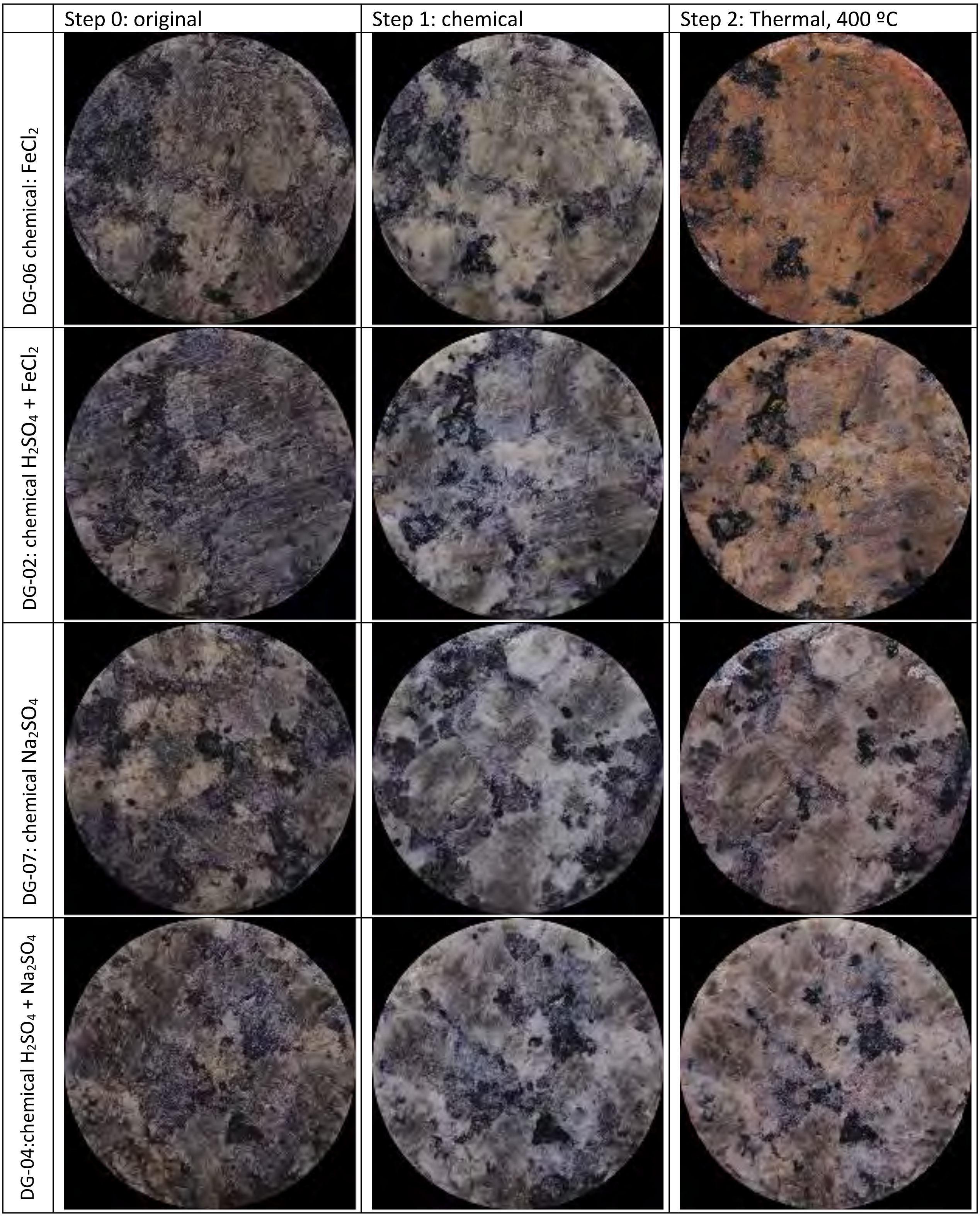

Figure 20 Dark green wiborgite sample surfaces; 1): original surface 2) after 1st treatment with chemicals ($FeCl_2$, and Na_2AO_4), and 3) after 2nd treatment step in 400ºC (30 min thermal treatment. ***The felsic minerals (light minerals) are coloured by FeCl2 in the first two tests and the treatments have disclosed mafic (dark coloured) and felsic (light coloured) minerals on the stone surface in the last two tests.***

3.2. SEM/EDS

The samples were analysed with SEM three times; as originals, after treatment 1 and after treatment 2. The SEM images of the samples in the different stages of treatment are presented in *Appendix SEM images of original and treated samples: Table* 19-Table 22. In the column 'Original' are pictured the original samples, in column 'Treatment 1' the samples after treatment 1 and in column 'Treatment 2' the samples after treatment 2. Some of the samples were only treated once, and therefore are not pictured in column 'Treatment 2'. SEM images were taken from only few of the original samples, and therefore pictures of some original samples are not available.

Below is an example of a granite surface before and phosphoric acid treatment. The aim of these studies is to see how the surface is affected by the different treatments (SEM part), also with the EDS images the distribution of elements along the surface of the samples can be assessed. When the analysis is done before and after the treatment, we can try to see if there is a difference in the elemental composition of the surface.

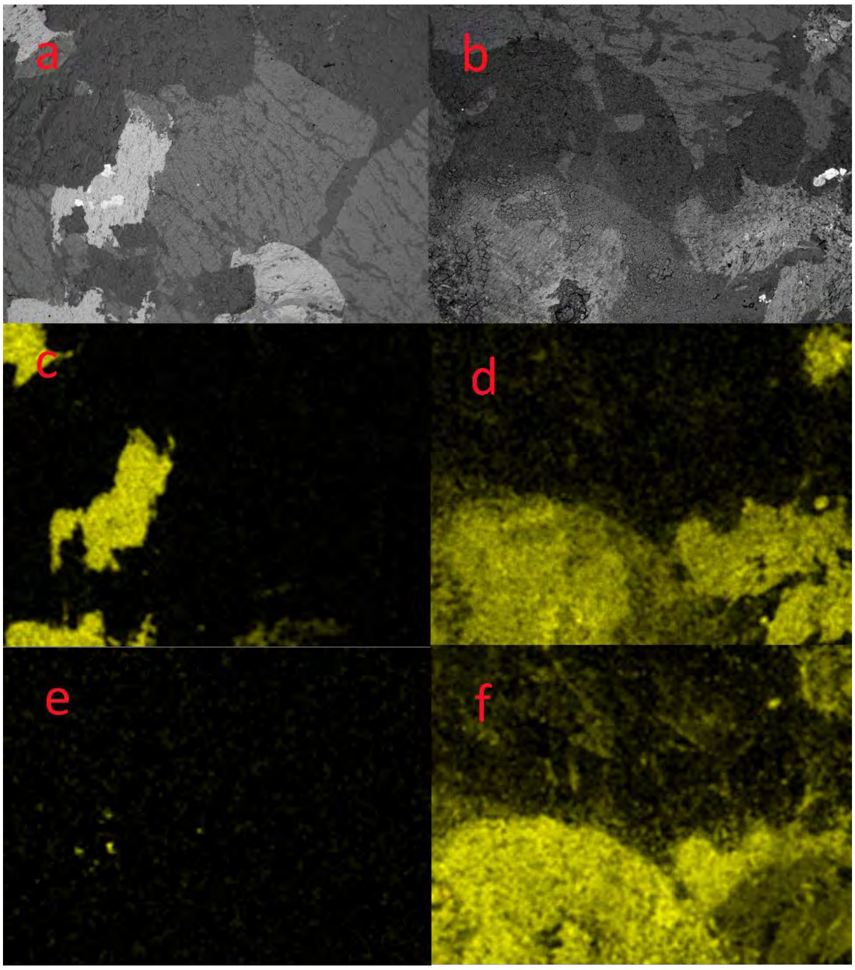

Figure 21 Two Pyterlite sample surfaces, left untreated sample surface and right phosphoric acid treated surface. SEM images (a,b), EDS mappings of iron (c,d) and of phosphorus (e,f).

In Figure 21, there is first a SEM images of the sample surface (a, b), followed by EDS mappings of Fe and P on these surfaces. In the left column is a surface of an untreated sample and on the right a surface after phosphoric acid treatment. In the SEM images the surfaces before and after are quite like each other, except that in the lower part of the after image (b), there is a flaky deposit on the surface. The EDS maps reveal that this residue is some form of iron phosphate. Based on this the phosphoric acid can react in with the iron in the stone (e.g., biotite parts), thus altering the surface. It should be noted that even though the residue seems flaky, the surfaces were washed before analysis, so the deposit is attached to the surface.

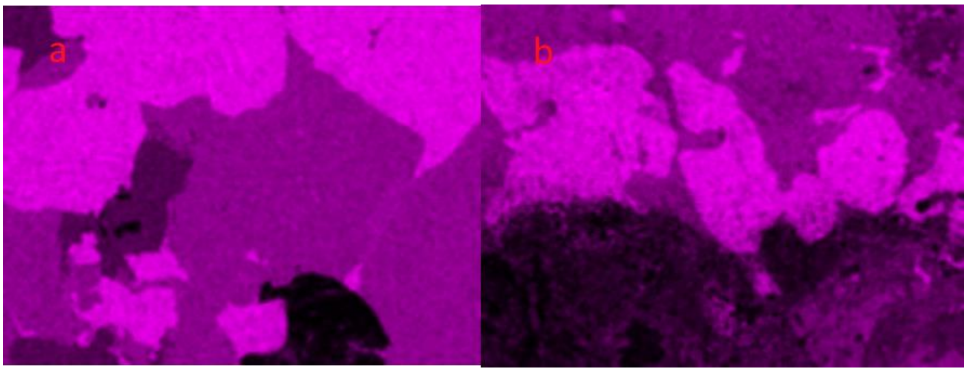

Figure 22 EDS mappings of Al on two Pyterlite sample surfaces, left untreated sample surface and right phosphoric acid treated surface.

In Figure 22, the EDS maps representing Al on the sample surfaces are given. Here we can see how the distribution of Al is similar before and after the treatment. In the treated sample, the deposition can be seen as the dark batches on the lower part of the image. Otherwise, the parts of the surface with strong Al signal are not so affected by the phosphoric acid treatment. Similarly other sets of samples and treatments can be studied from the SEM and EDS images given in the appendices.

4. Element concentration on surface (XRF analysis)

The meaning of XRF analysis is to examine the chemical composition of the sample surface before and during the different treatments used. Generally, treatment 1 means the chemical treatment and treatment 2 means the thermal treatment after chemical treatment. Element LE in the tables stands for light elements, which includes elements those atomic number is less than 12 Mg (such as Li, Be, C, F, and Na).

The sample surfaces were measured before and after each treatment with the handheld XRF instrument. Fist sample of each series was typically measured 10 times, and flowing samples 5 times randomly. There is no spatial information available from the measurements. The mean values for original (untreated) surfaces with their 95 % confidence limits are presented in Table 10 and visualized in Figure 23 - Figure 24. Total 35 elemental concentrations and sum of light elements (LE) were determined. However, several of the 35 elemental concentrations are highly uncertain due to low number of measurements exceeding the detection limit. Detection limits are experimentally detected and vary for each element and sample. For example, Mg average value for Dark Green wiborgite was 18092 mg/kg +/- 17602 mg/kg, which hardly differs from zero. Furthermore, only 8 measurements out of 50 exceeded the sample wise detection limits. Measurements results are presented in APPENDIX XRF results with standard deviations.

Univariate statistical approaches were applied to define changes during the treatments. Normality assumption of results might not be valid, but t test still can be applied to give an overview.

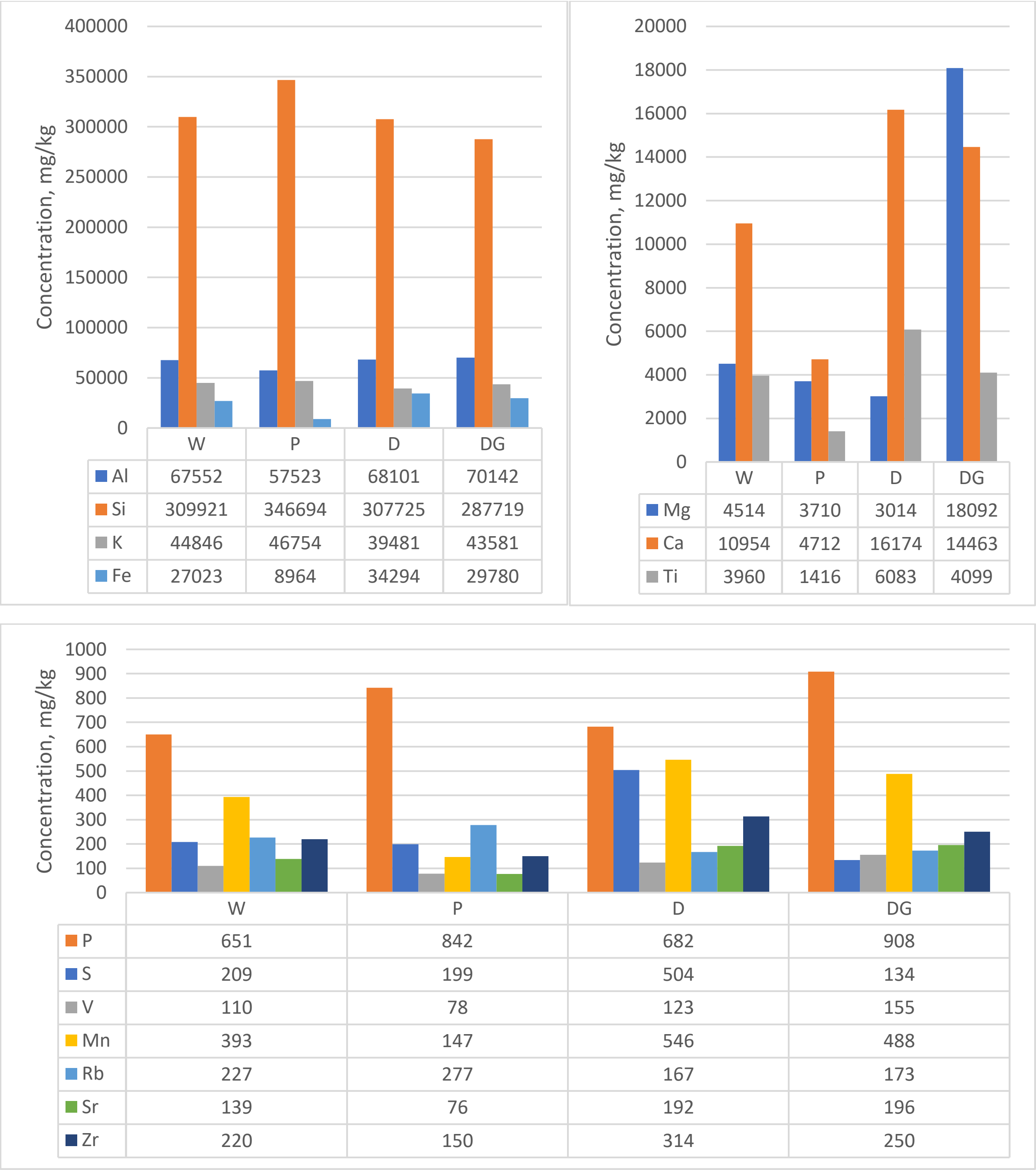

	W	P	D	DG
■ Al	67552	57523	68101	70142
■ Si	309921	346694	307725	287719
■ K	44846	46754	39481	43581
■ Fe	27023	8964	34294	29780

	W	P	D	DG
■ Mg	4514	3710	3014	18092
■ Ca	10954	4712	16174	14463
■ Ti	3960	1416	6083	4099

	W	P	D	DG
■ P	651	842	682	908
■ S	209	199	504	134
■ V	110	78	123	155
■ Mn	393	147	546	488
■ Rb	227	277	167	173
■ Sr	139	76	192	196
■ Zr	220	150	314	250

Figure 23 Mean concentrations of major and minor elements in the original samples. Amount of LEs in these 4 granite varieties were on similar level exceeding 50 m-% of surface: 525 000 – 540 000 mg/kg (D had the lowest and DG the highest amount).

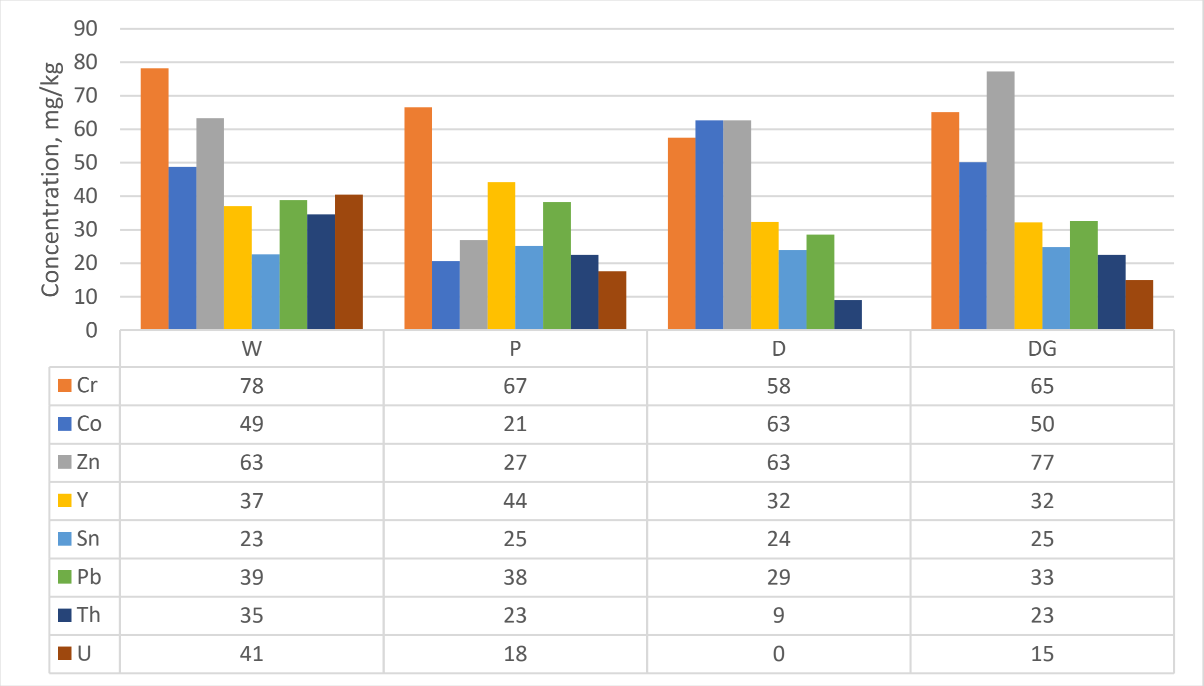

	W	P	D	DG
■ Cr	78	67	58	65
■ Co	49	21	63	50
■ Zn	63	27	63	77
■ Y	37	44	32	32
■ Sn	23	25	24	25
■ Pb	39	38	29	33
■ Th	35	23	9	23
■ U	41	18	0	15

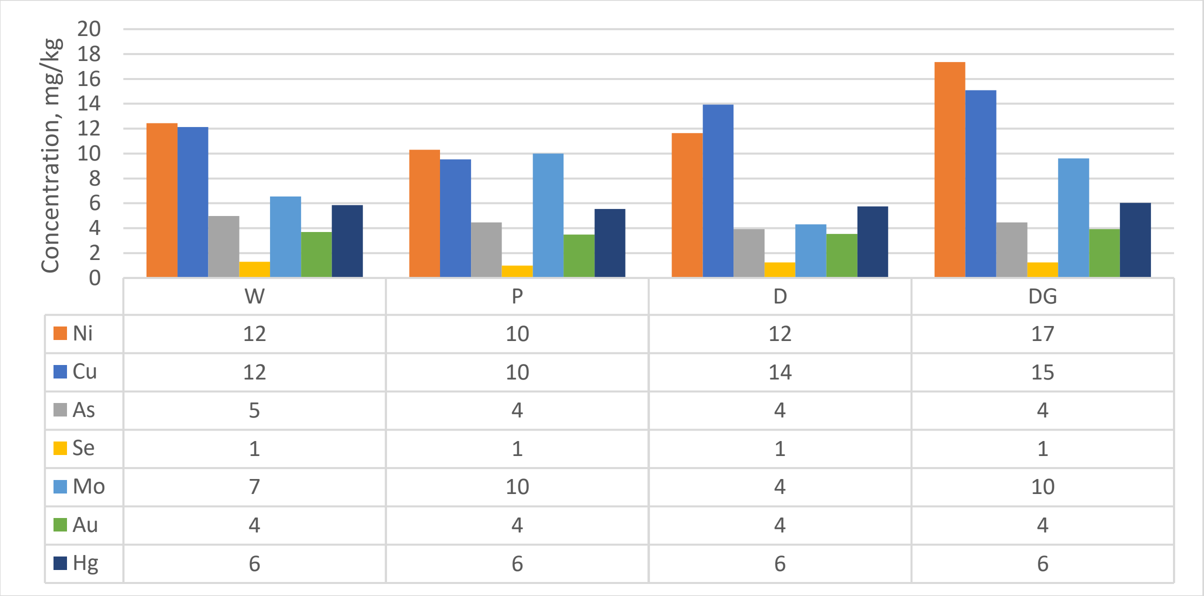

	W	P	D	DG
■ Ni	12	10	12	17
■ Cu	12	10	14	15
■ As	5	4	4	4
■ Se	1	1	1	1
■ Mo	7	10	4	10
■ Au	4	4	4	4
■ Hg	6	6	6	6

Figure 24 Mean concentrations of trace elements in the original samples. Ag, Cd, and Sb did not exceed the LOD in any sample and they were left out. The mean concentrations are computed only from samples exceeding the sample wise LOD. Therefore, the number of samples applied in computing the mean values vary. The mean values with expanded 95 % uncertainty is presented in Appendices.

Table 10 Mean concentrations of elements in original samples: W = Wiborgite, P = Pyterlite, D = Dark Rapakivi granite and DG = Dark Green wiborgite. Mean values are computed utilizing only the values exceeding LOD. N = number of samples. Element is marked with red colour if less than 50 % of the measurements have exceeded the LOD.. U95 = expanded standard uncertainty of the mean on 95 % confidence level. Total measurements: Ntot(W) = 99, Ntot(P, D, DG) = 50 with GEOCHEM program of the XRF instrument.

Element	**W**			**P**			**D**			**DG**		
	Mean	***U95***	***N***	***Mean***	***U95***	***n***	***Mean***	***U95***	***N***	***Mean***	***U95***	***N***
	mg/kg	**mg/kg**	**-**	**mg/kg**	**mg/kg**	**-**	**mg/kg**	**mg/kg**	**-**	**mg/kg**	**mg/kg**	**-**
Mg	4514	1049	13	3710	1223	3	3014	294	9	18092	17602	8
Al	67552	3596	99	57523	6216	50	68101	1386	50	70142	4709	50
Si	309921	4935	99	346694	11811	50	307725	2782	50	287719	8549	50
P	651	148	58	842	542	8	682	158	18	908	451	13
S	209	100	9	199	0	1	504	480	4	134	62	3
K	44846	3366	99	46754	5817	50	39481	1962	50	43581	6904	50
Ca	10954	1034	99	4712	1865	45	16174	1065	49	14463	2664	47
Ti	3960	599	99	1416	389	50	6083	572	50	4099	790	50
V	110	8	99	78	10	50	123	4	50	155	18	50
Cr	78	9	95	67	11	47	58	4	47	65	6	47
Mn	393	54	99	147	41	50	546	34	50	488	96	50
Fe	27023	4345	99	8964	3084	50	34294	2252	50	29780	6704	50
Co	49	16	12	21	3	10	63	9	8	50	17	9
Ni	12	1	89	10	2	45	12	1	46	17	4	45
Cu	12	1	98	10	2	41	14	3	43	15	3	42
Zn	63	11	99	27	8	50	63	4	50	77	17	50
As	5	0	77	4	0	42	4	0	42	4	0	42
Se	1	0	10	1	0	9	1	0	7	1	0	9
Rb	227	17	99	277	35	50	167	8	50	173	26	50
Sr	139	7	99	76	10	50	192	3	50	196	14	50
Y	37	8	98	44	16	50	32	4	50	32	10	50
Zr	220	47	99	150	64	50	314	25	50	250	81	50
Nb	16	3	67	18	9	19	9	2	26	16	6	24
Mo	7	1	32	10	8	3	4	1	6	10	4	6
Sn	23	2	17	25	3	6	24	1	7	25	2	8
W	15	2	10	12	2	8	13	1	6	14	2	7
Au	4	0	17	4	1	4	4	1	5	4	1	4
Hg	6	0	68	6	0	33	6	0	34	6	0	34
Pb	39	3	99	38	5	50	29	1	50	33	3	50
Bi	18	4	41	18	1	39	15	1	35	16	1	36
Th	35	37	13	23	5	8	9	0	9	23	12	9
U	41	69	2	18	9	9	n.d.	0	8	15	0	9
LE	533379	2690	99	533086	2826	50	525260	1350	50	540023	4374	50

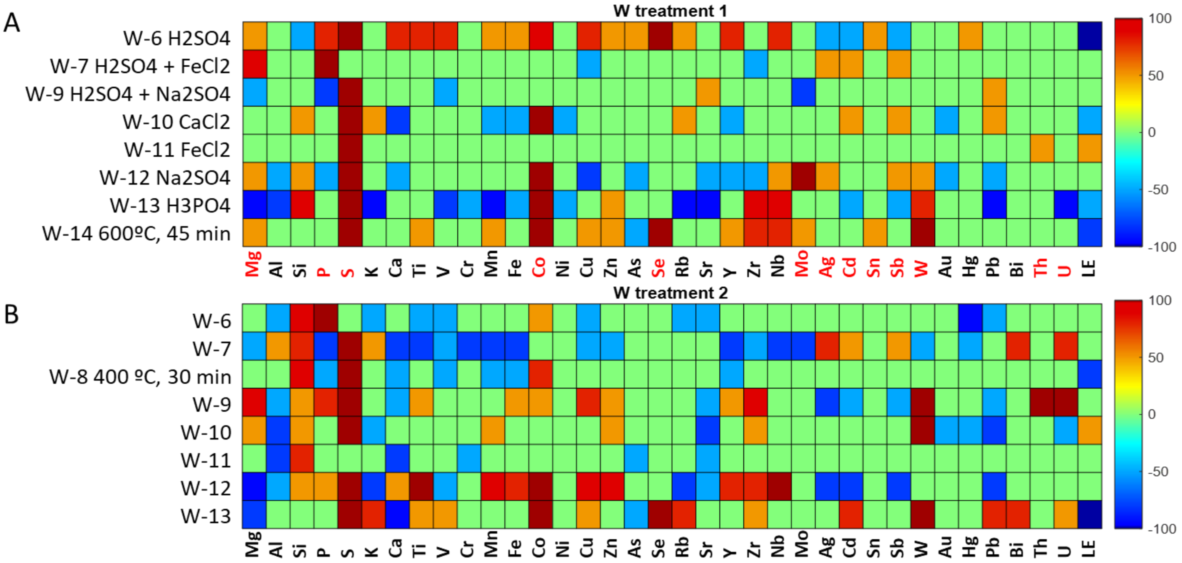

Figure 25 Wiborgite: Statistical significance of change in concentrations measured with the handheld XRF. Change is compared to the original sample. A) Treatment step 1 is typically chemical treatment. Exceptions are W-8 and W-14 in which the thermal treatment was the only step. B) Treatment step 2 was thermal treatment in 400 ºC. For comparison W-8 presented in subplot B.

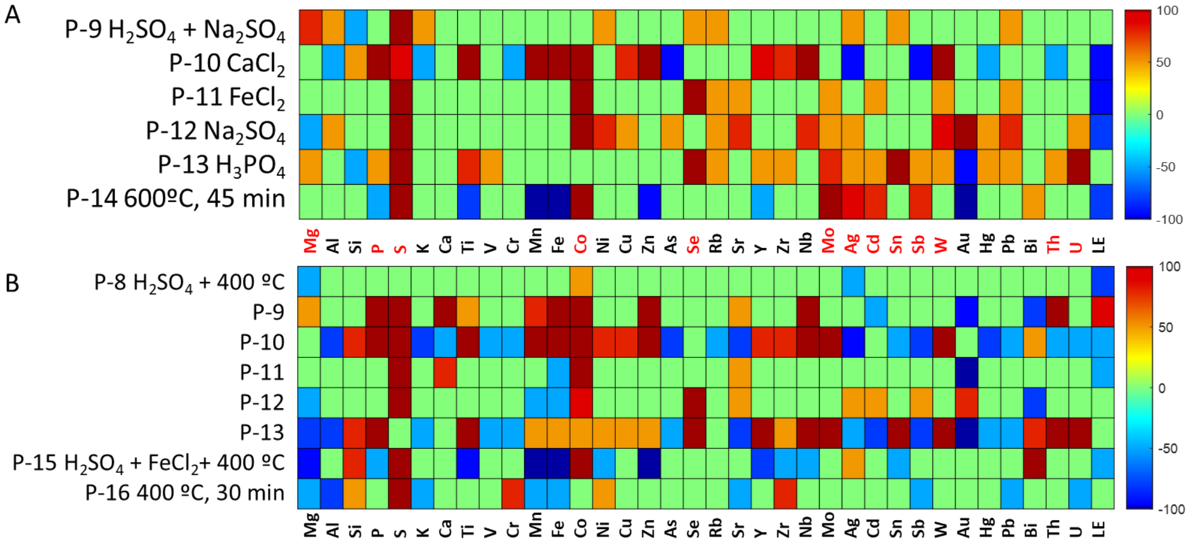

Figure 26 Pyterlite: Statistical significance of change in concentrations measured with the handheld XRF. Change is compared to the original sample. A) Treatment step 1 is typically chemical treatment. Exceptions are P-14 and P-16 in which the thermal treatment was the only step. B) Treatment step 2 was thermal treatment in 400 ºC. For comparison P-16 presented in subplot B. Samples P-8 and P-15 were not analysed after the first treatment step (due to human mistake).

General conclusion from XRF data is that more measurements on each individual sample should have been carried out. Each sample was measured 5-10 times. Results are uncertain, but conclusions such as sulphuric compounds (sulphides or even sulphates) are stable, and their relative amount (ppm) increased in most treatments of all granite varieties. Light elements (LE) tend to decrease. Wiborgite seems to be more sensitive to sulphate treatments and pyterlite to chloride treatments. The two acids (sulphuric and phosphoric acids) are both strong solvents and acids, but they differ as acids. Wiborgite is more sensitive to sulphuric acid (and other sulphuric compounds) while phosphoric acid affects the pyterlite surface composition more.

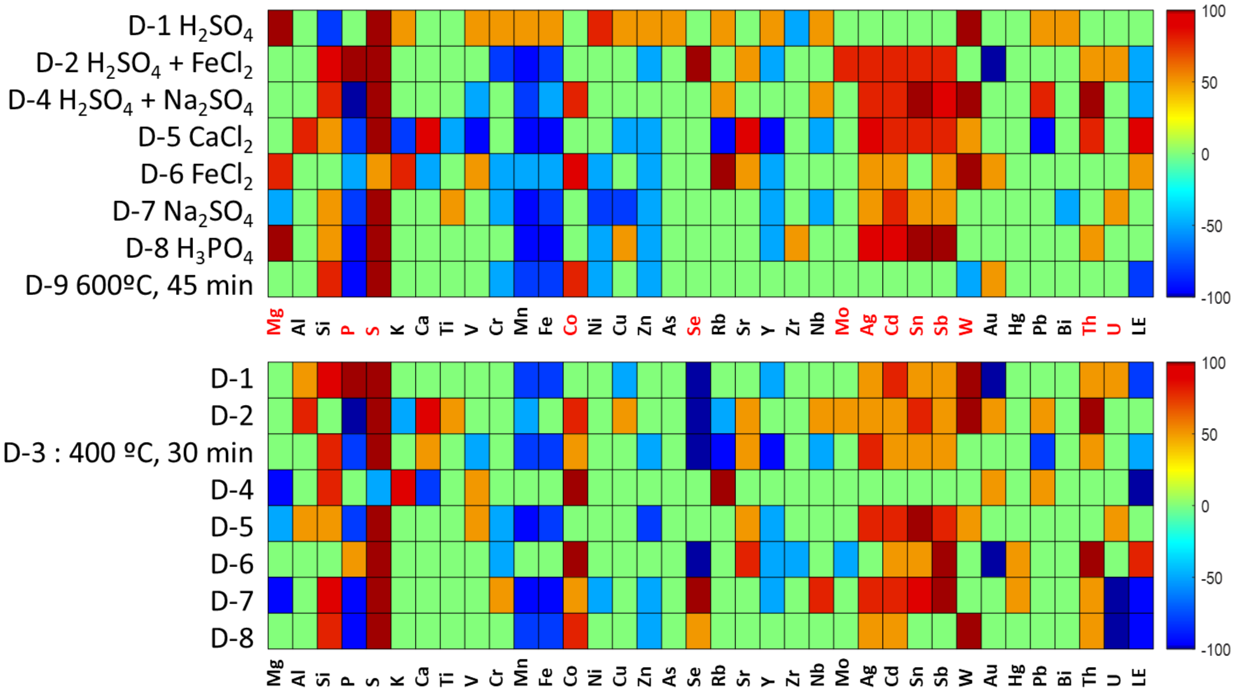

Figure 27 Dark rapakivi granite: Statistical significance of change in concentrations measured with the handheld XRF. Change is compared to the original sample. A) Treatment step 1 is typically a chemical treatment. Exceptions are D-3 and D9 in which the thermal treatment was the only step. B) Treatment step 2 was thermal treatment in 400 ºC. For comparison D-3 is presented in subplot B.

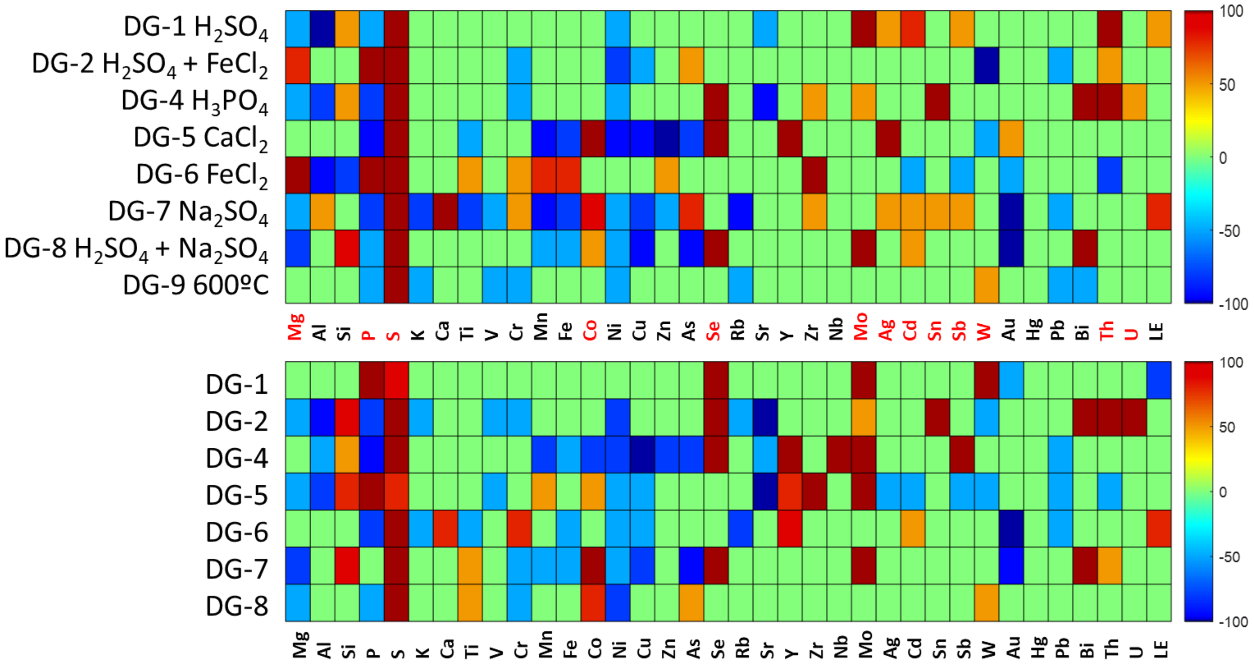

Figure 28 Dark green wiborgite: Statistical significance of change in concentrations measured with the handheld XRF. Change is compared to the original sample. A) Treatment step 1 is typically a chemical treatment. Exception is DG-9 in which the thermal treatment was the only step. B) Treatment step 2 was thermal treatment in 400 ºC.

Dark rapakivi granite and Dark Green wiborgite seem to be somewhere between Wiborgite and Pyterlite. Dark rapakivi is sensitive to sulphide and chloride treatments. Both acids also alter the chemical distribution. In thermal treatment, the trace elements ratio in surface increases, while light elements, iron, manganese, and phosphorus compounds decrease. Increase of silica compound is seen in all four granite varieties in thermal treatment, and in phosphoric acid treatments. The phenomena are statistically more significant in the two dark granite varieties. Dark rapakivi granite seems to behave in many treatments more similar to pyterlite than wiborgite. Also Dark green wiborgite has some features similar to pyterlite (e.g., in $CaCl_2$ treatment). However, their behaviour in both acid treatments is mixture of the phenomena seen in the wiborgite and pyterlite samples. Dark rapakivi granite seems to be the weakest material, when measured as changes and stability of chemical compounds on it's surface.

Na_2SO_4 treatment (with or without acid) has an interesting effect on surfaces. Occurrence of a set of trace elements (Mo, Ag, Cd, Sn, Sb, W) seems to increase on surface, which suggest that some minerals or compounds have dissolved due to sulphuric components.

5. Chemical balance in treatment solutions (ICP-MS)

After the stone samples were treated in chemical solutions, the solutions were analysed with ICP-MS. The results are presented as the concentration change in different elements in the specific solvents during the 72-hour leaching time when stone samples were treated. The elements either dissolved from the stone samples to the solvent or adsorbed to the stone surface from the solvent. The change in concentration was calculated by comparing the blank solutions results with the results of solutions after treatment. In the results, the area of the stone sample submerged into the treatment solution and the volume of the treatment solution have been taken into account which gives the results in mg/m^2 units.

The main ICP-MS results of each sample set are presented in separate tables Table 11, Table 12, Table 13 and Table 14. The tables are colour coded, and a green cell represents a result in which an element has dissolved from the stone sample to the solvent, and a red cell represents a result in which the element has been chemically bonded or adsorbed to the stone sample surface from the chemical solvent. In general, the limit of identification was from 10 ppb to 400 ppb with some exemptions. Some elements are left out from the results tables due to their small concentration change (less than 1 mg/m^2) or the results being under the limit of identification. All the results ICP-MS results are presented in Appendix: ICP-MS results.

During the ICP-MS analysis sodium went over the identification limit for almost all the samples in each series. Therefore, the results for sodium are only indicative. The high amount of sodium leached could be since the samples were kept in glass containers, and sodium could be leached from the glass walls of the containers as the glass consists of sodium.

For all the dark rapakivi granite (D) and the dark green wiborgite (DG) series samples treated with something else than $CaCl_2$, aluminium Al was adsorbed onto the stone surface, while for wiborgite (W) series and pyterlite (P) series the results are mixed. This could be due to Al for some samples going over the identification limit, and therefore the results being only indicative and possibly not accurate.

5.1. Wiborgite series (W)

The stone samples in series W were wiborgite commercial name Baltic Brown. In Table 11 are shown the ICP-MS results of treated samples from wiborgite series.

Table 11: ICP-MS results of treated samples from wiborgite series (W).

	W-6 H_2SO_4 Δc [mg/m^2]	W-7 H_2SO_4 + $FeCl_2$ Δc [mg/m^2]	W-9 H_2SO_4 + Na_2SO_4 Δc [mg/m^2]	W-10 $CaCl_2$ Δc [mg/m^2]	W-11 $FeCl_2$ Δc [mg/m^2]	W-12 Na_2SO_4 Δc [mg/m^2]	W-13 H_3PO_4 Δc [mg/m^2]
7 Li	**3461.1**	254.3	227.1	-463.0	188.3	88.9	216.0
24 Mg	774.8	**1539.3**	**827.0**	16.6	977.6	653.3	1019.5
27 Al	**3833.5**	**2355.8**	-400.8	0.0	926.3	-1537.6	2021.0
31 P	**4348.0**	-521.5	-2280.1	-2.4	-1167.0	3780.7	-63990.6
39 K	2861.6	**1795.5**	97.0	-38431.2	1211.4	701.5	1694.0
44 Ca	**3130.1**	**1884.1**	**719.7**	**-113806.7**	1824.6	741.9	2530.5
56 Fe	**14765.9**	**80348.2**	**7622.8**	**-2973.2**	**31393.7**	**2596.4**	**7141.2**
88 Sr	3.5	1.7	0.4	-13895.0	2.2	0.6	1.5

Wiborgite sample treated in sulfuric acid, the most leached elements were Fe, P, Al, Li, Ca and K. None of the studied elements were adsorbed to the sample surface.

The treatment in sulfuric acid and $FeCl_2$ caused Fe, Al, Ca, K and Mg to leach from its surface. Phosphorous was the only element adsorbing to the sample surface.

Wiborgite sample treated with sulfuric acid and Na_2SO_4, caused Fe, Mg and Ca to leach out from the sample surface. The elements adsorbed to the sample surface were P and Al.

The treatment of wiborgite sample with $CaCl_2$ caused mainly adsorption on the surface sample. The most adsorbed elements were Ca, K, Sr and Fe. Almost none of the elements were leached out.

Wiborgite sample treated with $FeCl_2$ solution caused Fe, Ca, K, Mg and Al to leach out from the sample surface. It also caused the adsorption of the P to the sample surface.

The Wiborgite sample treated with Na_2SO_4 solution, results showed that P, Fe, Ca, K, and Mg were the elements that leached the most from the sample surface during treatment. The treatment caused the adsorption of Al to the stone surface.

When wiborgite sample was treated with phosphoric acid, P was the element that was adsorbed to the sample surface. The most leached elements were Fe, Ca, Al, K and Mg.

5.2. Pyterlite (P)

The stone samples in series P (called also C1) were pyterlite, commercial name Carmen Red. In Table 12 are shown the results of ICP-MS analysis after the treatment for each sample.

Table 12: ICP-MS results of treated samples from pyterlite series.

	P-6 H_2SO_4 Δc [mg/m^2]	P-7 H_2SO_4 + $FeCl_2$ Δc [mg/m^2]	P-9 H_2SO_4 + Na_2SO_4 Δc [mg/m^2]	P-10 $CaCl_2$ Δc [mg/m^2]	P-11 $FeCl_2$ Δc [mg/m^2]	P-12 Na_2SO_4 Δc [mg/m^2]	P-13 H_3PO_4 Δc [mg/m^2]
7 Li	512.9	5091.9	-6765.7	-5567.1	4312.3	198.9	1556.3
9 Be	0.0	0.0	70.6	70.9	164.1	0.0	0.0
24 Mg	1361.4	106.0	618.9	31.2	864.9	612.8	847.0
27 Al	-4264.6	2002.2	1439.1	0.0	14207.3	-11210.8	2192.3
31 P	2892.7	-1240.6	-2810.4	1834.6	-91.6	1751.0	-79628.7
39 K	2921.5	1098.4	930.0	-34724.8	1308.4	1060.8	1552.3
44 Ca	4626.4	925.9	189.2	-120280.2	2383.4	259.6	811.9
45 Sc	21.9	5.3	5.5	0.0	9.9	6.4	8.1
55 Mn	196.0	91.6	59.2	0.0	122.7	65.3	97.9
56 Fe	12664.0	-93175.8	3108.1	-56.3	-98028.6	4002.6	6316.6
88 Sr	4.6	1.3	0.5	-319.5	1.9	0.8	1.6

For pyterlite samples treated in sulfuric acid, the most leached elements were Fe, Ca, K, P and Mg. The only adsorbed element was Al.

Pyterlite sample treated with both sulfuric acid and $FeCl_2$ caused Li, Al, K and Ca to leach out the most from the sample surface. The most adsorbed elements were P and Fe.

Pyterlite sample treated with sulfuric acid and Na_2SO_4, caused Fe, Al, K, Mg and Ca to leach out from the stone surface. The most adsorbed elements were Li and P.

Pyterlite sample treated with $CaCl_2$ results showed that only P was leached from the sample. However, Ca, K, Li and Sr seemed to chemically bond to the stone sample surface.

When pyterlite sample was treated with $FeCl_2$ solution. Mostly only the Fe-ions from the solution were adsorbed to the sample surface, and Al, Li, Ca and K were leached from the stone sample surface. This could indicate that Fe-ions took the place of these mentioned elements from the stone sample surface.

Pyterlite sample treated with Na_2SO_4 solution was shown to adsorb the Al-ions into the surface. The treatment leached Fe, P, K, Mg and Ca from the sample surface.

Pyterlite sample treated with phosphoric acid caused Fe, Al, Li, K, Mg and Ca to leach out from the sample surface. The most adsorbed elements was P.

5.3. Dark Rapakivi Granite (D)

The D series samples are dark rapakivi granite. Sample series was the only sample series where Li was left of out of the results table due to either low number of lithium found with ICP-MS or low change in concentration. Therefore, the results could indicate that the stone samples from this series do not have as much lithium in them as the other series.

In Table 13 are shown the ICP-MS results of concentration changes in the used solutions during the treatments.

Table 13: ICP-MS results of treated samples from Dark Rapakivi Granite (D) series.

	D-1 H_2SO_4 Δc [mg/m^2]	D-2 H_2SO_4 + $FeCl_2$ Δc [mg/m^2]	D-4 H_2SO_4 + Na_2SO_4 Δc [mg/m^2]	D-5 $CaCl_2$ Δc [mg/m^2]	D-6 $FeCl_2$ Δc [mg/m^2]	D-7 Na_2SO_4 Δc [mg/m^2]	D-8 H_3PO_4 Δc [mg/m^2]
23 Na	142.4	140.4	3323.7	291.3	-319.9	-3399.6	277.2
24 Mg	18.8	888.3	620.7	32.9	492.6	507.4	726.2
27 Al	-1161.9	-2957.3	-4203.0	0.0	-6600.8	-4195.7	-9699.4
31 P	2696.8	2240.3	5755.6	3782.7	641.8	9681.5	-12184.5
39 K	338.8	236.6	132.9	-23045.4	142.2	96.3	143.1
44 Ca	2842.4	2154.1	1145.1	-42208.0	1863.6	1307.2	5504.5
55 Mn	448.4	368.8	239.4	2.6	224.8	213.1	309.5
56 Fe	21067.9	86737.9	-29095.1	3036.8	5977.7	12127.6	16350.9

When treating dark rapakivi granite sample with sulphuric acid the most leached elements were Fe, Ca, P and Mn. The most adsorbed element was Al, similar to the rest of the samples in this series.

Treating dark rapakivi granite sample with sulphuric acid and $FeCl_2$ resulted Fe, P, Ca, and Mg to leach out from the surface while Al adsorbed into the sample surface

During the sulfuric acid + Na_2SO_4 treatment the most leached out elements were P, Ca and Mg. The most adsorbed elements were Fe and Al.

Dark rapakivi granite sample treated with $CaCl_2$ solution showed that the stone sample surface adsorbed Ca and K ions from the solution and P, Fe and Sr were leached into the solution.

When the sample was treated with $FeCl_2$ solution, the similar did not happen. Instead, it showed that Fe was leached from the stone sample, together with Ca, P and Mg. Al was the only element to absorb into the surface.

Na_2SO_4 treated sample adsorbed Al ions into the surface. The most leached elements were Fe, P, Ca and Mg.

If dark rapakivi granite sample was treated with phosphoric acid, it caused a lot of elements to leach out of the sample. Highest leaching was observed with Fe, Ca, Mg and Mn. The P in the acid however seemed to adsorb to the stone sample surface, as amount of P were lower than before the treatment. According to the results, Al was also adsorbed to the stone sample.

5.4 Dark Green Wiborgite -series (DG)

In Table 14 are shown the results of ICP-MS analysis for concentration changes during chemical treatment for these samples.

Table 14: ICP-MS results of treated samples from dark green wiborgite series.

	DG-1 H_2SO_4 Δc [mg/m^2]	DG-2 H_2SO_4 + $FeCl_2$ Δc [mg/m^2]	DG-4 H_2SO_4 + Na_2SO_4 Δc [mg/m^2]	DG-5 $CaCl_2$ Δc [mg/m^2]	DG-6 $FeCl_2$ Δc [mg/m^2]	DG-7 Na_2SO_4 Δc [mg/m^2]	DG-8 H_3PO_4 Δc [mg/m^2]
7 Li	1260.0	16.7	-155.7	-98.2	8.0	203.2	15.8
9 Be	4.6	5.0	0.0	5.0	12.3	-5.2	-10.2
24 Mg	59.1	59.1	34.4	4.1	35.0	32.6	53.3
27 Al	-252.4	-314.4	-2786.0	2.4	-52.9	106.5	-479.0
31 P	206.3	238.3	79.9	-1.0	-89.0	630.4	5654.2
39 K	5.6	92.7	79.3	-2426.2	6.2	73.0	9.0
44 Ca	244.7	177.7	85.1	-5294.6	214.3	123.2	521.1
56 Fe	2119.6	-840.7	1054.2	-4.1	-3751.8	943.4	1386.7

Dark Green Wiborgite treated with sulfuric acid caused Fe, Li, Ca and P leached into the solution. Al was the only element that was adsorbed into the stone sample surface.

When this sample type was treated with sulfuric acid and $FeCl_2$, the most leached element from the stone sample surface was P. Fe and Al were adsorbed to the surface.

When sample was treated with sulfuric acid and Na_2SO_4, Fe was the main element to leach out. Al and LI were only elements which adsorbed into the surface.

If dark green wiborgite samples were treated with $CaCl_2$, none of the elements were clearly leached into the solution. However, the adsorption of K and Ca seemed to be significant in this sample.

When this sample type was treated with $FeCl_2$ solution, the most leached elements were P and Ca. The most adsorbed element to the stone surface was Fe.

Sample treated with Na_2SO_4 solution the most leached elements were Fe, P, Li and Ca.

When sample was treated with phosphoric acid, the elements which adsorbed most were Fe and Ca.

6. SPECTRAL ANALYSIS

6.1 Raman test study

Raman spectroscopy has been used in identifying minerals from stone samples (Wojcieszak & Wadley, 2019). For this project the intended use of raman was to study differences between untreated and treated surfaces of stones. Two methods of Raman analysis were employed. First a single sample was mapped overnight, to see the distribution of minerals (different spectra) on the stone surface. The software compares the recorded spectra directly to a library of spectra and divides the sample surface to areas according to the matches.

Thermo scientific DXR3xi Raman Imaging Microscope was used to study different minerals on the rapakivi sample surfaces. Microscope allows the user to aim for the areas of interest and gather the spectra. In the study it was noticed that some of the minerals on the surface gave poor raman response or had problems with fluorescence.

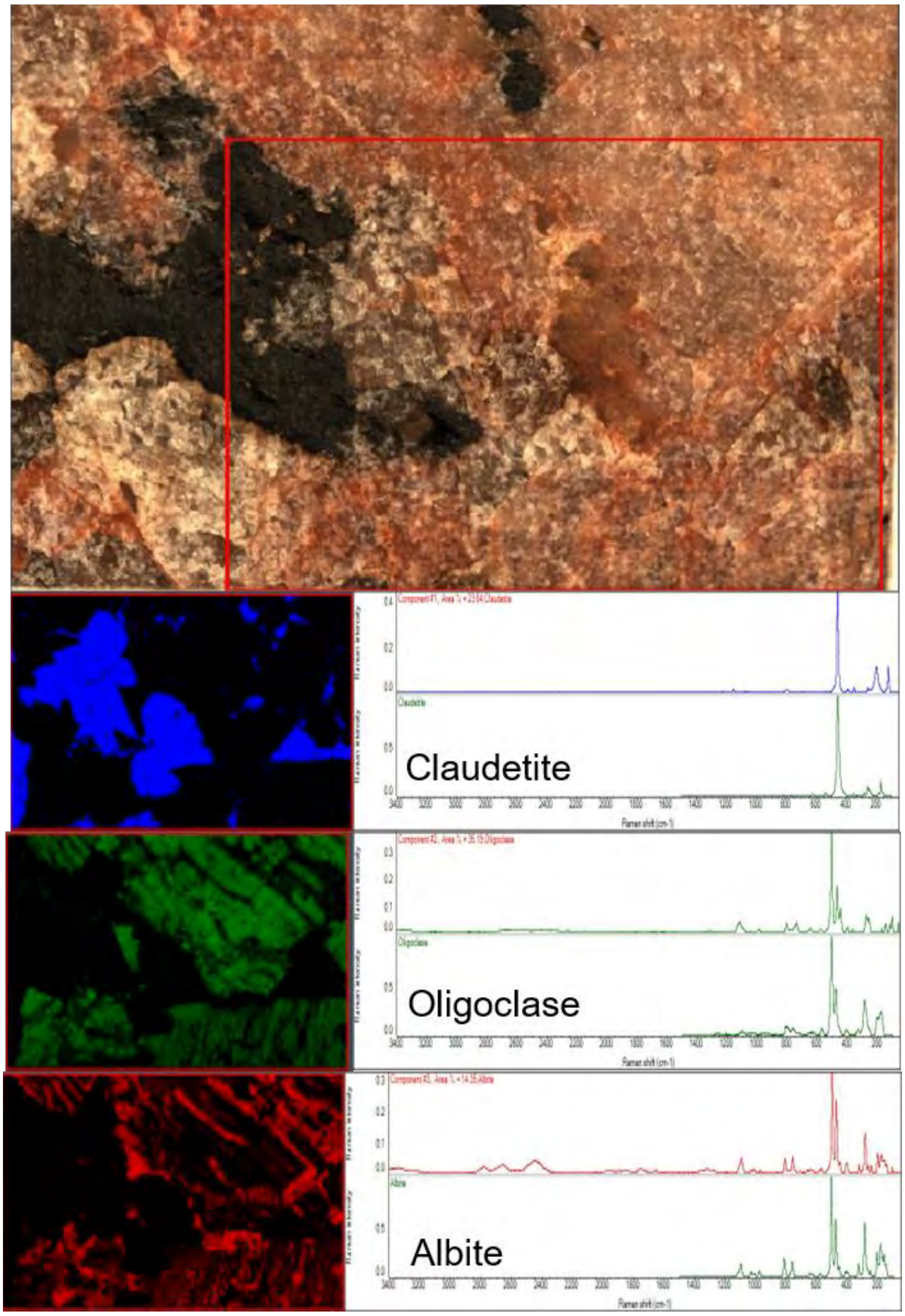

Figure 29 Raman microscopy study of Wiborgite. Area of study marked with the red rectangle. Three main areas identified with raman spectra and their corresponding spectra and the closest match from the spectral library. Together these three minerals make up about 73% of the sample surface.

In Figure 29, the main minerals identified in raman scanning study are presented. For these measurements the spectra look clean and are identified by comparison to spectra found in the instruments libraries. However, these library matches were not checked further, and it is possible that the automatic library search has made mistakes, as for example claudetite and quartz raman spectra are very similar. According to the results these three minerals comprise about 73 % of the sample surface. However, in Figure 30, some of the not so clear results of the raman scan are given. With these it is seen that some of the minerals on the sample cause for example fluorescence problems and the minerals cannot be reliably identified using the spectral library.

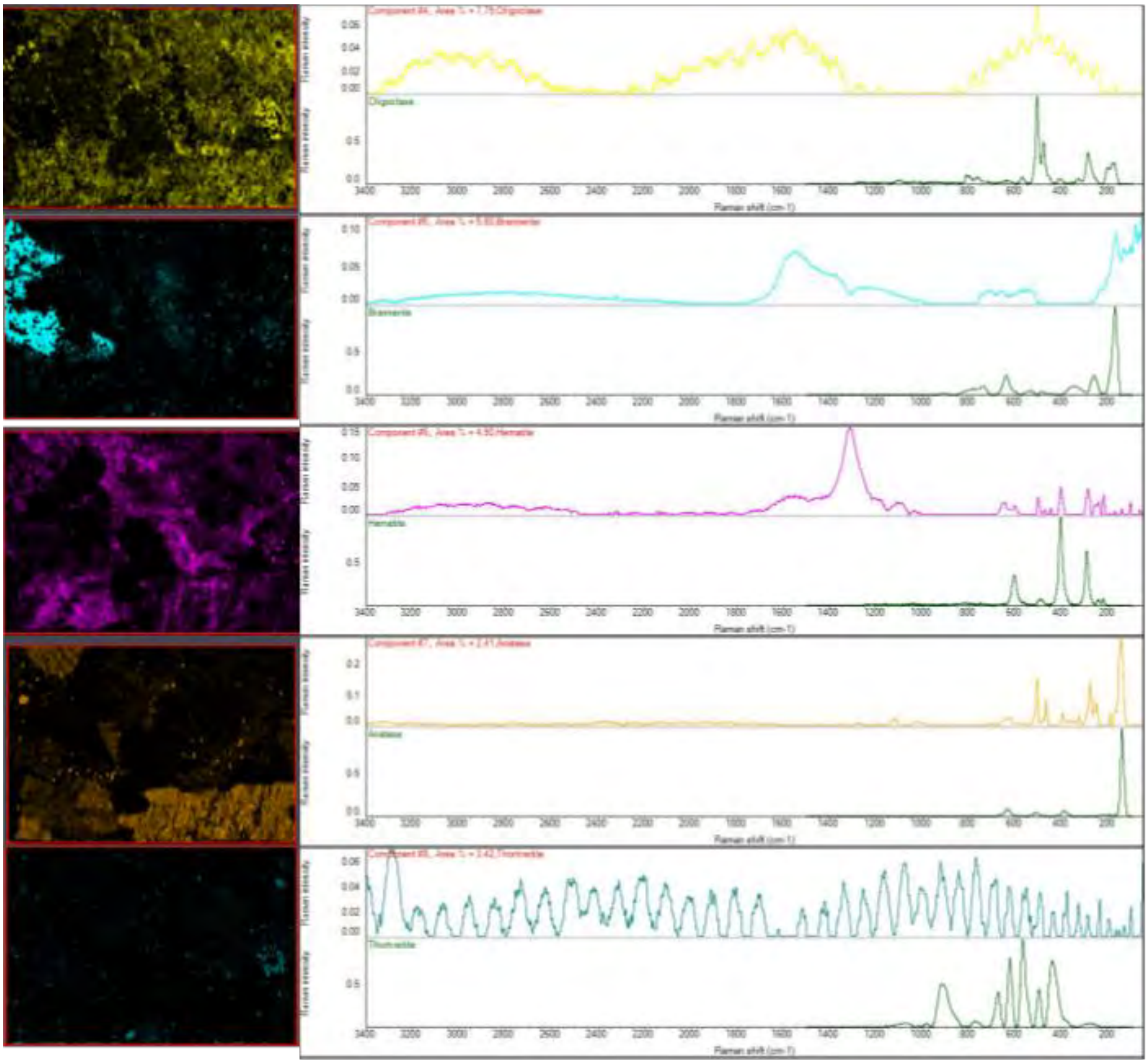

Figure 30 Badly identified regions of the stone sample. Together these parts cover about 24% of the sample surface.

As the scanning study gave promising results but was not feasible with a larger set of samples (the scan took a whole night). It was decided to try and do a spot vise study, by selecting points from the surface randomly, covering visually different regions. Using this method three wiborgite samples and two pyterlite samples were studied. Results for one wiborgite sample are presented in Figure 31. From there it is evident that the results are not as good as in the scanning study.

Looking at the spectra from Figure 31, we can see some of the same features as in the scanning spectra, however with a larger amount of noise. Also, many of the spectra suffer from fluorescence problems.

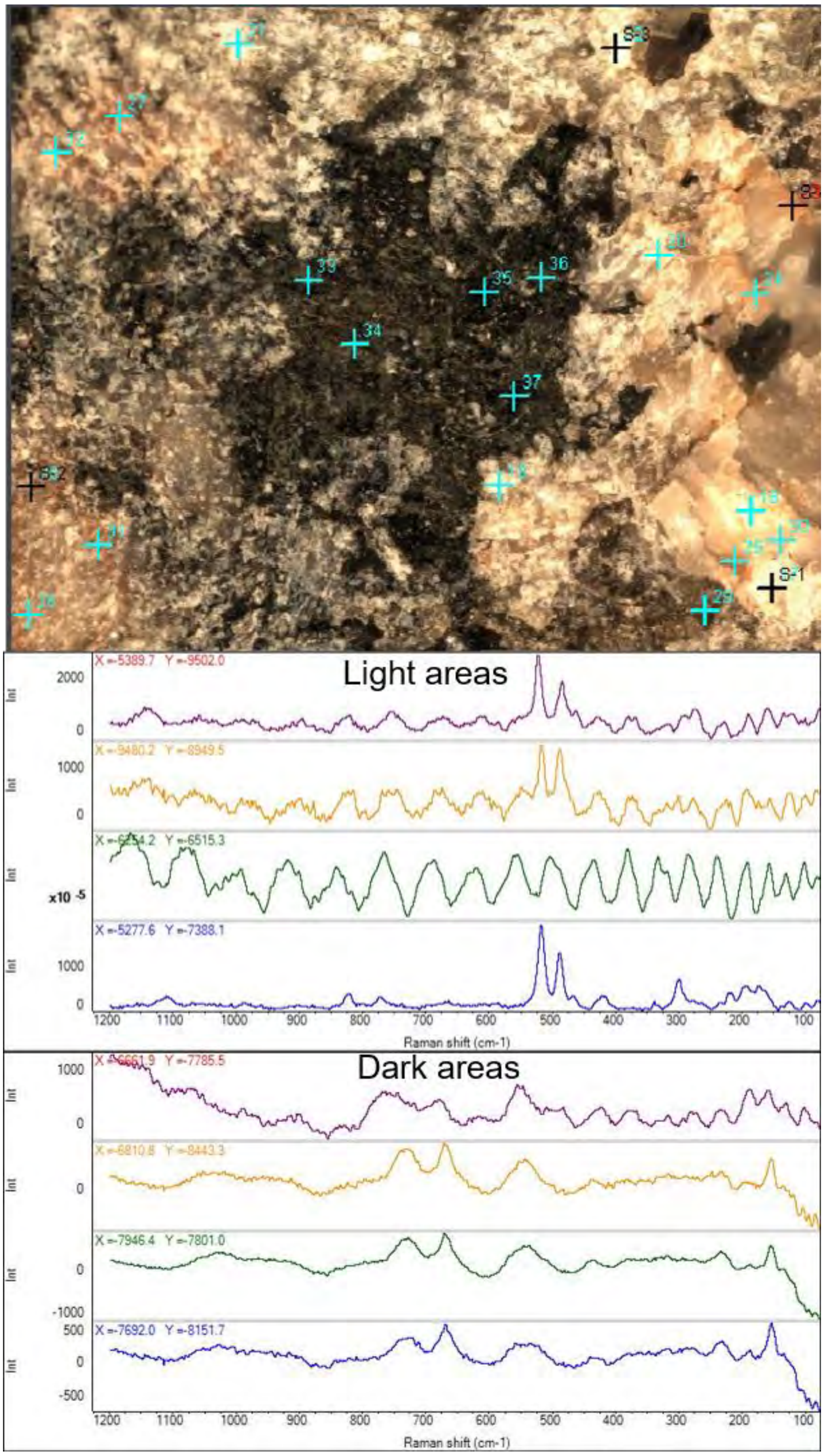

Figure 31 Sample surface of the point vise raman analysis. Included four spectra from the points selected in the "light areas" and fours spectra from the "dark areas" on the sample surface. d

Surface scanning method seems to be the more feasible one, but it also takes more time. For point vise analysis, more study is needed to find the required number of spectra to represent the surface of the rock and all the features that are interesting. Point and shoot method can be tricky as the surface image on the microscope can seem clear, but the spectra in similar looking areas can be different minerals.

6.2 FT-IR results

Reference spectra

FT-IR spectra were measures from the original stones and treated stones. The sample series are introduced in the first chapters: Wiborgite, Baltic Brown (W or A), Pyterlite, Carmen Red (P or C), Dark green wiborgite, Baltic Green (DG or BG), Dark rapakivi granite (D or B).

All samples were treated thermally as 1st or 2nd step in the treatment procedure. The handheld FT-IR instrument arrived only after the first treatment, and therefore reference spectra were measured from reference samples. These reference spectra represent “original stone before any treatment”. Number of reference samples varied from 3-6. From each reference sample 20 FT-IR spectra were measured (60-120 reference spectra for each series). Samples were analysed by GTK in LUT laboratory facilities, where samples were treated.

The average spectra of the reference samples are presented in *Figure* 32. W, P and even DG rapakivi granites provide very similar spectra. It would be difficult to identify the rapakivi type based on the spectra in this range of handheld FT-IR (650-4000 cm^{-1}).

shows typical spectra of main minerals occurring in these granite varieties.

Table 16 and Table 16 show the main frequencies that are present in the granite spectra. The spectra have many common main peaks, such as:

- Si-O: 725, 1008-1012, 1040, 1055, 1073, 1140, 1172
- Quartz Si-O: 780, 800, Sulphate: 1090, P: 1190 cm^{-1}

Main spectral profiles from samples could be extracted. However, their utilization was not in scope of this research. In *Figure* 32 - *Figure* 41 average spectra of the granite samples are presented and compared: original surfaces and treated surface.

Table 15 Adsorption bands in ATR-FTIR spectra of reference minerals in study of (Bosch-Reig, Gimeno-Adelantado, Bosch-Mossi, & Doménech-Carbó, 2017) or database of Whiley and Sons.

Mineral Bands on wavenumbers [cm^{-1}]	Spectra presented in (Bosch-Reig, Gimeno-Adelantado, Bosch-Mossi, & Doménech-Carbó, 2017)
Na-Feldspar (a) 1145, 1095, 1040, 994, 786, 761, 743, 724, 692, 648	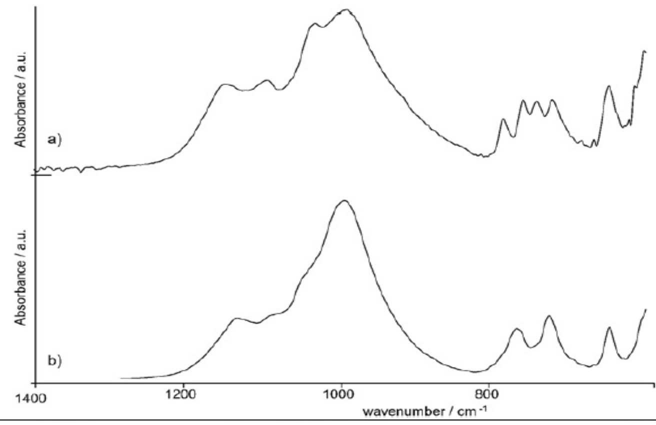
K-Feldspar (b) 1140, 1090, 1045, 992, 767, 725, 647	
Quarts 1160, 1090, 796, 777, 690	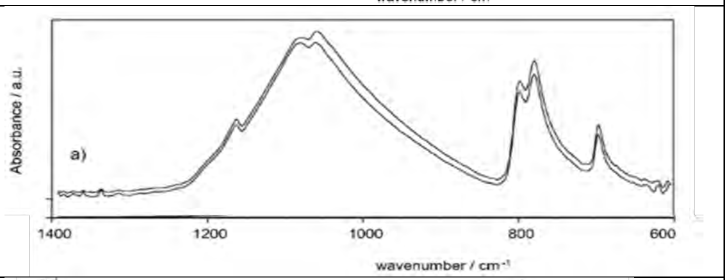
Biotite 1628, 990, 960	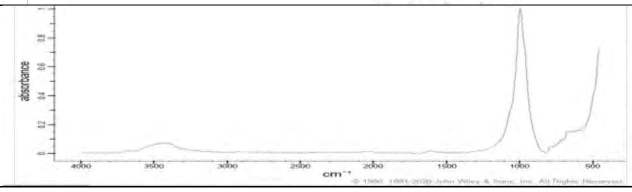

Table 16 Relevant wavenumbers in the ATR-FTIR spectra of granite samples gathered from previous studies (Pozo, et al., 2013), (Senthil Kumar & Rajkumar, 2013) (Pernet-Fisher, Joy, Martin, & Donaldson Hanna, 2017), (Yang, Xia, & Zhang, 2015), (Bosch-Reig, Gimeno-Adelantado, Bosch-Mossi, & Doménech-Carbó, 2017) (Sontevska, Jovanovski, Makreski, & Raskovska, 2008)). (Rubio-Ordóñez, García-Moreno, Terente, García-Guinea, & Tormo, 2019) (Hlavay, Jonas, Elek, & J., 1978)

Wavenumber, cm^{-1}	Description	Found in ref spectra
3906. 3856, 3840, 3820, 3808, 3753, 3737, 3714	Small peaks common in all four rapakivi stones	W, P, DG (D)
3680	Board, -OH stretching for Al-OH	Spectra of W, P, (DG)
3580	Weak, -OH stretching for Si-OH	n.d.
3400, 3417-3100	Board, -OH stretching for absorbed water	n.d. but D is lower
3100-2800	C-H stretching CH2 and CH3	n.d. but D is in lower level
3070, 3026	N-H stretching (amine)	n.d.
1900-1870	Board, Si-OH of quartz	n.d.
1772	Feldspar Si–O stretching	W, P, DG really weak
1725	Weak, H-O-H bending	n.d.
1210	Wide	(W, P, D, DG)
1190	PO_2^- symmetric stretching	(W, P, D, DG)
1170-1015	Si–O–Si, asymmetric oxygen bridging	Main in all
1175, 1100	*Quartz, Si-O asymmetric stretching*	W, P, D, DG
1159	Si–O stretching, Anorthite CaAl2Si2O8	negative peak in ref spectra
1140	wide	W, P, DG
1122	PO stretching of phosphodiester and C-O stretching	(W, P, DG)
1113	Si–O–Si stretching, microcline feldspar	(P)
1090	Symmetric stretching of SO_4^{2-}	(W, P)
1080-1072	Si–O–Si	W, P, D, DG
1040, 1055, 1073	Si–O?	W, P, DG
1019-1012	1019 Hydrous feldspar, O-H	W, P, DG
990	Wide or belongs to 1012	W, P, DG
894	*Goethite* (FeOH), O-H bending	n.d. or wide in all
800, 785	*Quartz, Si-O symmetric stretching*	W, P, D, DG
775, 735	*Feldspar Al-O-Si component vibrations*	W, P, DG
755	Al–O–Si in Dickite (Al2Si2O5(OH)4)	DGc, others 750
727	Si–O stretching mode vibration, microcline feldspar	DG
724-720	Al-O-Si in Biotite	W, P, (D, DG)
700-550	Si-O-Si bending (biotite)	D (DG) 710-715
695	Quartz Si-O symmetrical bending	W, P, D, DG

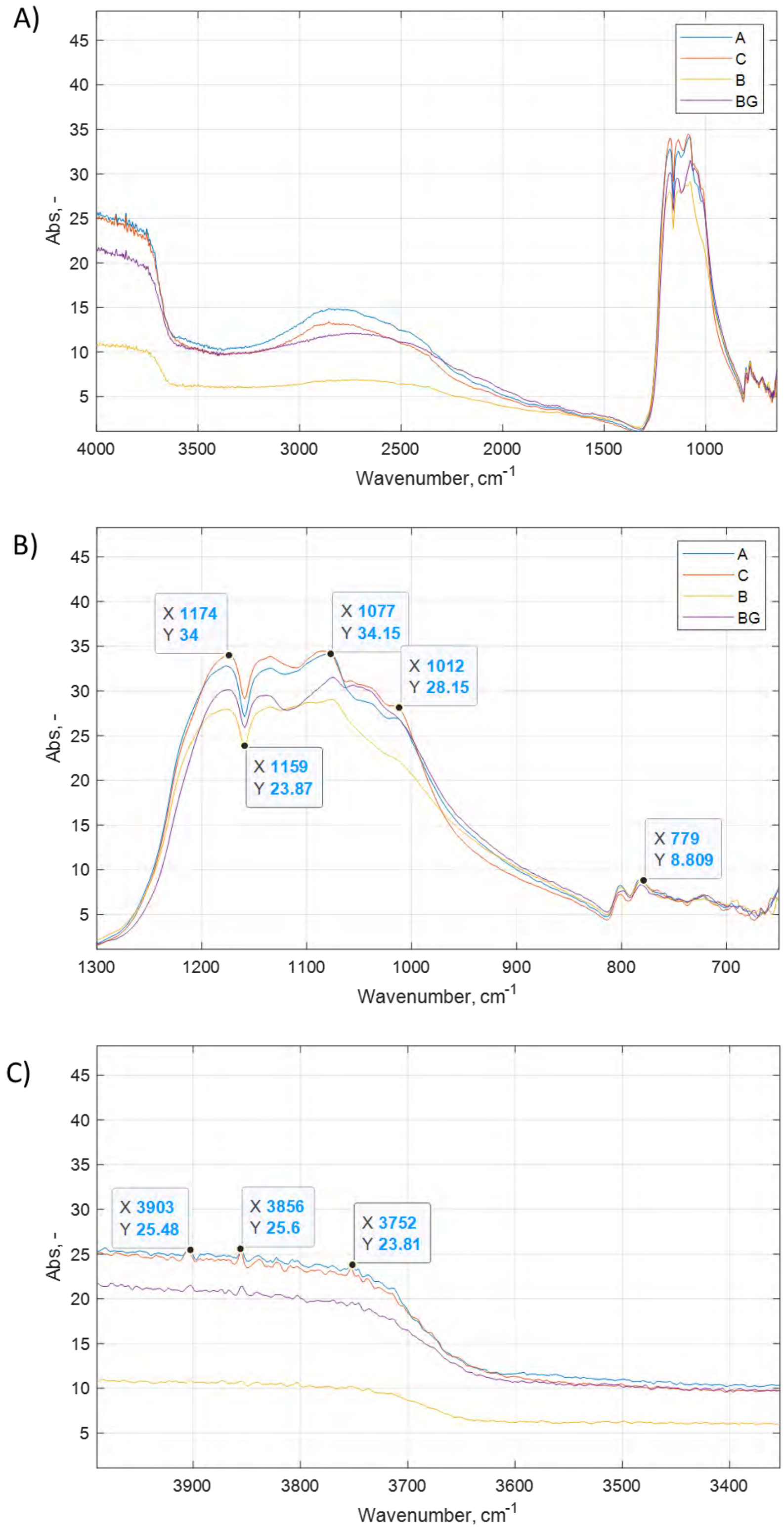

Figure 32 *Average spectra of 60-110 measurements of untreated sample (Reference spectra of the series): W = Wiborgite, Baltic Brown (A), P = Pyterlite, Carmen Red (C), DG = Dark green wiborgite, Baltic Green (BG), D = Dark rapakivi granite, Black granite (B). Subplots A) Full measurement range 650.4 – 3999.4 cm^{-1}, B) wavelength range near 650-1300 cm^{-1}. All stones show Si-O-Si bands in range 1000-1200 cm^{-1}, C) wavelength range near 3300-4000 cm^{-1}. Black stone most relevant difference is on frequency 1010-1050 cm^{-1}, where the other stones have stronger Si-O-Si bonds typical for biotite and quartz. However, it has the 782 and 780 cm^{-1}characteristics to quartz. In average spectra biotite shows only minor peak at 3712 cm^{-1}.*

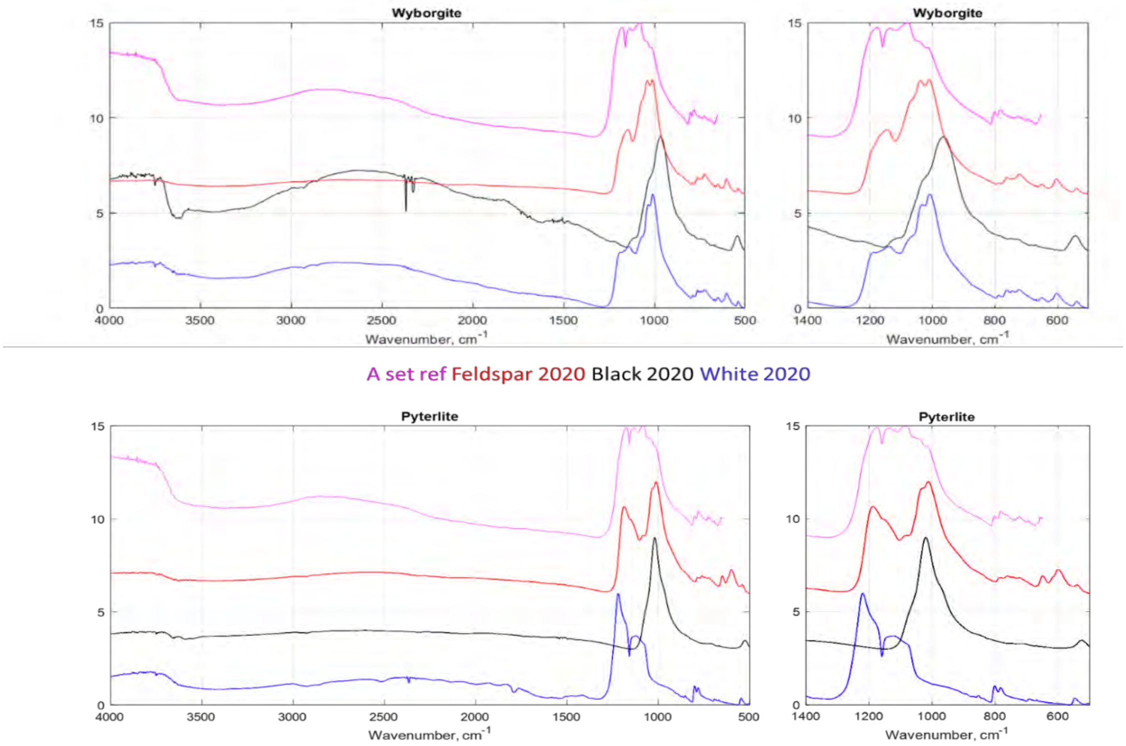

Figure 33 *Wiborgite and Pyrite spectra: average spectra from stone samples measured with the handheld FT-IR and average spectra measured with laboratory FT-IR instrument from colour tones occurring in the stone samples. Brownish or reddish regions provided repeatable spectra and it was defined as feldspar. The black/dark and white/light regions provided more heterogenous spectra. Spectra of Wiborgite white regions is a typical quartz spectra with peaks at 780, 800, 1008, 1036, 1190 cm^{-1}. Pyterlite spectra from white regions: the Si-O-Si peak from 1008 cm^{-1} is missing, and new peak at 1122 cm^{-1} suggesting PO presence has appeared. Dark or black regions tend to have Si-O bands in 964 cm^{-1} (Wiborgite) or 1008 cm^{-1}(Pyterlite). Biotite spectra could be expected to have Si-O-Si peak at 1000-1015 cm^{-1}, and peak at 550 cm^{-1}. Spectra are scaled [to variation 6] and lifted [by step of 3] for visualization purposes.*

Figure 33 illustrates average spectra measured from Wiborgite and Pyterlite samples, and from different colors (minerals) in them. The average spectra are same as in *Figure* 32 measured with handheld instrument, while the feldspar, white/light, and black/dark areas are measured with laboratory FT-IR instrument. Thus, the wavenumber range is wider in latter spectra. Spectra from black regions have clear features of biotite spectra. Feldspar and white regions spectra are obviously mixtures of minerals. The white regions have quartz, and the reddish/brownish felspar visible in the spectra.

FT-IR of treated Wiborgite

Wiborgite samples were measured 20 times after the treatments. The average spectra are illustrated in *Figure* 34, and change is visualized in *Figure* 35 as *(treated average spectrum)-(untreated average spectrum)*. Reference spectra is mean of untreated W2-W5 samples. Sample W1 was removed from reference set since the spectra clearly deviated from the other samples in W set. It can be due to analytical issues (first measurements with the FT-IR instrument) or due to the sample surface. Sample had been stored long time, and it was the surface sample that might have been exposed to various factors.

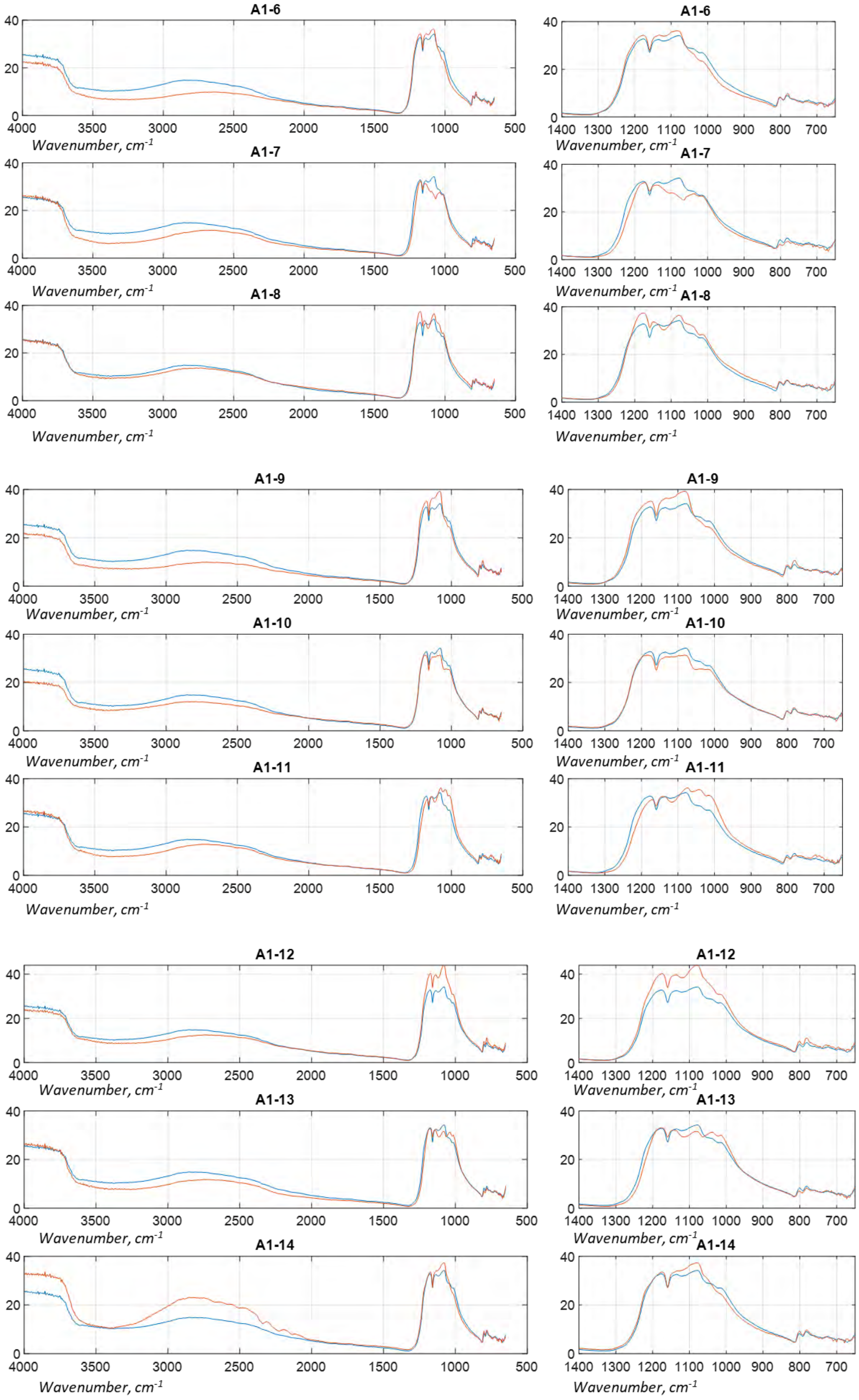

Figure 34 W set: Wiborgite spectra of treated samples (red), and untreated samples (blue). Samples labelled as A1-# (set W).

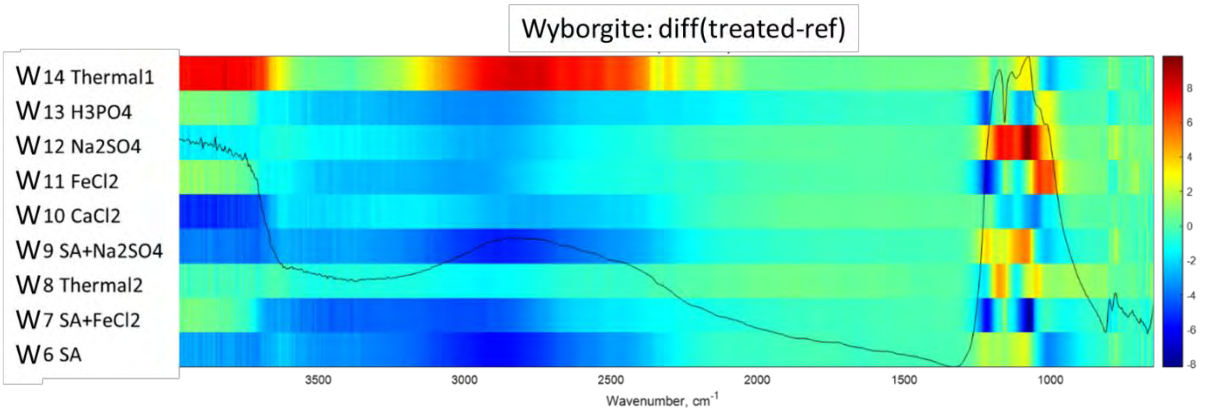

Figure 35 *Change in FT-IR spectra during the 1st treatment: W set (Wiborgite). Main changes are in the Si-O range 980-1190 cm*$^{-1}$*. Sulphuric acid affects to Si-O-Si bonds typical for biotite. Sodium sulphate seems to increase Si-O-Si bonds typical for feldspar. Iron and phosphoric acid treatments decrease occurrence of bonds typical to quartz. Also P-O and C-O bands may appear near 1020 cm*$^{-1}$*. Thermal treatment in higher temperature decreased obviously bonds typical for biotite spectra.*

FT-IR of treated Pyterlite

P set (Pyterlite, Carmen Red) were treated similar to other sample series. The reference samples and treated samples were analyzed with the handheld FT-IR. 20 spectra from each sample were taken, and after removal of obvious outliers the average spectra were computed as taking mean on each wavenumber. Resulting spectra are presented in *Figure* 36, and difference between treated and untreated spectra in *Figure* 37. Reference samples utilized were: P1-P5, and P17, total 120 spectra.

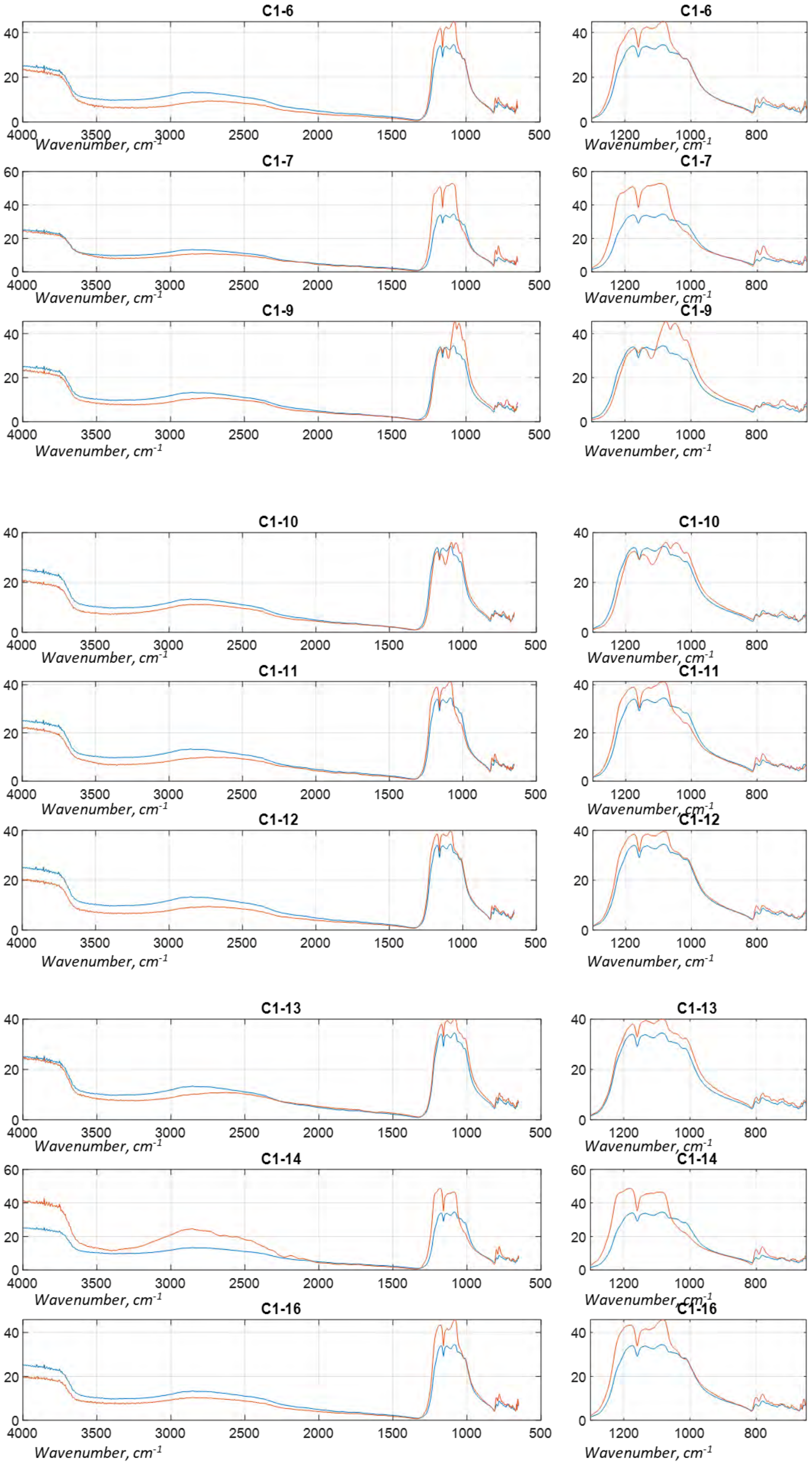

Figure 36. *P set: Pyterlite (Carmen Red, C1 samples) spectra of treated samples (red), and untreated samples (blue). Spectra after 1st treatment reveals stronger features of feldspar or white regions of untreated stone.*

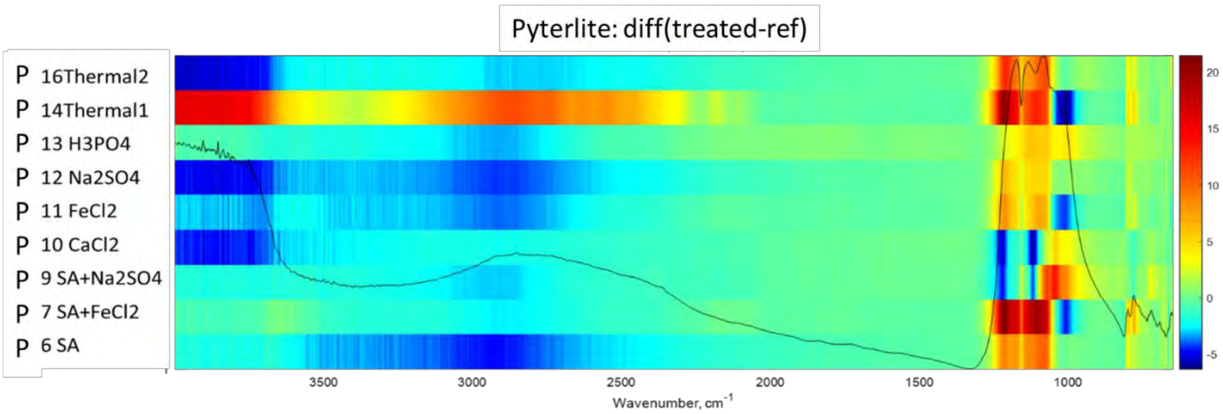

Figure 37*. Change in FT-IR spectra during the 1st treatment: P set (Pyterlite).*

Main changes are in the Si-O range 980-1190 cm^{-1}. NaSO4 bonds can also be identified from that region: characteristics for Sodium sulphate are peaks at 1185, 1094, 1034 and 940 cm^{-1}. Iron with sulphate and treatment in higher temperature have had an effect on appearance of Si-O-Si bonds typical for biotite. Most treatments seem to increase Si-O-Si bonds typical for feldspar and quartz. Calsium chloride and acidic Sodium seems to effect more quartz and feldspar than biotite. Thermal treatment in higher temperature decreased obviously bonds typical for biotite while the oven treatment in lower temperature was clearly less visible in the spectra.

FT-IR of treated Dark Rapakivi Granite series (D)

D samples represent granite that is most different from the others. It has bonds that are common to feldspar and quartz, but it has less bonds typical for biotite. Biotite is a black mineral but the main black mineral in this D samples is not biotite.

Handheld FT-IR instrument were applied to analyze treated and untreated stone samples. The untreated samples D-10, …, D-15 were applied to define the reference spectra (total 120 spectra). From the treated samples 20 spectra from each stone sample were analyzed.

Average spectra are presented in *Figure* 38 and the change is illustrated in *Figure* 39. Conclusions are in figure captions.

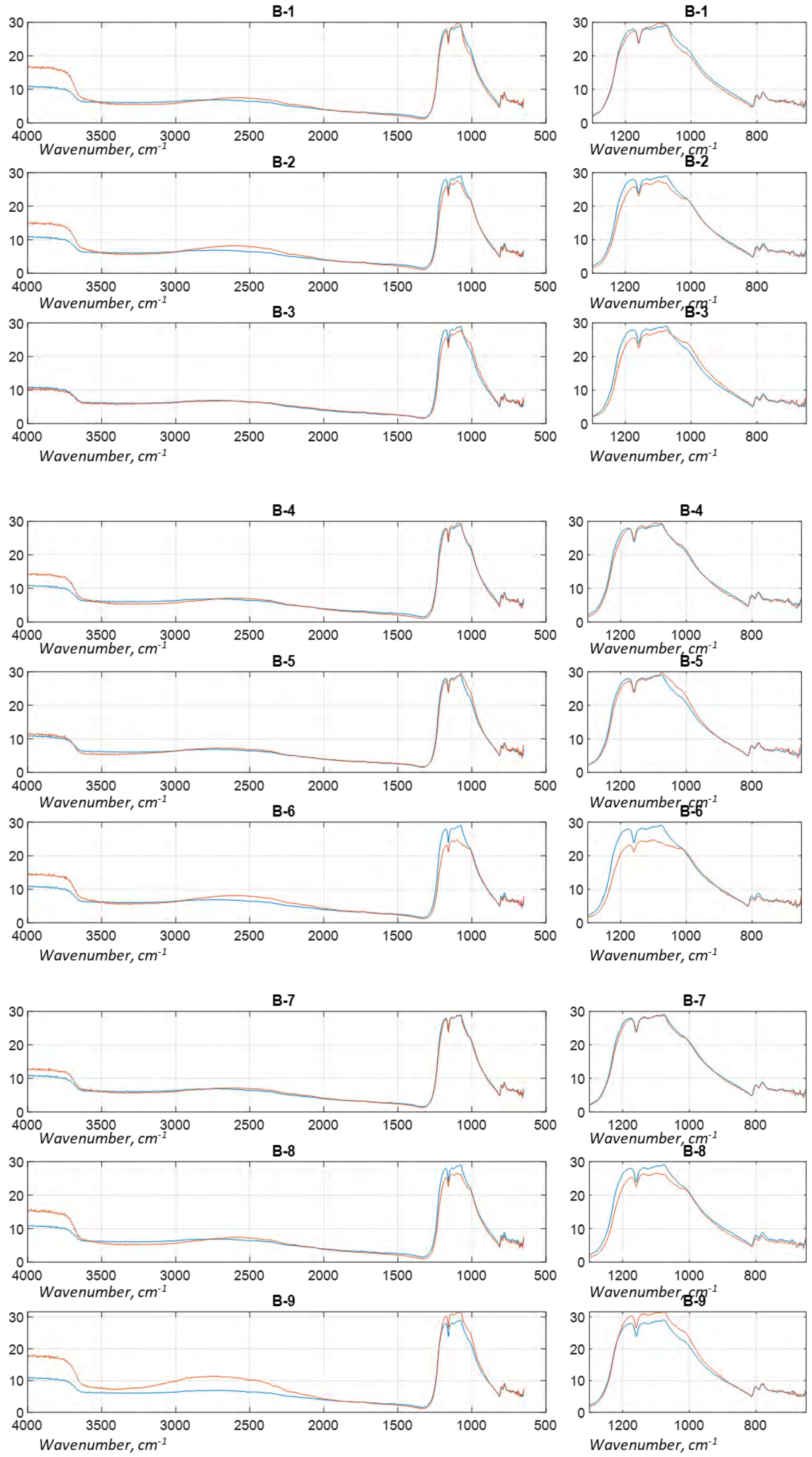

Figure 38. D set (Dark Rapakivi Granite, named as B samples). Spectra of treated samples (red), and untreated samples (blue). Spectra after 1st treatment reveals only minor changes compared to the untreated stone.

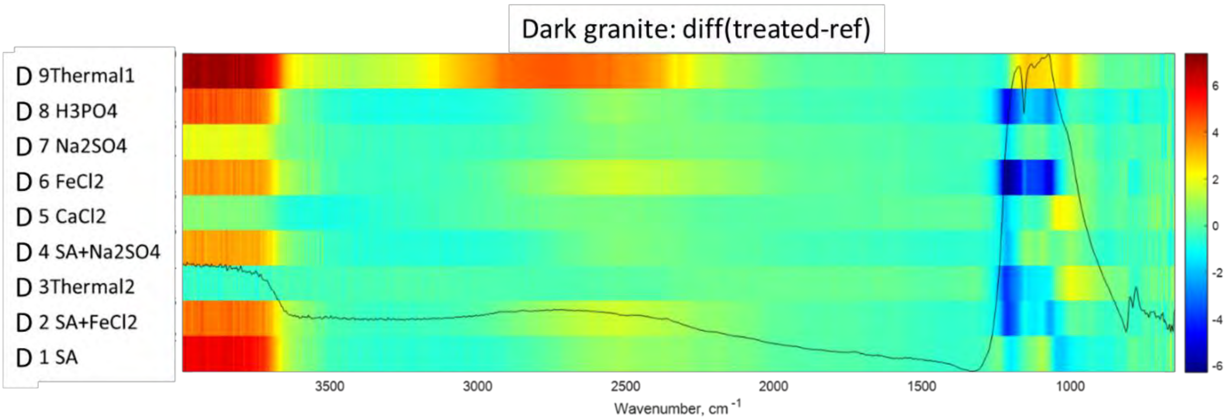

Figure 39. *Change in FT-IR spectra during the 1st treatment: D set (Dark rapakivi granite). Main changes are in the Si-O range 980-1190 cm^{-1}and in 3600-4000 cm^{-1}. OH band(s) appear at 3645 cm^{-1}. However, the latter wavelength range is not generally considered important nor containing specific information to characterize samples. The thermal treatment in 600ºC oven did destroy the sample surface. Main changes in samples appeared at 1190-1220 cm^{-1}, which could refer to PO2 or Si-O-Si bonds. Iron chloride, phosphoric acid and thermal treatment seem to decrease these bonds.*

FT-IR of treated DG series (Dark Green wiborgite)

Dark Green wiborgite (*Baltic Green*) is rapakivi granite with dark green appearance. There were 3 reference samples: DG-10, DG-11 and DG-12. With the FT-IR instrument 20 times from each stone sample resulting total 60 reference spectra. DG-1, … , DG-9 samples were treated and 20 spectra from each were analyzed from each sample after the treatments.

The average spectra of treated and reference samples are presented in *Figure* 40. *Figure* 41 shows changes as difference *treated – untreated*.

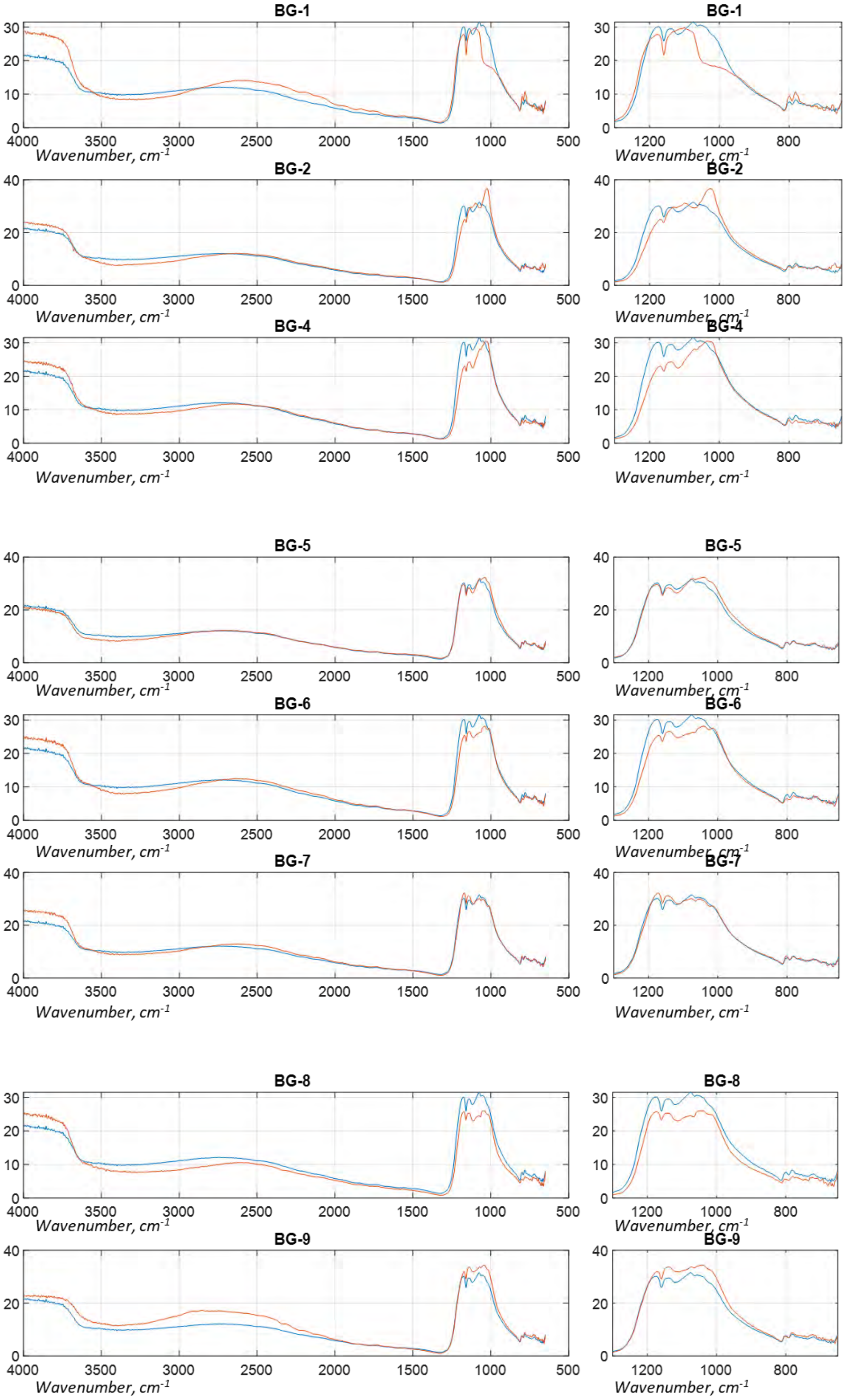

Figure 40 *DG (BG) set: Dark Green Wiborgite spectra of treated samples (red), and untreated samples (blue). Spectra after 1st treatment with Na2SO4 (DG7) and CaCl (DG5) reveals only minor changes compared to the untreated stone.*

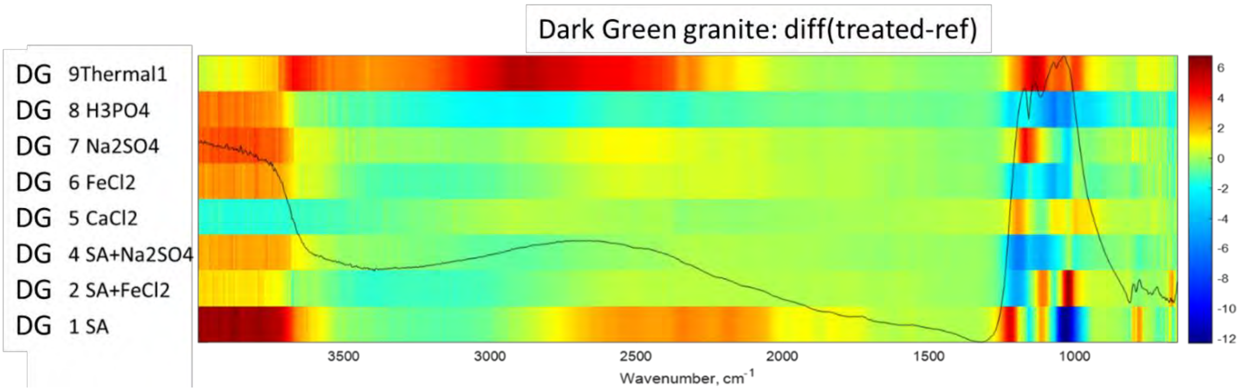

Figure 41 Change in FT-IR spectra during the 1st treatment: DG set (Baltic Green). Main changes are in the Si-O range 980-1190 cm^{-1}and in 3600-4000 cm^{-1}. OH band(s) appear at 3645 cm^{-1}. However, the latter wavelength range is not generally considered important nor containing specific information to characterize samples. The thermal treatment in 600ºC oven have had a clear effect on the sample surface. Main changes in samples appeared at 1190-1220 cm^{-1}, which could refer to PO2 or Si-O-Si bonds. Iron chloride, phosphoric acid and thermal treatment seem to decrease these bonds.

4.1.6 Conclusions from FT-IR measurements

General conclusions

- When comparing the reference spectra, it was found that they are very similar, and typical for granite stones
- Dark rapakivi granite (D) has less biotite (bands) than the other granite varieties.
- Dark Green wiborgite (DG) samples indicated less Si-O-Si bands. However, the ratio of bonds is very similar to W and P series. W and P (Wiborgite and Pyterlite) are impossible to distinguish from each another based on reference spectra.
- Thermal treatment in 600ºC had strong effect on the spectra, which supports the visual inspection of the surfaces. Dark minerals are more sensitive to thermal treatment and their durability is weaker, than silica or reddish/brownish feldspar minerals.
- Increase in wide spectral range 2000-3000 cm^{-1} might be due to C-H bands appearing in burning.
- Si-O-Si bands characteristics to biotite generally decreased while the silica bands in feldspars increased in surface.
- Thermal treatment in lower temperature had less effect compared to higher temperature.
- Sulphuric acid and phosphoric acid have different effects
- Sulphuric effects more on biotite type bonds
- Phosphoric acid effects more on quartz and feldspar
- Iron chloride seems to decrease peaks related to quartz, and SA increase these phenomena.
- Sodium sulphate effects depend on the stone set. In some cases, the dominant effect seems to sulphate, while in other cases sodium itself might have formed new compound.
- $CaCl_2$ caused the mildest effects on the spectra.

5. DISCUSSION AND RECOMMENDATIONS

An overview of the main results is presented in Table 17 and Table 18. During the chemical treatment, the red areas tend to increase, and the dark regions decreased during all treatments. Thermal treatment seemed to also increase the red area independent from chemical treatment or granite variety. Opaque light layer was found to cover dark minerals. Tone of red colours changed in thermal and iron treatments. Natural weathering of stone was a clear phenomena namely in Dark Green Wiborgite and in Dark Rapakivi granite. Wiborgite was found to be sensitive and surface alteration was clear with sulphite chemical, while effect of chloride compounds was strongest on pyterlite. This suggests presence of different dominating weathering phenomena. Dark green wiborgite was clearly more sensitive to chloride than wiborgite, but still affected by the sulphite chemicals. Dark Rapakivi granite is the most sensitive one for high temperatures. At 600 ºC crackles appeared on surface.

The experiments revealed adsorption to surface layer via new forming chemical compounds and cation exchange. Acidic treatments dissolved light elements, and trace elements from the surface. The trace elements originates from the dark regions. Sulphuric acid is a strong acid and phosphoric acid is classified as a weak acid. They both could be applied, if chemical weathering of granite is aimed. Phosphorus in phosphoric acid might be involved and catalyse reactions with iron or other metals leaching out from the surface. P adsorption occurred in phosphoric acid treatment, while in sulphuric acid treatment several metal compounds leached out and mainly aluminium sorption was verified. In thermal treatments S content was increased. The most common S compounds are sulphides and sulphates, and it can be expected that several dissolved metal ions have formed these compounds.

Recommendation:

Sulphuric acid: strong acid, widely applied in manufacturing industry. Can be applied safely and efficiently in low concentrations (2 mg/L) to speed natural weathering of granites.

Thermal treatment: treatment in 400 ºC can be applied safely and efficiently to alter the surface appearance. Short 30 min treatment time is sufficient. Higher temperatures might damage the stone. The temperature range was not optimized, but 600 ºC already damaged the structure.

Table 17. H_2SO_4 and H_3PO_4 treated samples: Visual changes, Changes according to FT-IR, and changes is elemental concentrations based of XRF.

Method	W6 H_2SO_4 W13 H_3PO_4	P8 H_2SO_4 P13 H_3PO_4	D1 H_2SO_4 D8 H_3PO_4	DG1 H_2SO_4 DG8 H_3PO_4
Visual, Reddish	+, +	+, +	-, -	-, -
Visual, Black	-, -	-, -	-, -	-, -
Visual, White	-, -	-, +	+, +	+, +
FTIR, Feldspar	+, -	+, +	0, -	-, -
FTIR, Biotite	-, +	0, +	-, -	-, -
FTIR: Quartz	0, -	+, +	0, -	+, -
Conclusions based on XRF and ICP/MS results				
Dissolving H_2SO_4	Mg, Al, P, K, Ca, Fe, Sr (Li)	Li, Mg, P, K, Ca, Mn, Fe, Sr	Mg, P, K, Ca, Mn, Fe	Li, Be, Mg, P, K, Ca, Fe
H_3PO_4	Mg, Al, K, Ca, Fe, Sr (Li)	Li, Mg, Al, K, Ca, Mn, Fe, Sr	Mg, K, Ca, Mn, Fe	Mg, P, K, Ca, Fe
Sorption H_2SO_4	-	Al	Al	Al
H_3PO_4	P	P	P, Al	P, Al
Other H_2SO_4	SA cleans the top layer and metal compounds leach out. Occurrence of Si, trace and LE elements increase. S compounds increase: metal sulfides and sulphates increase			
H_3PO_4	PA is weak acid and with properties close to SA S compounds increase Occurrence of Si and trace elements increase, but LE decreases.			

Table 18. Thermally treated samples: Visual changes, Changes according to FT-IR, and changes is elemental concentrations based of XRF.

Method	W14, W8	P14, P16	D9, D3	DG9,
Visual, Reddish	+, +	+, +	+, +	+, -
Visual, Black	-, -	-, -	-, -	-, +
Visual, White	-, -	+, +	+, -	+, -
FTIR, Feldspar	+, mixed	+, +	+, -	+, +
FTIR, Biotite	-, 0	-, 0	+, +	+, +
FTIR: Quartz	+, -	+, +	0, -	+, +
XRF				
Decreasing in surface 600 °C	LE	P, Mn, Fe, LE	P, Mn, Fe, LE	P, K, trace
400 °C	LE, P, Mn, Fe	LE (Mg)	P, Mn, Fe, LE	n.a.
Increase 600 °C	S, trace	S, trace	Si, S, trace	S
400 °C	Si, S	LE (Mg)	Si, S, trace	n.a.
Other 600 °C	Trace elements are revealed	Trace elements are revealed in 600 C, durable	Trace elements are revealed	Not durable, crackles
400 °C				

References

Bosch-Reig, F., Gimeno-Adelantado, J. V., Bosch-Mossi, F., & Doménech-Carbó, A. (2017). Quantification of minerals from ATR-FTIR spectra with spectral interferences using the MRC method. *Spectrochimica Acta Part A Molecular and Biomolecular Spectroscopy, 181*, 7-12.

Hlavay, J., Jonas, K., Elek, S., & J., I. (1978). Characterization of the Particle Size and the Crystallinity of Certain Minerals by IR Spectrophotometry and other Instrumental Methods—II. Investigations on Quartz and Feldspar. *Clays and Clay Minerals, 2*(26), 139-143.

Ilonen, J. (2020). *Aging of stone surface.* LUT University, B, Sc, Thesis. Retrieved from https://urn.fi/URN:NBN:fi-fe20201211100394

Pernet-Fisher, J., Joy, K., Martin, D., & Donaldson Hanna, K. (2017). Assessing the shock state of the lunar highlands: Implications for the petrogenesis and chronology of crustal anorthosites. *Scientific Reports*.

Pozo, S., Montojo, C., Rivas, T., López-Díaz, A. J., Fiorucci, M. P., & López de Silanes, M. E. (2013). Comparison between Methods of Biological Crust Removal on Granite. *Engineering Materials, 548*, 317-325.

Rubio-Ordóñez, A., García-Moreno, O., Terente, L. M., García-Guinea, J., & Tormo, L. (2019). Chondrite Shock Metamorphism History Assessed by Non-Destructive Analyses on Ca-Phosphates and Feldspars in the Cangas de Onís Regolith Breccia. *European Journal of Mineralogy*. doi:10.3390/min9070417

Senthil Kumar, R., & Rajkumar, P. (2013). Characterization of minerals in air dust particles in the state of Tamilnadu, India through ftir spectroscopy. *Atmos. Chem. Phys. Discuss, 13*, 22221–22248.

Sontevska, V., Jovanovski, G., Makreski, P., & Raskovska, A. (2008). Minerals From Macedonia. XXI. Vibrational Spectroscopy as Identificational Tool for Some Phyllosilicate Minerals. *Acta Chimica Slovenica, 55*(4), 757-766.

Wojcieszak, M., & Wadley, L. (2019). A Raman micro-spectroscopy study of 77,000 to 71,000 year old ochre processing tools from Sibudu, KwaZulu-Natal. *South Africa. Herit Sci, 7*(24). Retrieved from https://doi.org/10.1186/s40494-019-0267-9

Yang, Y., Xia, Q., & Zhang, P. (2015). Evolution of OH groups in diopside and feldspars with temperature. *Eur. J. Mineral., 2*, 185 - 192. doi:10.1127/ejm/2015/0027-2424

APPENDIX UV treatment

The intensity of noon summer sunlight at 340 nm is 0,68 W/m^2. An UV oven Q-Sun Xenon Test Chamber (Figure 42) was used to mimic these conditions in 24-hour intervals.

Figure 42 Q-Sun Xenon Test Chamber used for in UV light treatment.

3 samples of rocks were used, 2 unpretreated pyterlite rock samples and 1 sample of rapakivi granite pytherlite pretreated in 0,1 M H_3PO_4 for one day. Unpretreated samples were exposed to the UV-rays for 11 days and acid pretreated sample was exposed to the UV rays for 10 days. The total test time was 264 hours with total of 986,8 kJ/m^2 UV-light exposed to the rock samples.

RESULTS

The pyterlite samples treated with UV light, named U1 and U2, are shown below in Figure 43. On the left are the 2 samples before treatment and on the right after treatment. There are not many visual changes seen in the treated samples.

Figure 43 Samples treated with UV light treatment for 11 days. Samples U1 and U2 on the left are untreated and on the right U1 and U2 after UV light treatment.

In Figure 44 are shown the FT-IR picture and optical microscope picture of U1 side by side.

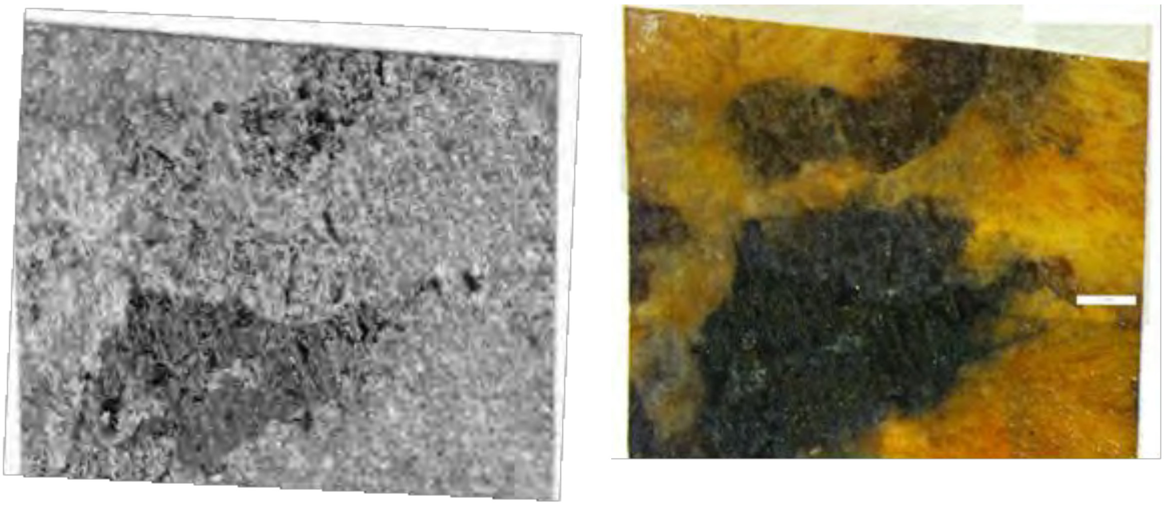

Figure 44 The UV light treated pyterlite sample U1. Optical microscope picture on the right and FT-IR picture on the left.

In

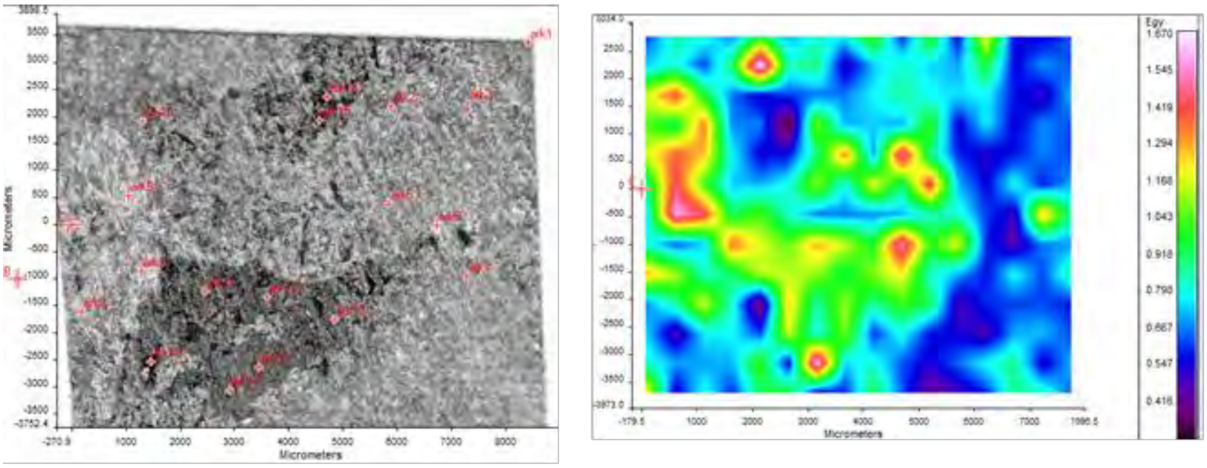

Figure 45*, the specific examined spots are shown as markers, where the IR spectra of that marker was taken from the surface and analyzed. Next to the markers is also shown the measured energy map of the examined area.*

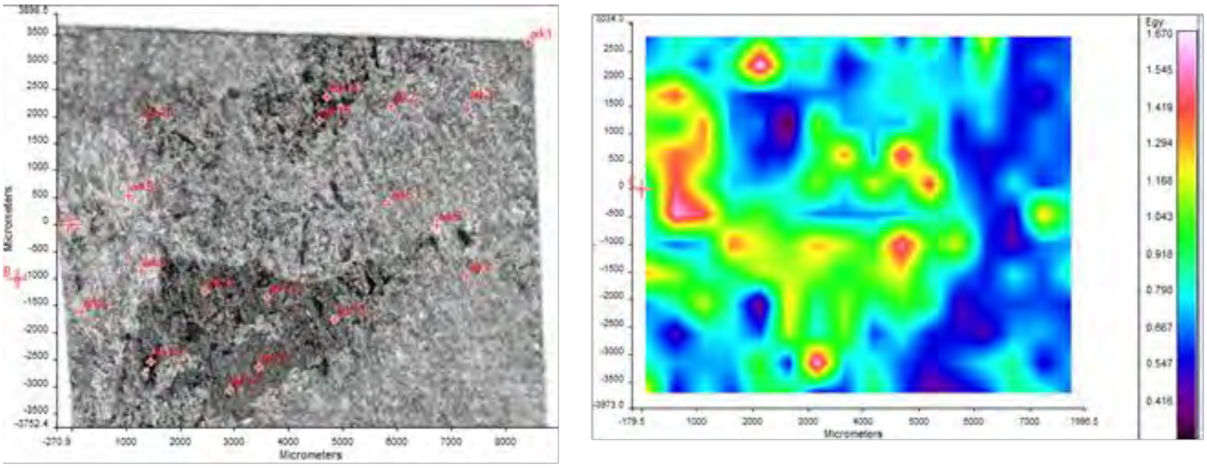

Figure 45 Sample UV1 FT-IR picture with marked IR spectra analyzed spots examined energy map area. Average energy of this mapped area on the right.

IR reflectance spectra of each marker examined of sample UV1 surface is shown in Figure 46.

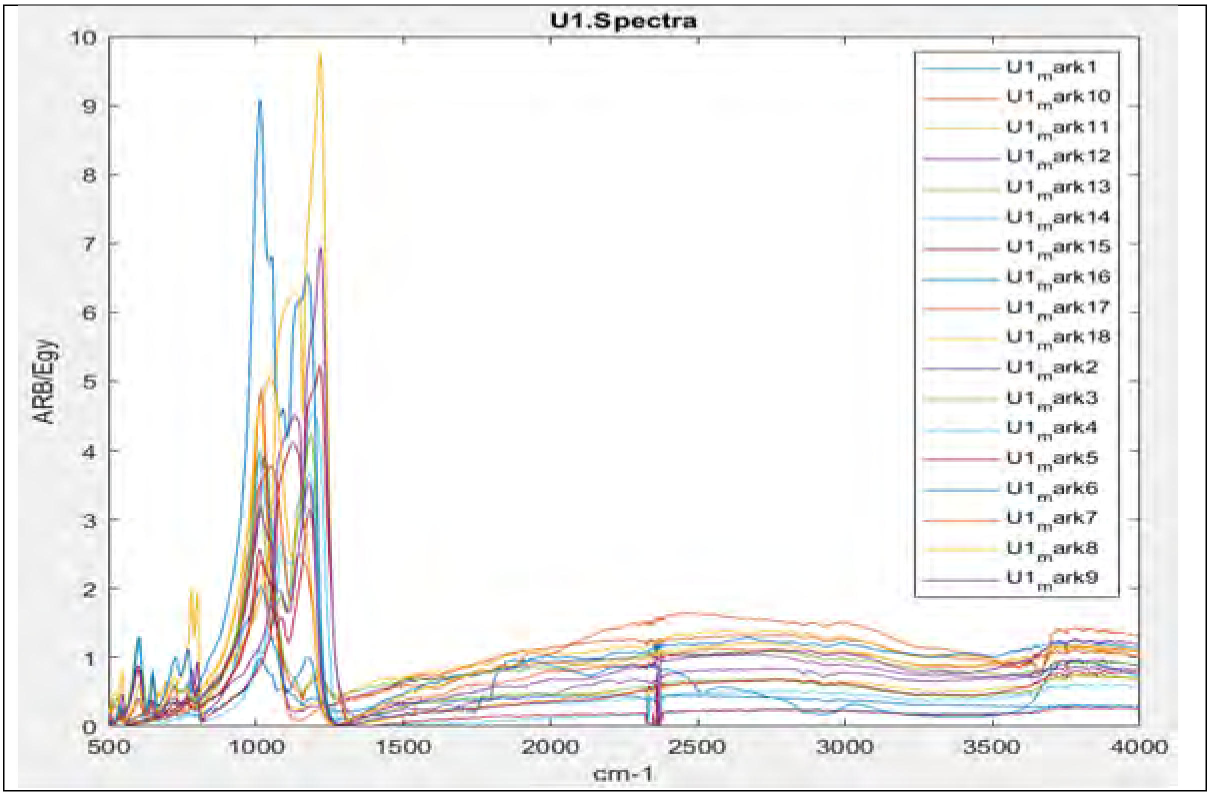

Figure 46 Sample U1 spectra of thermally treated granite in furnace. Marker spots are shown above in Figure 33. Y-axel unit is energy.

APPENDIX: CHANGE IN VISUAL APPEARANCE: COLORIMETRIC APPROACH

Appendix consist of large colorimetric work report available in pdf format + manuscript of unpublished scientific paper. Appendices are available on request for one year from publishing date of this report. Requests: satu-pia.reinikainen@lut.fi.

Introduction to the annex:

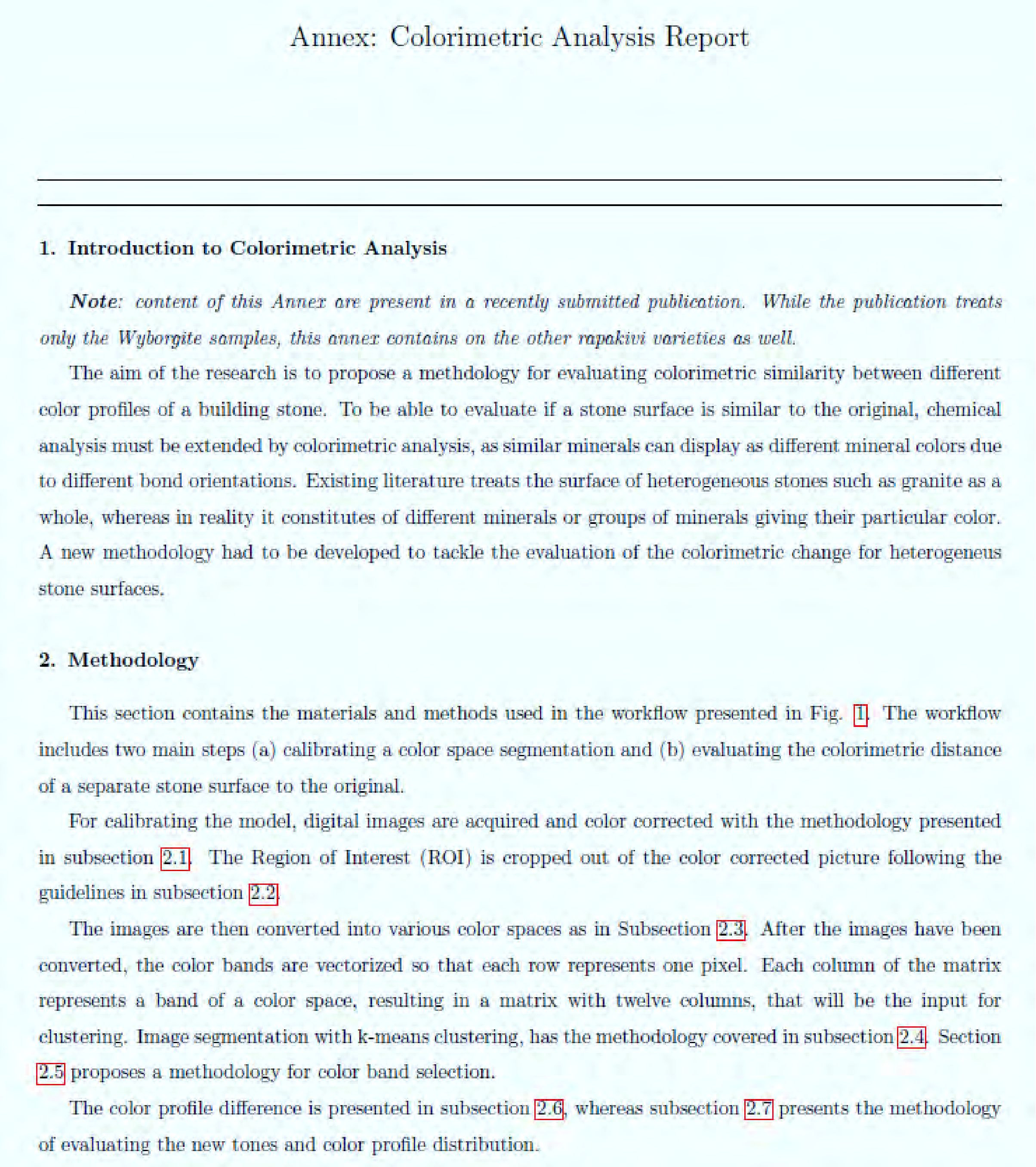

Annex: Colorimetric Analysis Report

1. Introduction to Colorimetric Analysis

Note: *content of this Annex are present in a recently submitted publication. While the publication treats only the Wyborgite samples, this annex contains on the other rapakivi varieties as well.*

The aim of the research is to propose a methdology for evaluating colorimetric similarity between different color profiles of a building stone. To be able to evaluate if a stone surface is similar to the original, chemical analysis must be extended by colorimetric analysis, as similar minerals can display as different mineral colors due to different bond orientations. Existing literature treats the surface of heterogeneous stones such as granite as a whole, whereas in reality it constitutes of different minerals or groups of minerals giving their particular color. A new methodology had to be developed to tackle the evaluation of the colorimetric change for heterogeneus stone surfaces.

2. Methodology

This section contains the materials and methods used in the workflow presented in Fig. 1. The workflow includes two main steps (a) calibrating a color space segmentation and (b) evaluating the colorimetric distance of a separate stone surface to the original.

For calibrating the model, digital images are acquired and color corrected with the methodology presented in subsection 2.1. The Region of Interest (ROI) is cropped out of the color corrected picture following the guidelines in subsection 2.2.

The images are then converted into various color spaces as in Subsection 2.3. After the images have been converted, the color bands are vectorized so that each row represents one pixel. Each column of the matrix represents a band of a color space, resulting in a matrix with twelve columns, that will be the input for clustering. Image segmentation with k-means clustering, has the methodology covered in subsection 2.4. Section 2.5 proposes a methodology for color band selection.

The color profile difference is presented in subsection 2.6, whereas subsection 2.7 presents the methodology of evaluating the new tones and color profile distribution.

Appendix SEM images of original and treated samples

Wiborgite-series (W)

Table 19. SEM pictures of sample series wiborgite.

	Step 0	**Step 1 chemical**	**Step 2 thermal**
6 **H_2SO_4**	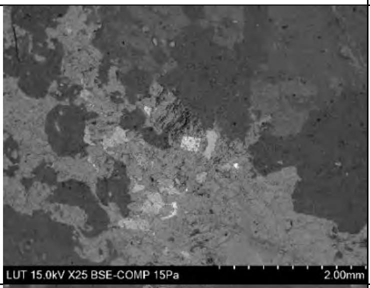	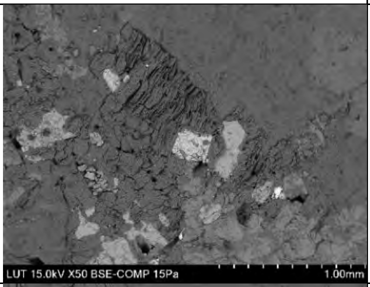	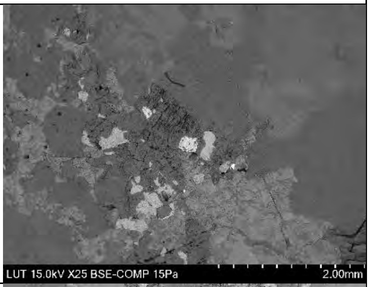
7 **H_2SO_4 + $FeCl_2$**	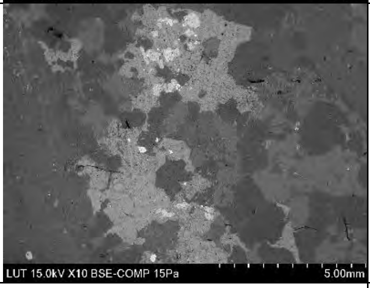	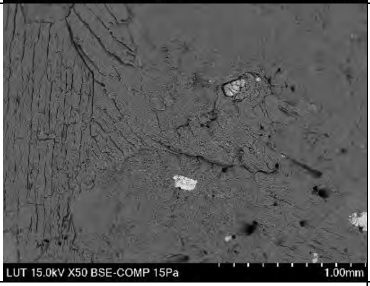	
8 **Thermal[2]**			
9 **H_2SO_4 + Na_2SO_4**		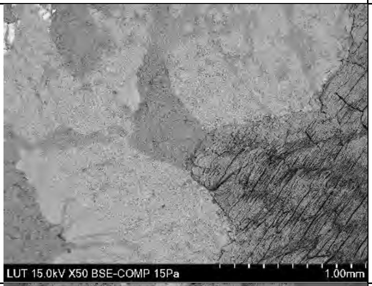	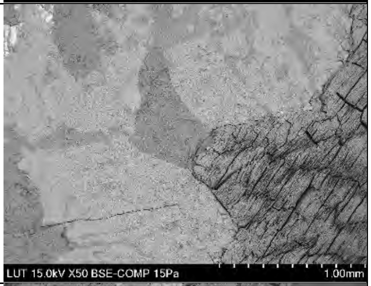
10 **$CaCl_2$**		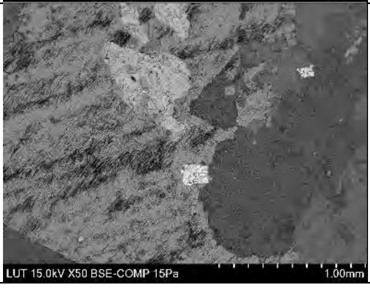	

11 **$FeCl_2$**		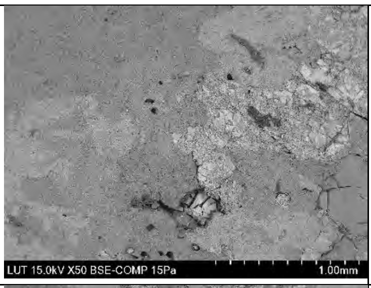	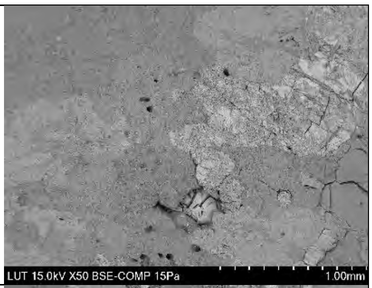
12 **Na_2SO_4**		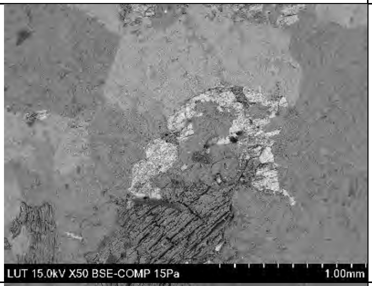	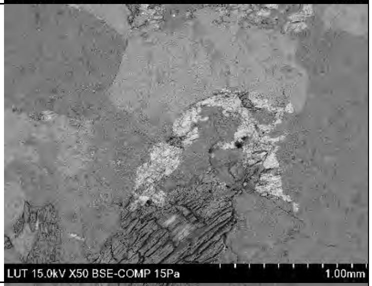
13 **H_3PO_4**			
14 **Thermal[1]**			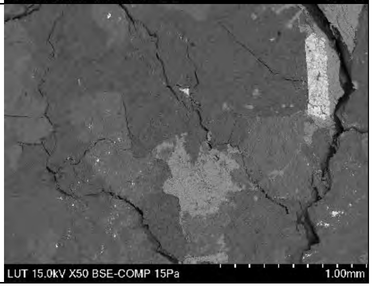

Pyterlite-series (P)

Table 20. SEM pictures of sample series Pyterlite.

	Step 0	**Step 1**	**Step 2**
8 **H_2SO_4**	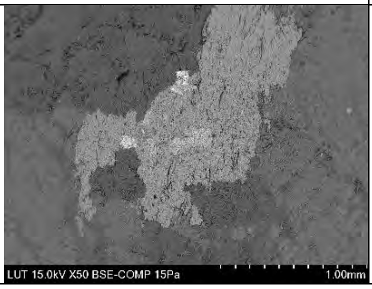	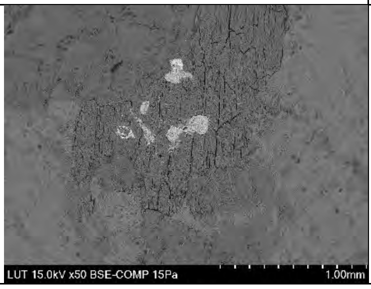	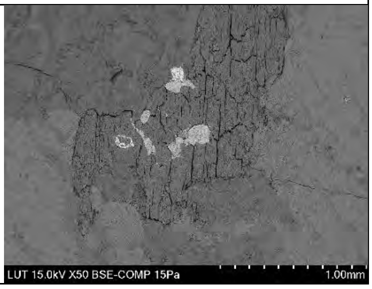

9 **$H_2SO_4 + Na_2SO_4$**	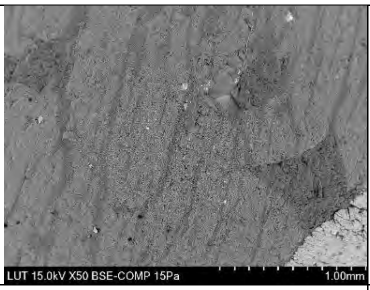		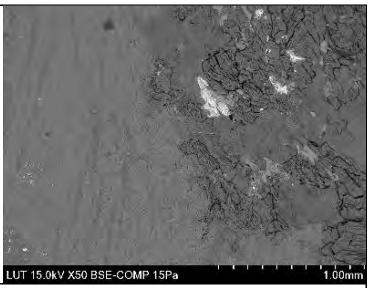
10 **$CaCl_2$**		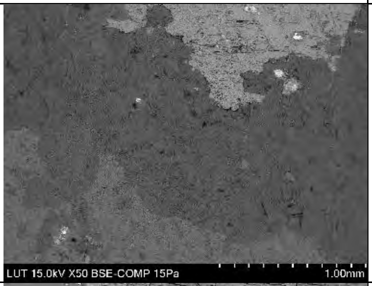	
11 **$FeCl_2$**		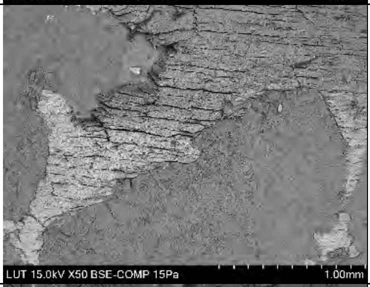	
12 **Na_2SO_4**		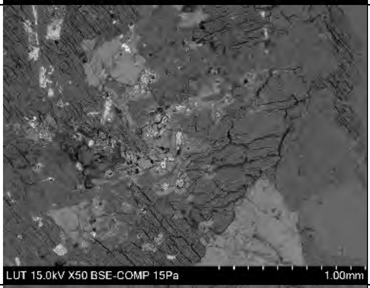	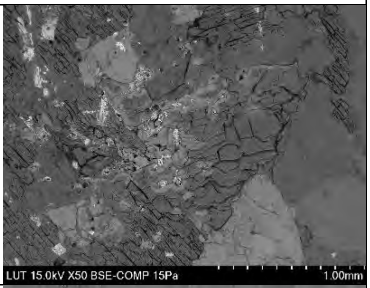
13 **H_3PO_4**			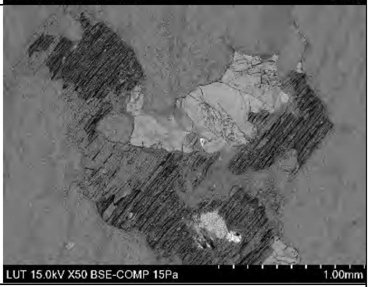
14 **Thermal[1]**		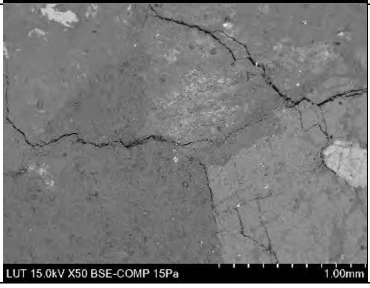	

15 H_2SO_4 + $FeCl_2$		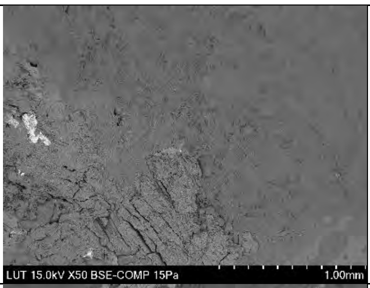	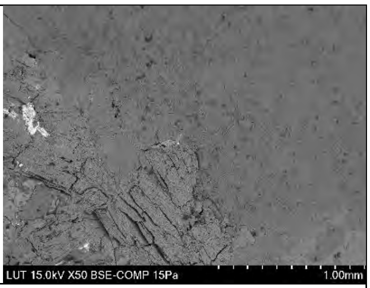
16 Thermal^2		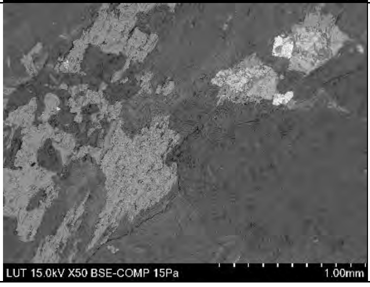	

Dark Rapakivi Granite-series (D)

Table 21. SEM pictures of sample series D (Dark Rapakivi granite).

	Step 0	**Step 1**	**Step 2**
1 H_2SO_4	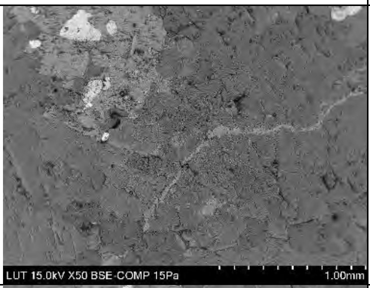	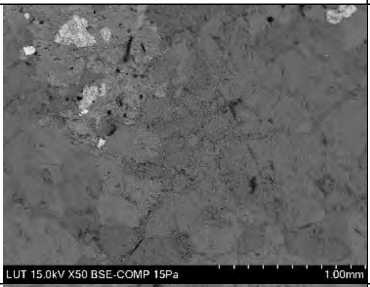	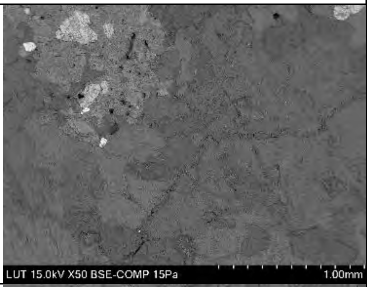
2 H_2SO_4 + $FeCl_2$	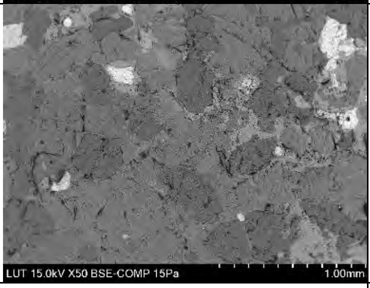	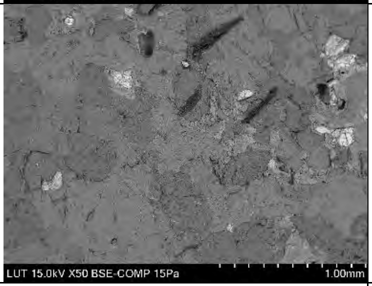	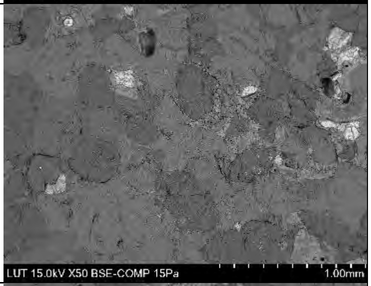
3 Ther-mal^2			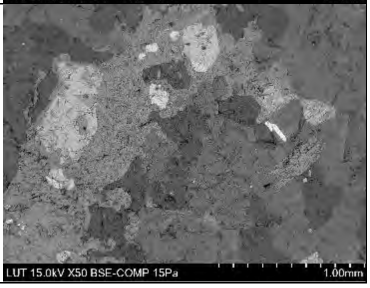

4 **H_2SO_4 + Na_2SO_4**			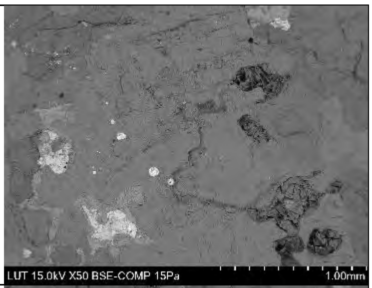
5 **$CaCl_2$**			
6 **$FeCl_2$**		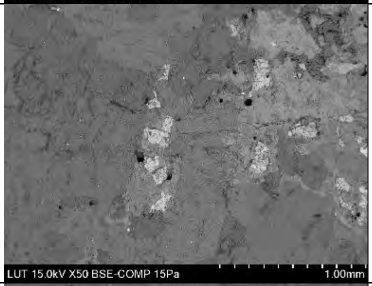	
7 **Na_2SO_4**		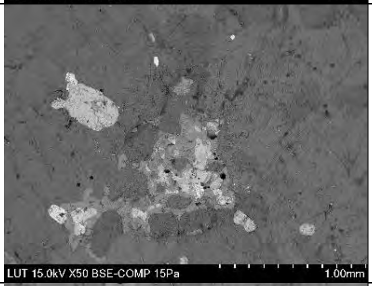	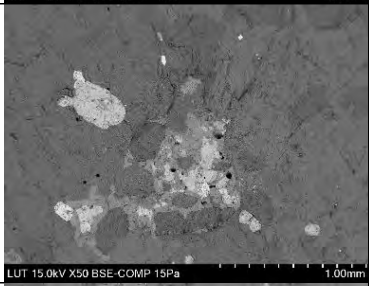
8 **H_3PO_4**		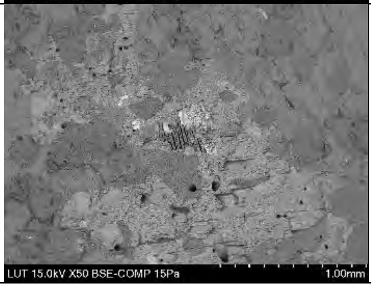	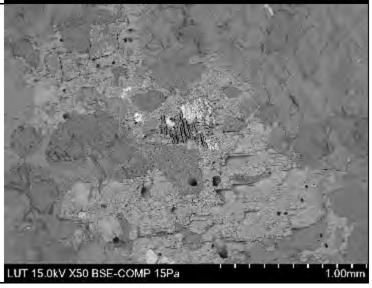

Dark Green Wiborgite-series (DG)

Table 22. SEM pictures of sample series DG (dark green wiborgite).

	Step 0	Step 1	Step 2
1 H_2SO_4	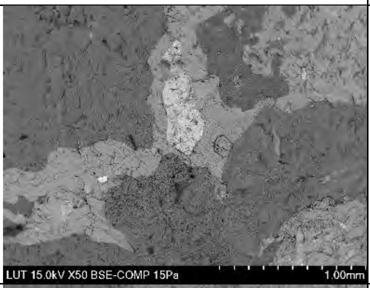	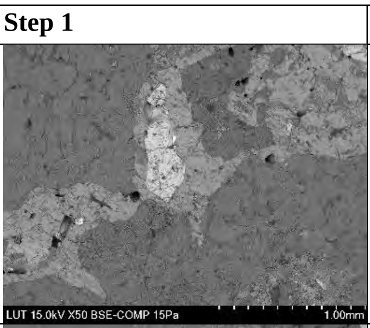	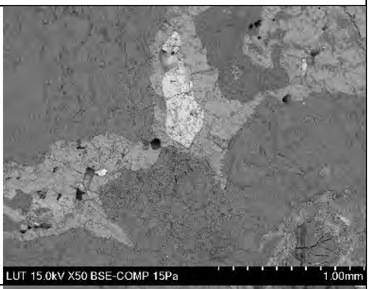
2 $H_2SO_4 + FeCl_2$			
4 $H_2SO_4 + Na_2SO_4$			
5 $CaCl_2$		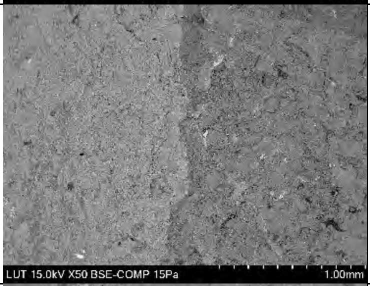	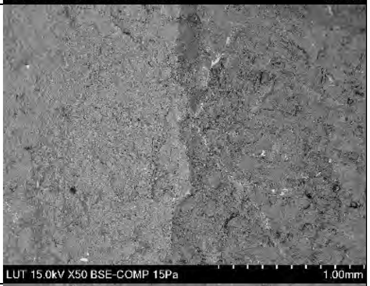
6 $FeCl_2$		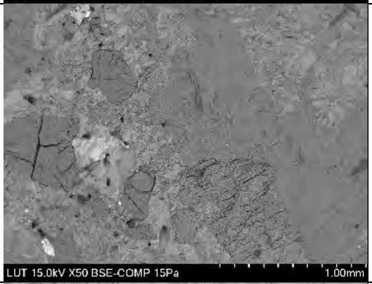	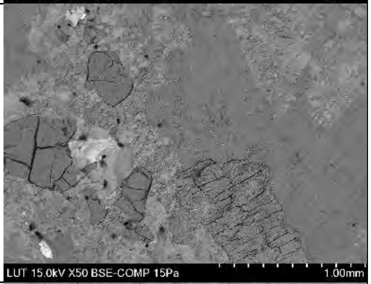
7 Na_2SO_4		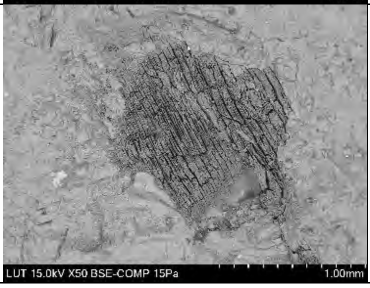	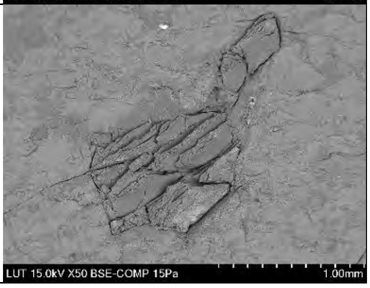

8 **H_3PO_4**		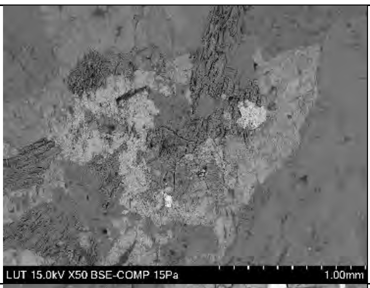	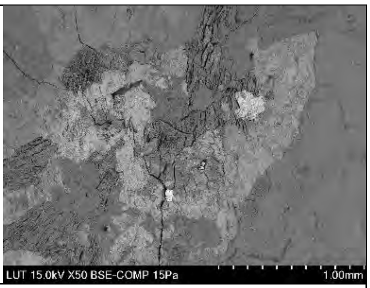
9 **Ther-mal[1]**		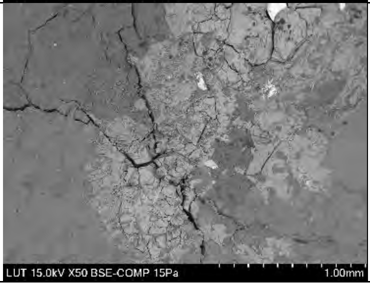	

Appendix: EDS example “Iron distribution on sample surfaces”

Energy Dispersive X-Ray Spectroscopy (EDS) was used to detect the element composition on the sample surfaces. Thermo Scientific UltraDry SDD EDS, dual detector

Wiborgite -series (W)

Table 23. Table with the amount of Fe on the wiborgite-series samples surface according to EDS: original distribution, distribution after chemical treatment and after completing the treatment in oven.

	Original	**After chemical treatment**	**After thermal treatment**
6 **H_2SO_4**	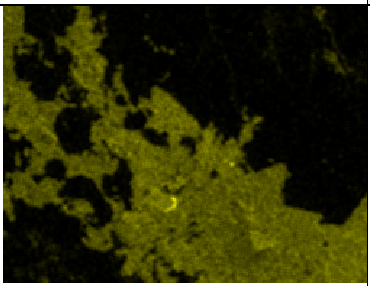	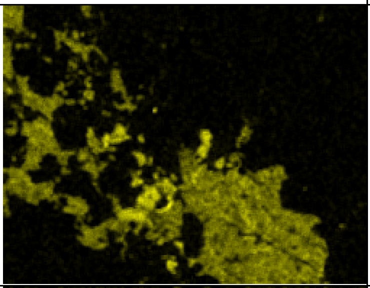	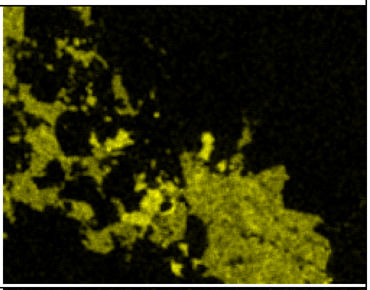
7 **H_2SO_4 + $FeCl_2$**	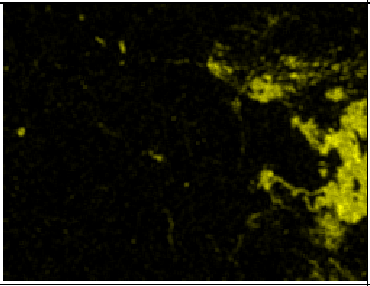	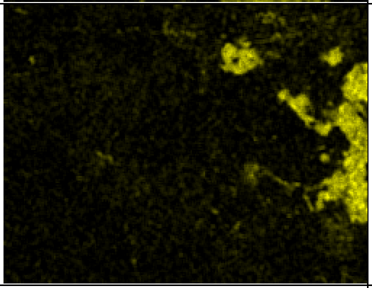	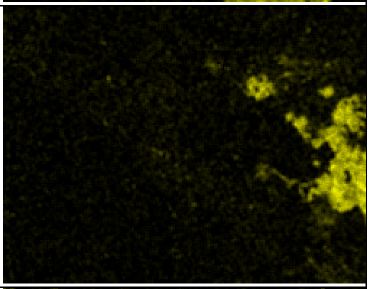
8 **Thermal^2, 400 C**			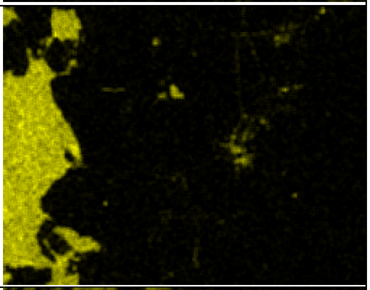
9 **H_2SO_4 + Na_2SO_4**		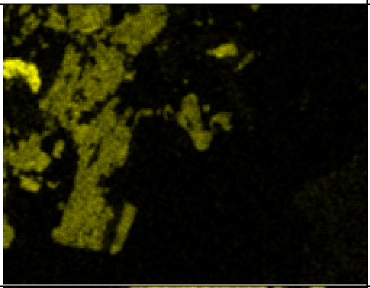	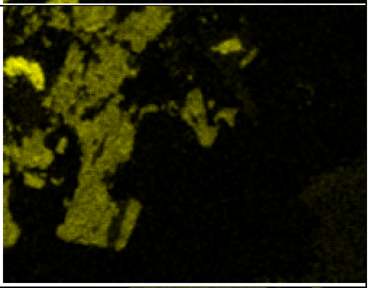
10 **$CaCl_2$**		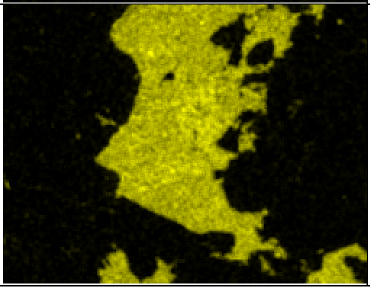	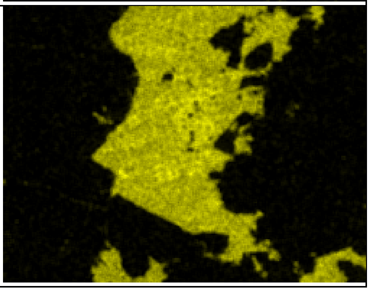

11 **$FeCl_2$**		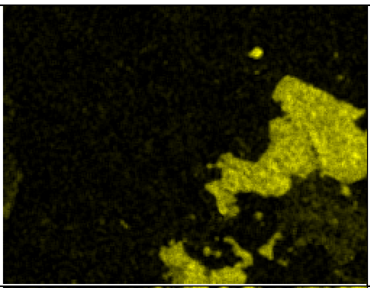	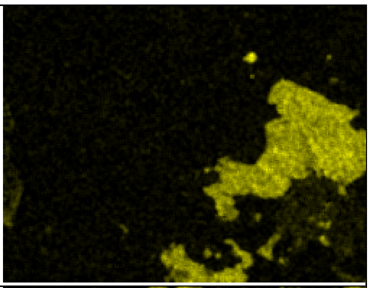
12 **Na_2SO_4**		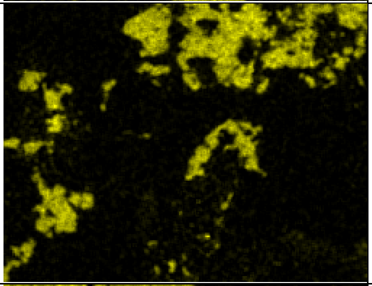	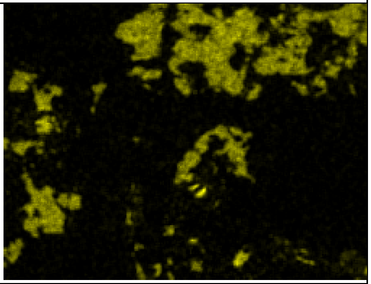
13 **H_3PO_4**		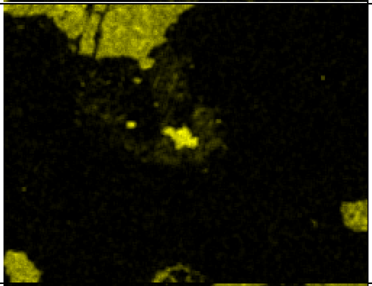	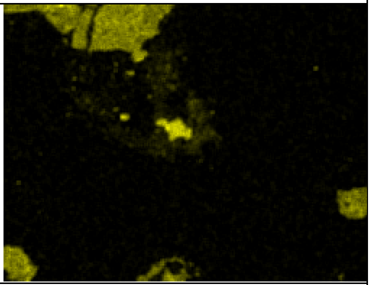
14 **Thermal[1], 600 C**		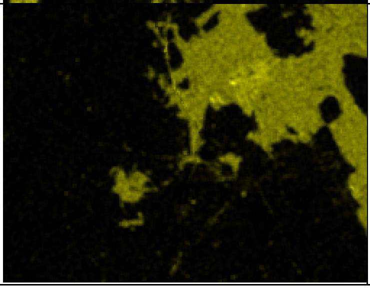	

Pyterlite-series (P)

Table 24. Table with the amount of Fe on the Pyterlite-series samples surface according to EDS during different treatments.

	Original	**After chemical treatment**	**After thermal treatment**
6 H_2SO_4		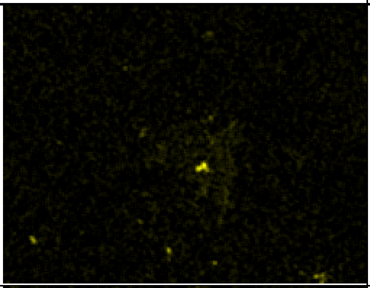	
7 $H_2SO_4 + FeCl_2$		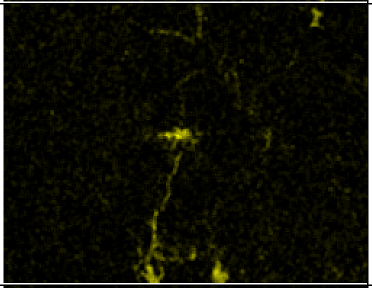	
8 H_2SO_4	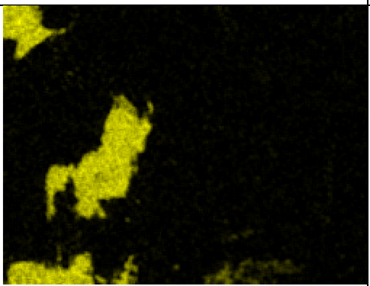	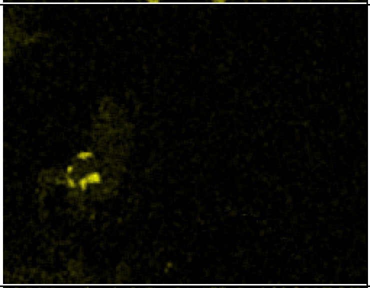	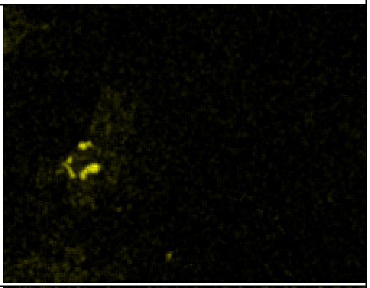
9 $H_2SO_4 + Na_2SO_4$	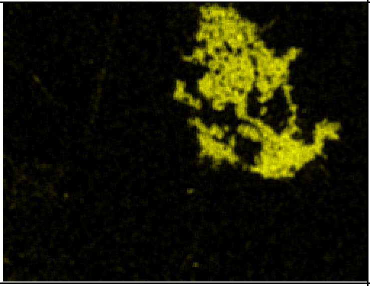	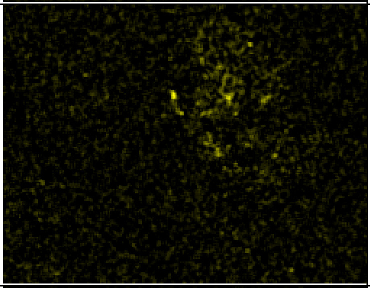	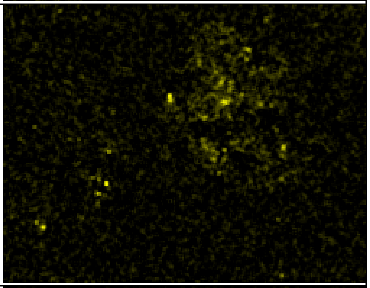
10 $CaCl_2$		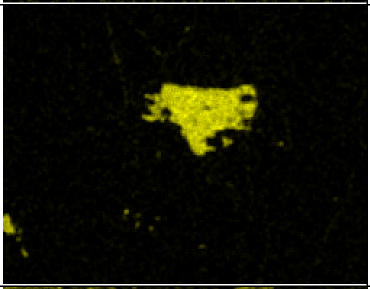	
11 $FeCl_2$		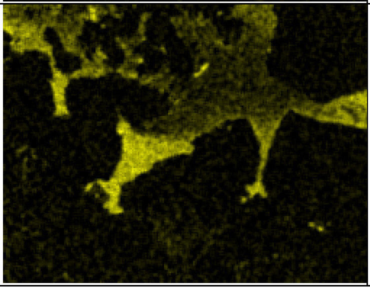	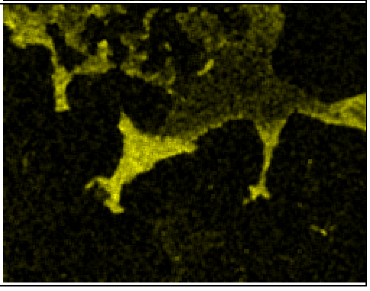

12 **Na$_2$SO$_4$**		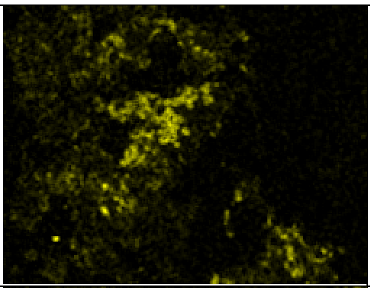	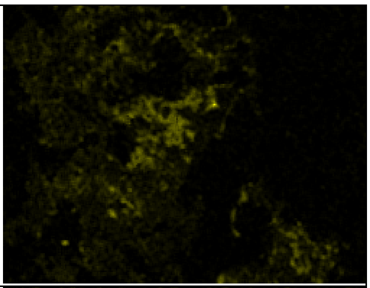
13 **H$_3$PO$_4$**		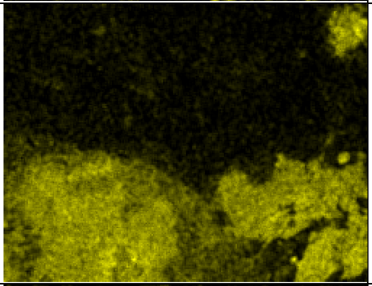	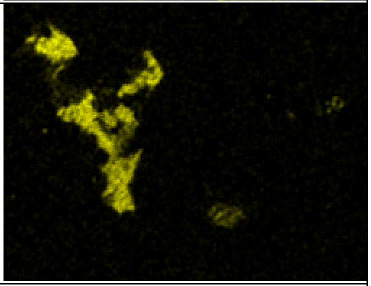
14 **Thermal[1], 600 C**		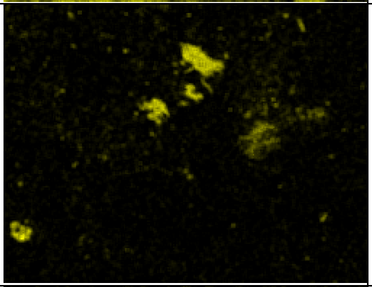	
15 **H$_2$SO$_4$ + FeCl$_2$**		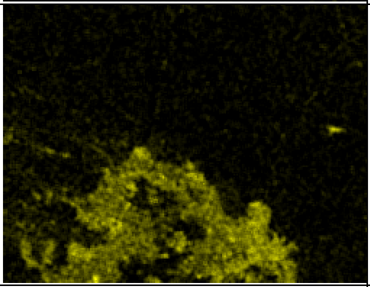	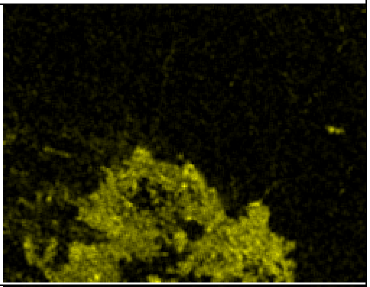
16 **Thermal[2], 400 C**			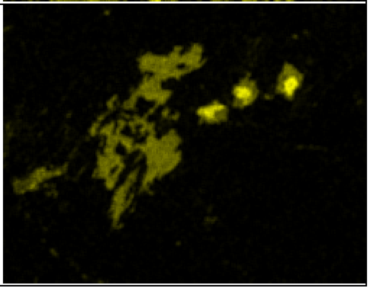

Dark Rapakivi Granite-series (D)

Table 25. Table with the amount of Fe on the D (dark Rapakivi Granite)-series samples surface according to EDS during different treatments.

	Original	**After chemical treatment**	**After thermal treatment**
1 H_2SO_4	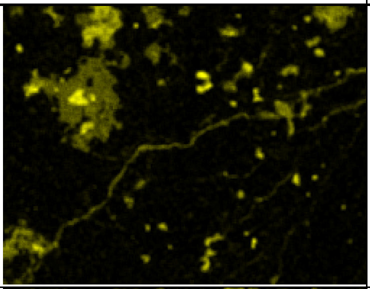	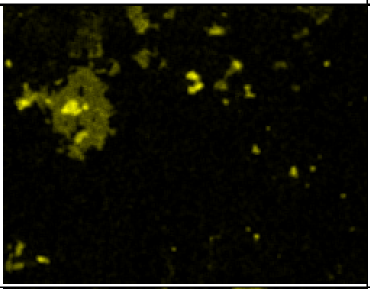	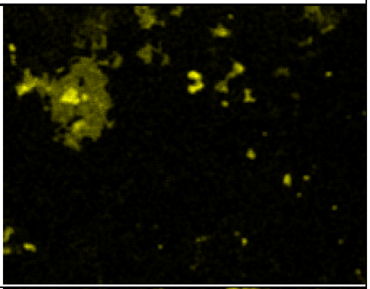
2 $H_2SO_4 + FeCl_2$	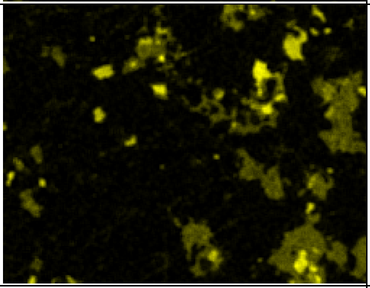	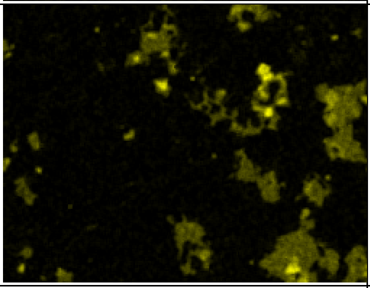	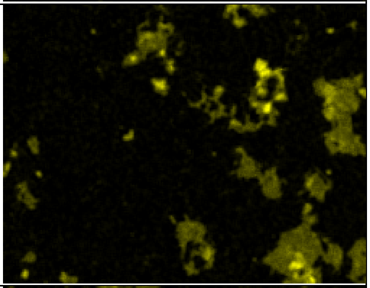
3 Thermal[2], 400 C			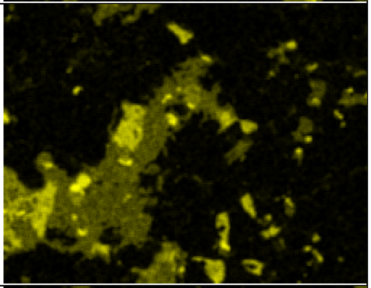
4 $H_2SO_4 + Na_2SO_4$		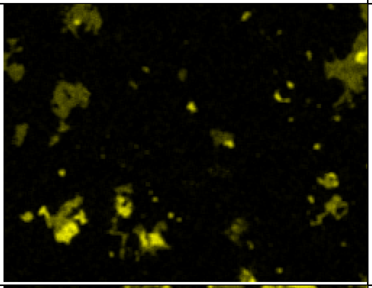	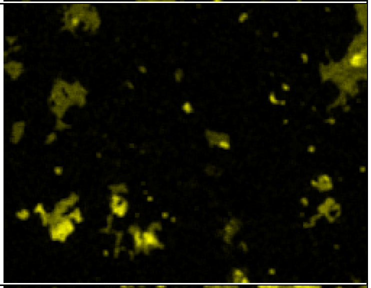
5 $CaCl_2$		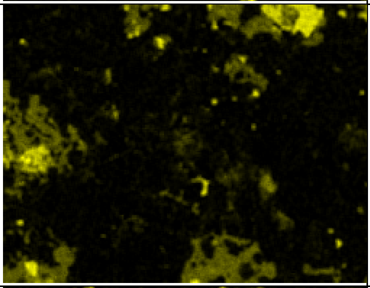	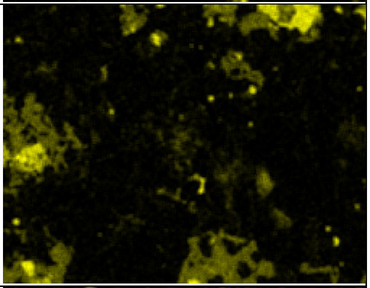
6 $FeCl_2$		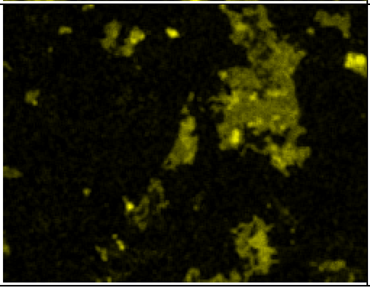	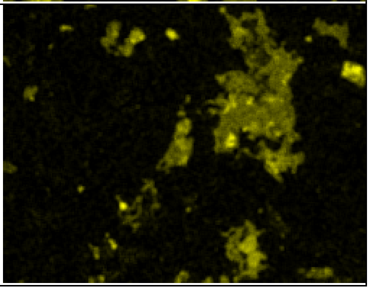

7 **Na_2SO_4**		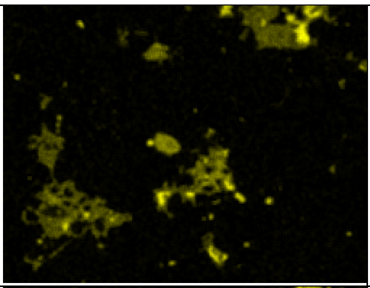	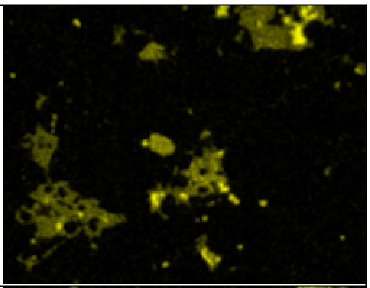
8 **H_3PO_4**		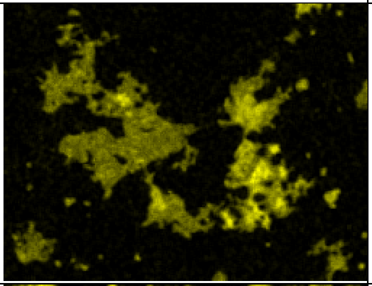	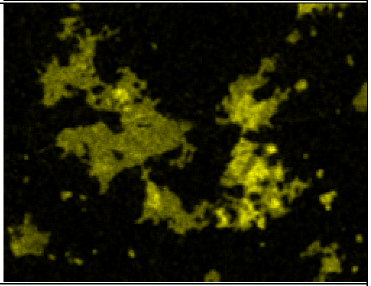
9 **Thermal[1], 600 C**		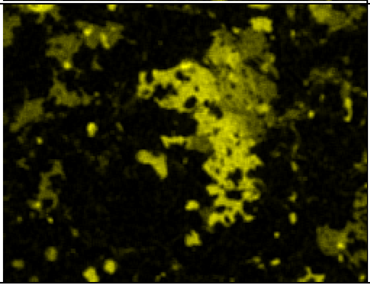	

Dark Green Wiborgite-series (DG)

Table 26. Table with the amount of Fe on the DG (dark green wiborgite)-series samples surface according to EDS.

	Original	**After chemical treatment**	**After thermal treatment**
1 H_2SO_4	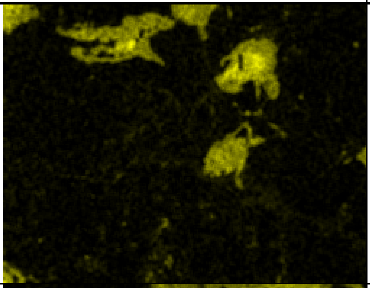	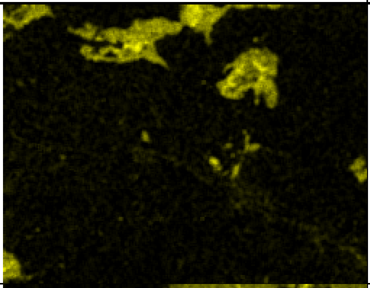	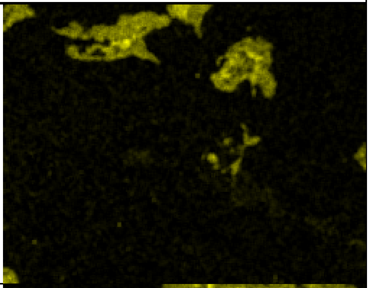
2 $H_2SO_4 + FeCl_2$	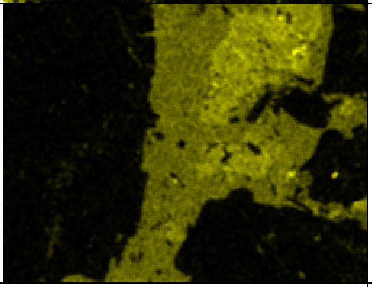	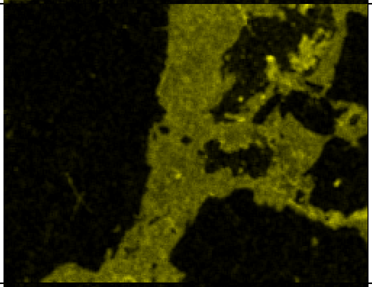	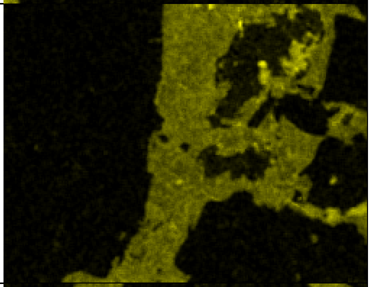
4 $H_2SO_4 + Na_2SO_4$		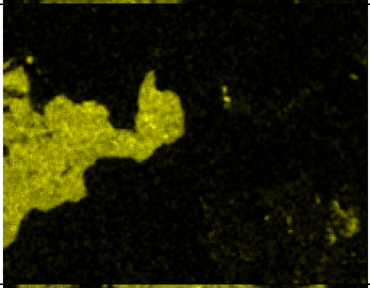	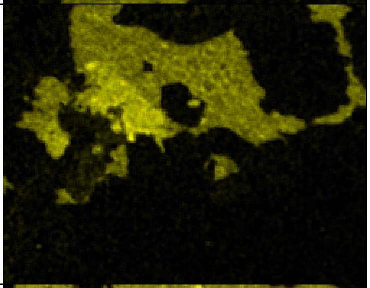
5 $CaCl_2$		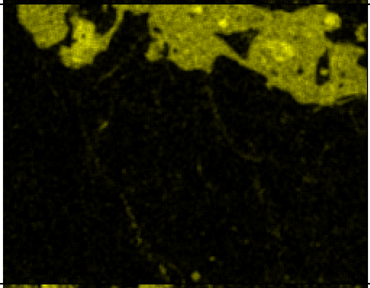	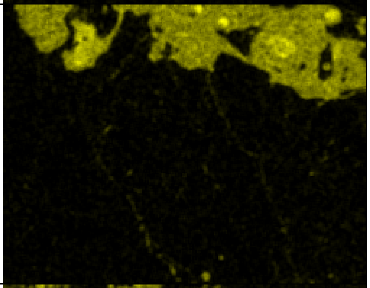
6 $FeCl_2$		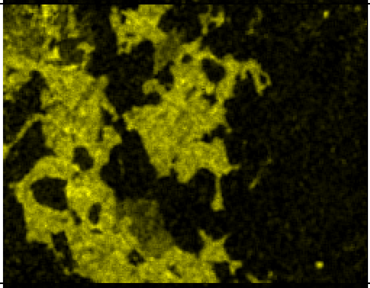	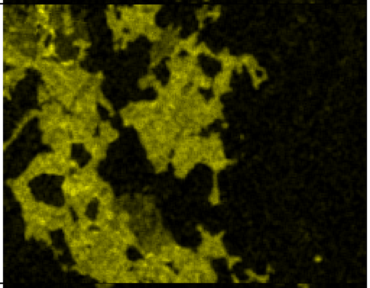
7 Na_2SO_4		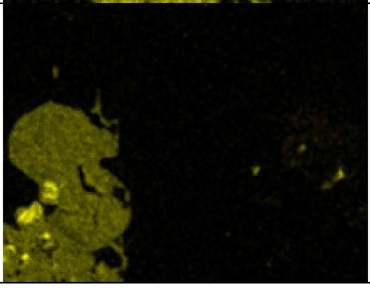	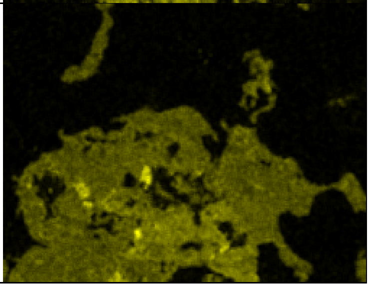

8 **H_3PO_4**			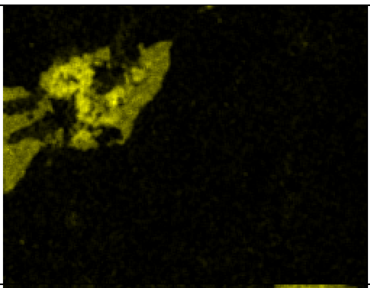	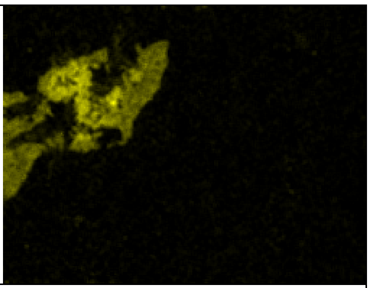
9 **Thermal[1], 600 C**			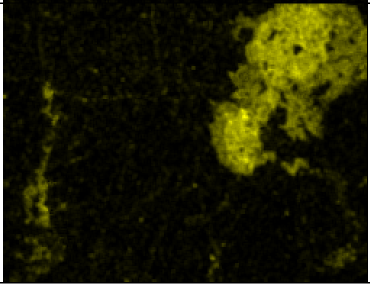	

APPENDIX XRF results with standard deviations

Appendix is an Excel file containing all XRF measurements, and their mean values from each sample. The file can be requested from: satu-pia.reinikainen@lut.fi before 1.3.2024 (one year after this work report published).

Appendix: ICP-MS results

Table 27. ICP-MS results of treated samples from wiborgite series (W).

	W-6 H_2SO_4 Δc $[mg/m^2]$	W-7 H_2SO_4 + $FeCl_2$ Δc $[mg/m^2]$	W-9 H_2SO_4 + Na_2SO_4 Δc $[mg/m^2]$	W-10 $CaCl_2$ Δc $[mg/m^2]$	W-11 $FeCl_2$ Δc $[mg/m^2]$	W-12 Na_2SO_4 Δc $[mg/m^2]$	W-13 H_3PO_4 Δc $[mg/m^2]$
7 Li	3461.1	254.3	227.1	-463.0	188.3	88.9	216.0
23 Na	340.2	37780.2	4695.1	-694.4	-542.2	-24364.3	1146.0
24 Mg	774.8	1539.3	827.0	16.6	977.6	653.3	1019.5
27 Al	3833.5	2355.8	-400.8	0.0	926.3	-1537.6	2021.0
31 P	4348.0	-521.5	-2280.1	-2.4	-1167.0	3780.7	-63990.6
39 K	2861.6	1795.5	97.0	-38431.2	1211.4	701.5	1694.0
44 Ca	3130.1	1884.1	719.7	-113806.7	1824.6	741.9	2530.5
45 Sc	11.5	6.7	3.5	0.1	4.3	2.7	6.2
55 Mn	144.2	111.4	77.5	0.0	67.4	35.1	87.9
56 Fe	14765.9	80348.2	7622.8	-2973.2	31393.7	2596.4	7141.2
66 Zn	35.4	25.3	19.3	0.0	13.4	7.2	17.2
88 Sr	3.5	1.7	0.4	-13895.0	2.2	0.6	1.5
89 Y	32.8	23.8	4.5	0.0	15.1	5.4	16.6
139 La	177.0	146.2	6.1	0.0	63.9	6.5	24.3
140 Ce	341.1	248.2	11.2	0.0	122.1	12.4	47.9
141 Pr	31.6	22.4	1.2	0.0	12.1	1.4	5.4
146 Nd	100.9	70.3	4.9	0.0	41.4	5.4	21.8
147 Sm	14.9	9.1	0.9	0.0	6.4	1.0	4.0
163 Dy	7.4	4.8	0.8	0.0	3.1	1.0	3.3
166 Er	3.5	2.4	0.5	0.0	1.5	0.6	1.8
172 Yb	2.8	2.0	0.4	0.0	1.2	0.6	1.5
208 Pb	1.6	98.1	0.6	0.3	4.3	1.0	6.4
232 Th	71.2	41.5	1.0	0.0	11.1	4.2	14.0
238 U	16.5	5.7	1.3	0.0	3.9	2.0	4.1

Table 28: ICP-MS results of treated samples from pyterlite series.

	P-6 H_2SO_4 Δc [mg/m^2]	P-7 H_2SO_4 + $FeCl_2$ Δc [mg/m^2]	P-9 H_2SO_4 + Na_2SO_4 Δc [mg/m^2]	P-10 $CaCl_2$ Δc [mg/m^2]	P-11 $FeCl_2$ Δc [mg/m^2]	P-12 Na_2SO_4 Δc [mg/m^2]	P-13 H_3PO_4 Δc [mg/m^2]
7 Li	512.9	5091.9	-6765.7	-5567.1	4312.3	198.9	1556.3
9 Be	0.0	0.0	70.6	70.9	164.1	0.0	0.0
23 Na	0.0	21342.6	-1125998.5	71.8	856557.4	-976564.6	-110695.5
24 Mg	1361.4	106.0	618.9	31.2	864.9	612.8	847.0
27 Al	-4264.6	2002.2	1439.1	0.0	14207.3	-11210.8	2192.3
31 P	2892.7	-1240.6	-2810.4	1834.6	-91.6	1751.0	-79628.7
39 K	2921.5	1098.4	930.0	-34724.8	1308.4	1060.8	1552.3
44 Ca	4626.4	925.9	189.2	-120280.2	2383.4	259.6	811.9
45 Sc	21.9	5.3	5.5	0.0	9.9	6.4	8.1
55 Mn	196.0	91.6	59.2	0.0	122.7	65.3	97.9
56 Fe	12664.0	-93175.8	3108.1	-56.3	-98028.6	4002.6	6316.6
66 Zn	55.0	25.9	20.5	0.3	25.2	21.9	32.4
88 Sr	4.6	1.3	0.5	-319.5	1.9	0.8	1.6
89 Y	65.4	57.9	5.2	0.1	38.9	11.5	13.0
137 Ba	1.4	0.1	1.0	0.5	1.1	1.6	11.3
139 La	75.8	45.9	2.2	0.2	57.1	14.4	20.2
140 Ce	148.7	89.8	4.3	0.3	109.8	25.2	34.6
141 Pr	18.0	10.6	0.5	0.0	13.0	2.7	4.0
146 Nd	72.1	42.4	2.1	0.0	53.4	10.7	16.9
147 Sm	15.3	9.9	0.6	0.0	10.7	1.9	4.1
163 Dy	13.8	12.4	0.8	0.0	8.5	2.1	2.8
166 Er	7.5	7.3	0.6	0.0	4.3	1.2	1.1
172 Yb	6.4	6.2	0.6	0.0	3.3	0.9	0.8
232 Th	38.8	95.6	1.5	0.0	32.1	7.0	2.5
238 U	34.4	31.7	6.4	0.1	11.9	3.5	1.4

Table 29: ICP-MS results of treated samples from Dark Rapakivi Granite (D) series.

	D-1 H_2SO_4 Δc [mg/m^2]	D-2 H_2SO_4 + $FeCl_2$ Δc [mg/m^2]	D-4 H_2SO_4 + Na_2SO_4 Δc [mg/m^2]	D-5 $CaCl_2$ Δc [mg/m^2]	D-6 $FeCl_2$ Δc [mg/m^2]	D-7 Na_2SO_4 Δc [mg/m^2]	D-8 H_3PO_4 Δc [mg/m^2]
23 Na	142.4	140.4	3323.7	291.3	-319.9	-3399.6	277.2
24 Mg	18.8	888.3	620.7	32.9	492.6	507.4	726.2
27 Al	-1161.9	-2957.3	-4203.0	0.0	-6600.8	-4195.7	-9699.4
31 P	2696.8	2240.3	5755.6	3782.7	641.8	9681.5	-12184.5
39 K	338.8	236.6	132.9	-23045.4	142.2	96.3	143.1
44 Ca	2842.4	2154.1	1145.1	-42208.0	1863.6	1307.2	5504.5
45 Sc	5.4	4.3	2.2	0.1	2.5	2.3	4.2
51 V	3.0	5.3	1.0	0.0	2.6	0.4	4.9
55 Mn	448.4	368.8	239.4	2.6	224.8	213.1	309.5
56 Fe	21067.9	86737.9	-29095.1	3036.8	5977.7	12127.6	16350.9
66 Zn	53.1	37.1	27.4	0.2	21.4	25.2	16.5
88 Sr	2.6	1.8	1.5	333.8	1.6	1.1	2.8
89 Y	13.3	15.9	4.2	0.0	11.2	5.9	18.2
139 La	19.6	21.2	4.7	0.0	17.0	7.4	28.3
140 Ce	40.7	43.4	9.8	0.0	34.9	15.5	59.5
141 Pr	4.7	4.9	1.1	0.0	4.0	1.8	6.9
146 Nd	19.0	19.9	4.4	0.0	16.5	7.2	28.2
147 Sm	3.4	3.9	1.0	0.0	3.0	1.4	5.2
163 Dy	2.7	3.2	0.8	0.0	2.2	1.1	3.9
166 Er	1.5	1.7	0.5	0.0	1.2	0.6	2.1
232 Th	10.3	6.9	1.6	0.0	4.2	2.2	5.3

Table 30: ICP-MS results of treated samples from dark green wiborgite series.

	DG-1 H_2SO_4 Δc $[mg/m^2]$	DG-2 H_2SO_4 + $FeCl_2$ Δc $[mg/m^2]$	DG-4 H_2SO_4 + Na_2SO_4 Δc $[mg/m^2]$	DG-5 $CaCl_2$ Δc $[mg/m^2]$	DG-6 $FeCl_2$ Δc $[mg/m^2]$	DG-7 Na_2SO_4 Δc $[mg/m^2]$	DG-8 H_3PO_4 Δc $[mg/m^2]$
7 Li	1260.0	16.7	-155.7	-98.2	8.0	203.2	15.8
9 Be	4.6	5.0	0.0	5.0	12.3	-5.2	-10.2
23 Na	13092.9	6349.7	13190.4	3234.2	1597.4	12235.8	2448.8
24 Mg	59.1	59.1	34.4	4.1	35.0	32.6	53.3
27 Al	-252.4	-314.4	-2786.0	2.4	-52.9	106.5	-479.0
31 P	206.3	238.3	79.9	-1.0	-89.0	630.4	5654.2
39 K	5.6	92.7	79.3	-2426.2	6.2	73.0	9.0
44 Ca	244.7	177.7	85.1	-5294.6	214.3	123.2	521.1
55 Mn	30.0	32.3	17.2	0.2	22.2	16.9	26.2
56 Fe	2119.6	-840.7	1054.2	-4.1	-3751.8	943.4	1386.7
66 Zn	4.4	3.5	2.5	0.0	2.5	2.8	3.3
88 Sr	0.2	0.2	0.1	11.3	0.4	0.1	0.3
89 Y	1.2	1.3	0.4	0.0	1.0	0.6	1.7
137 Ba	0.0	0.0	0.1	0.2	0.0	0.1	1.6
139 La	2.3	2.1	0.4	0.0	1.8	0.7	2.6
140 Ce	4.3	3.9	0.8	0.0	3.4	1.3	5.2
146 Nd	1.8	1.6	0.3	0.0	1.5	0.6	2.4
232 Th	2.0	1.3	0.5	0.0	1.0	0.5	1.2